12-1957

The Infrared Spectrum of Formyl Fluoride

Roy Franklin Stratton
University of Tennessee - Knoxville

To the Graduate Council:

I am submitting herewith a dissertation written by Roy Franklin Stratton entitled "The Infrared Spectrum of Formyl Fluoride." I have examined the final electronic copy of this dissertation for form and content and recommend that it be accepted in partial fulfillment of the requirements for the degree of Doctor of Philosophy, with a major in Physics.

Alvin H. Nielsen, Major Professor

We have read this dissertation and recommend its acceptance:

William H. Fletcher, Dewy W. Morgan, W. E. Deeds, Isabel H. Tipton

Accepted for the Council:

Carolyn R. Hodges

Vice Provost and Dean of the Graduate School

(Original signatures are on file with official student records.)

December 5, 1957

To the Graduate Council:

I am submitting herewith a thesis written by Roy Franklin Stratton entitled "The Infrared Spectrum of Formyl Fluoride." I recommend that it be accepted in partial fulfillment of the requirements for the degree of Doctor of Philosophy, with a major in Physics.

Major Professor

We have read this thesis and recommend its acceptance:

William H. Fletcher

Henry W. Morgan

W. E. Deeds

Dale H. Tapton

Accepted for the Council:

Dean of the Graduate School

THE INFRARED SPECTRUM OF FORMYL FLUORIDE

A THESIS

Submitted to
The Graduate Council
of
The University of Tennessee
in
Partial Fulfillment of the Requirements
for the degree of
Doctor of Philosophy

---

by

Roy Franklin Stratton

December 1957

ACKNOWLEDGEMENT

The author wishes to acknowledge his thanks to the Department of Physics of The University of Tennessee for the use of the infrared spectrometer and the materials used throughout this investigation. The author wishes, in particular, to express his sincere thanks to Mr. H. W. Morgan and Mr. P. A. Staats of Oak Ridge National Laboratory for having supplied the samples of HCOF and DCOF used throughout the work, and to Dr. Alvin H. Nielsen, who suggested the problem, for his guidance and encouragement throughout the course of the investigation. The financial assistance received from the Office of Ordnance Research under Contract No. DA 33-008 ORD-1166 is greatly appreciated. Finally, the author wishes to acknowledge with thanks the many persons who have contributed to the completion of this work.

TABLE OF CONTENTS

CHAPTER PAGE

LIST OF TABLES

TABLE PAGE

TABLE PAGE

LIST OF FIGURES

FIGURE PAGE

FIGURE PAGE

FIGURE PAGE

CHAPTER I

INTRODUCTION

History

Formyl fluoride, shown diagrammatically in Figure 1, is a relatively stable compound which was first reported by Nesmejanow and Kahn[1] in 1934, and later, independently, by Mashentsev[2] in 1946.

Morgan, Staats and Goldstein[3] have examined the vibrational spectra of formyl fluoride (HCOF) and deutro-formyl fluoride (DCOF) with a prism spectrometer between 500 cm^{-1} and 5000 cm^{-1} and by means of the Raman effect. They assigned wave numbers to the five planar vibrations, and made a tentative assignment for the out-of-plane vibration in DCOF. They also applied a normal coordinate analysis to the planar vibrations of HCOF and obtained a set of force constants which predicted the isotopic shift in DCOF reasonably well.

Some of the interatomic distances have been determined

---

[1] A. N. Nesmejanow and E. J. Kahn, Ber. 67B, 370 (1934).

[2] A. I. Mashentsev, J. Gen. Chem. (U.S.S.R.) 16, 203 (1946).

[3] H. W. Morgan, P. A. Staats, and J. H. Goldstein, J. Chem. Phys. 25, 337 (1956).

by Jones, Hedberg, and Schomaker[4] by electron diffraction methods. They obtained: (C-F) = 1.351 ±0.013 Å, (C=O) = 1.192 ±0.011 Å, (O ....F) = 2.225 ±0.019 Å, (C-F/C=O) = 1.134 ±0.005, and F-C=O angle = 121.9 ±0.9°.

Since our work was started it has been learned that Wilson[5] and Wilkinson have been working on the spectra of both molecules at the University of London with high dispersion at frequencies greater than about 1500 cm^{-1}.

More recently K. N. Rao[6] at the Ohio State University has observed the pure rotational spectrum of DCOF and is planning in the near future to study also the pure rotational spectrum of HCOF.

The Problem

The work of Morgan, Staats, and Goldstein indicated that it would be profitable to examine the spectra of HCOF and DCOF under high resolution in order to determine the moments of inertia, better values for the band centers and, perhaps, some of the anharmonic constants. Late in 1953 it

---

[4] M. E. Jones, K. Hedberg, and V. Shomaker, J. Amer. Chem. Soc. 77, 5278 (1955).

[5] M. Kent Wilson, private communication.

[6] K. N. Rao, private communication.

was decided to examine these molecules with the University of Tennessee high-resolution grating spectrometer. However, measurements were not actually begun until early in the spring of 1955.

It was originally planned that we would examine, and attempt to resolve, all of the bands reported by Morgan, Staats, and Goldstein. They observed eleven bands in HCOF, five of them fundamentals, and fifteen bands in DCOF, six of them fundamentals. The missing fundamental in HCOF is thought to be obscured by ν_4, which is very intense.

This plan was modified after we learned of the work of Wilson and Wilkinson. Even so, we measured all of the bands at wave numbers lower than 3000 cm^{-1}, as well as $2\nu_2$ in both molecules which lies at about 3500 cm^{-1}. There is some question about our measurement of $(\nu_3+\nu_4)$ in HCOF because it was the last band in HCOF to be examined. The sample is known to have been impure, and there was not a sufficient amount of the sample to obtain good absorption so the results were poor. While our results on some of the other bands were almost equally poor, some of the bands were very well resolved. The bands which were measured are discussed individually in a later chapter.

CHAPTER II

THEORY

According to quantum mechanics a molecule can have only certain discrete energy levels, and by the use of quantum mechanics we can write an equation describing these energy levels for any molecule. Unfortunately, these equations cannot be solved exactly. We are, therefore, forced to make approximations. For the purposes of infrared spectroscopy it is usually assumed that the Hamiltonian for a molecule may be written as the sum of an electronic Hamiltonian, the Hamiltonian for a non-rotating vibrator, and the Hamiltonian for a rigid rotator. With this approximation the wave equation separates into three equations so that the total energy, E, of the molecule is given by[1,2]:

$$E = E_e + E_v + E_r \qquad (1)$$

where E_e= the electronic energy,

E_v= the vibrational energy, and

E_r= the rotational energy.

These energies may be obtained from the three new and

---

[1] David M. Dennison, Rev. Mod. Phys. 3, 306f (1931).

[2] L. I. Schiff, Quantum Mechanics (McGraw-Hill Book Company, Inc., New York, 1949) p. 288.

simpler equations into which the original equation separates. Each of these three energies will be determined by specifying a set of one or more quantum numbers.

In this report we shall consider only the absorption spectra of HCOF and DCOF in the gaseous state in the infrared region. For a study of this type the gas being studied is at about room temperature, and, hence, essentially all of the molecules will be in the ground (lowest) electronic and vibrational state. Since the rotational energies of the molecule are of the same order as thermal energies there will be a distribution of rotational energies[3].

A molecule may absorb radiation if the radiation satisfies the Bohr frequency condition that

$$h\nu' = hc\nu = E_1 - E_2 \qquad (2)$$

where h = Planck's constant,

ν' = frequency of the radiation in sec^{-1},

ν = frequency of the radiation in cm^{-1},

E_1 and E_2 are energy levels of the molecule,

c is the speed of light,

and if the electric dipole transition probability between the states E_1 and E_2 is non-zero. The transition probability

---

[3] Gerhard Herzberg, Molecular Spectra and Molecular Structure II. Infrared and Raman Spectra of Polyatomic Molecules, (D. Van Nostrand Company, Inc., New York 1945) p. 29.

may be determined from quantum mechanics. Statistically speaking, the strength of absorption will depend on the magnitude of the transition probability and on the number of molecules in the initial state. Since the frequency of the radiation needed to induce a change in the electronic energy will (usually) be much higher than infrared frequencies, the electronic state will usually be the same and may be neglected in a study of infrared spectra.

We must now consider the rotation and vibration of the molecule and their interaction, which is not included in the above approximation. The interaction is taken into account by using perturbation methods. In general the correction terms due to this interaction are included by modifying the constants in the rotational terms.

Vibration

In general 3N coordinates are required to locate the N atoms of a molecule exactly in space. Three of these coordinates locate the center of mass of the molecule. These three coordinates contribute only to the translational energy of the molecule and do not concern us. This leaves 3N-3 coordinates to describe the rotation-vibration of the molecule. For a non-linear molecule three coordinates are needed to describe the rotation of the molecule, leaving 3N-6 coordinates to describe the vibration. There are,

therefore, 3N-6 vibrational degrees of freedom.

Classically, each of these 3N-6 degrees of freedom will be represented by a vibrational mode which, in general, may involve a motion of all N of the atoms. If these vibrations are described by ordinary Cartesian coordinates, each will usually involve all 3N of the original coordinates. However, by assuming small oscillations, and transforming to a special set of coordinates, called normal coordinates, each type of vibration may be described as a simple harmonic motion using only one of the 3N-6 normal coordinates. Only squared terms appear in the kinetic and potential energy if normal coordinates are used.

Assuming small oscillations and transforming to normal coordinates, we find that the vibrational part of the Schrödinger equation breaks into 3N-6 equations each of the form of the equation for the simple harmonic oscillator. Therefore, the total vibrational energy, E_v, of the molecule may be written as[4]:

$$E_v = \sum_i E_i = \sum_i hc\omega_i(v_i+\tfrac{1}{2}) \qquad v_i = 0, 1, 2, \text{---} \qquad (3)$$

where E_i = the energy of the i^{th} vibration,

h = Planck's constant,

ω_i = the frequency of the i^{th} vibration (cm^{-1}),

c = the speed of light, and

v_i = the quantum number of the i^{th} vibration.

---

[4]Herzberg, p. 77.

While the above is a good approximation, it is not quite right because the oscillations of a molecule are not sufficiently small, the potential is not strictly harmonic, and there are couplings between the vibrations. When these are taken into account the following equation is obtained[5]:

$$G(v_1,v_2,\text{--}) = \sum_i \omega_i (v_i+\tfrac{1}{2}) + \sum_{ij} x_{ij} (v_i+\tfrac{1}{2})(v_j+\tfrac{1}{2}) \qquad (4)$$

$$v_i = 0,\ 1,\ 2,\ \text{---}$$

where $G(v_1,v_2,\text{--})$ is the term value (energy level expressed in cm^{-1}) as a function of the quantum numbers v_i.

ω_i is the frequency of the i^{th} vibration in cm^{-1}, and

x_{ij} are the anharmonic constants.

Since the molecule is never in an energy state below the ground state, and since (almost) all of the energy transitions which interest us are measured from the ground state, it is convenient to consider only differences from the ground state. Therefore we define[5]:

$$G_o(v_1,v_2,\text{--}) = G(v_1,v_2,\text{--}) - G(0,0,\text{---},0) \qquad (5)$$

$$= \sum_i \omega_i^o v_i + \tfrac{1}{2}\sum_{ij} x_{ij}^o v_i v_j$$

where $\omega_i^o = \omega_i + \sum \frac{1}{2} x_{ij}$

$x_{ij}^o = x_{ij}$ as long as no powers higher than the second in v occur.

---

[5] Herzberg, p. 205 f.

Selection Rules

It has already been mentioned that a transition between states can be caused by radiation only if the transition probability is non-zero. The transition probability between two states, a and b, may be written as[6]:

$$\left[\int \Psi_a \vec{M} \Psi_b^* d\tau\right]^2 \qquad (6)$$

where Ψ_i is the complete wave function for the i^{th} state,

* indicates the complex conjugate,

$\vec{M}$ is the dipole moment,

and the integral is over all space, $d\tau$ being the element of volume.

For the approximation that we have made,

$$\Psi_i = \psi_e \psi_r \psi_v \qquad (7)$$

where ψ_e = the electronic wave function,

ψ_r = the rotational wave function,

ψ_v = the vibrational wave function,

and where the time dependence is ignored. In infrared spectroscopy the electronic wave function will be the same in the upper and lower state, and hence will contribute only a constant to the transition probability. For pure vibrational spectra, the same may be said of the rotational

---

[6] Herzberg, p. 252.

wave function, and the transition probability will be proportional to:

$$\left[\Psi_{v_1} \vec{M} \Psi_{v_2} \, d\tau'\right]^2 \qquad (8)$$

where v_1 is the wave function for the i^{th} vibrational level,

$\vec{M}$ is the dipole moment, and

$d\tau'$ is the new differential element of volume.

In order for this to be non-zero, at least one component of the integrand must be totally symmetric since the limits are symmetric[7].

In this particular case the molecules (HCOF and DCOF) are expected to have symmetry C_s [8] so that all of the vibrations are either symmetric, or antisymmetric with respect to reflection in the plane of the molecule, and, M_x and M_y are symmetric while M_z is antisymmetric[7]. Therefore, at least one component of the integrand will be symmetric for any pair of vibrational levels, and hence none of the fundamental, overtone, or combination bands are forbidden in the infrared. Naturally, not all possible combinations are observed since their transition probabilities may be very small. For a simple harmonic oscillator $\Delta v = \pm 1$; and, since the molecular vibrations are nearly harmonic, we would

---

[7] Herzberg, p. 252 f.

[8] H. W. Morgan, P. A. Staats, and J. H. Goldstein, J. Chem. Phys. 25, 337 (1956).

expect that the transition probability corresponding to $\Delta v = \pm 1$ would be much larger than any other.

Rotation

A molecule has three principle moments of inertia, usually referred to as I_a, I_b, and I_c, along three mutually perpendicular axes a, b, and c. Frequently these axes are chosen so that $I_a \leq I_b \leq I_c$.

HCOF and DCOF are accidentally nearly symmetric tops[9]. That is to say that two of their moments of inertia (I_b and I_c) are nearly equal; thus they are nearly symmetric rotors. We say that they are accidentally nearly symmetric tops because there are no symmetrical or structural reasons to cause one to expect that they would be nearly symmetrical before they are examined.

Classically the motion of a force-free symmetric top may be represented as a rotation about the symmetry axis together with a precession of this axis about the line of the total angular momentum[10]. The motion of a force-free asymmetric top may be represented as a rotation about the axis of the greatest or least moment of inertia together

---

[9] Morgan, Staats, and Goldstein.

[10] Herbert Goldstein, Classical Mechanics (Addison-Wesley Press Inc., Cambridge, Mass., 1951) p. 159f.

with a precession and nutation (of commensurable period) of this axis about the line of the total angular momentum[11]. The classical solution of the symmetric top case is simple, while the solution of the asymmetric top is rather complex, involving elliptic functions. The quantum mechanical situation is similar. Both tops have three degrees of freedom, but they both have only two constants of the motion; we would expect, therefore, that the energy, however complex, would involve only two quantum numbers[11].

The Asymmetric Top

To obtain a representation of the energy levels of an asymmetric top by quantitative formula would require fairly elaborate calculations. We might use the energy equation derived by Ray[12] for which tables have been compiled or we might use the relation derived by Wang[12,13]. Wang's equation is:

$$F(J_\tau) = \tfrac{1}{2}(B+C)J(J+1) + \left[A - \tfrac{1}{2}(B+C)\right] W_\tau \qquad (9)$$
$$= \overline{B}\, J(J+1) + (A-\overline{B})W_\tau$$

where $J = 0, 1, 2, \cdots$;

$F(J_\tau)$ is the term value in cm^{-1} corresponding to the τ^{th} sublevel of the J^{th} level;

---

[11] Dennison, p. 317.

[12] Herzberg, p. 46.

[13] S. C. Wang, Phys. Rev. 34, 243 (1929).

$A = h/8\pi cI_a$; $B = h/8\pi cI_b$; $C = h/8\pi cI_c$; $\bar{B} = \frac{1}{2}(B+C)$;

c is the speed of light.

The quantum number J corresponds to the classical total angular momentum. The τ's are numbers, without physical significance, which are used to order the sublevels; for the highest sublevel we set $\tau = J$, and for the lowest sublevel we set $\tau = -J$. Since there are 2J+1 sublevels, there are 2J+1 τ's. The sublevels are actually determined by the W_τ's which are also just numbers. In order to find the W_τ's one must solve a set of algebraic equations whose order increases linearly with J. Wang's equation seems to be the better for our purposes since it is I_b and I_c which are nearly equal in HCOF and DCOF. We will use an approximation, however, rather than solve the equations.

The Symmetric Top

While the derivation of an equation representing the energy levels of a symmetric top is not simple, the result may be quoted easily[14,15].

$$F(J,K) = BJ(J+1) + (A-B)K^2 \qquad (10)$$

where $J = 0,1,2,3,---$; $K = -J,--,0,1,--,+J$.

Here again J corresponds to the classical total angular momentum. K corresponds to the component of the angular

---

[14] Dennison, p. 306f.

[15] Herzberg, p. 24.

momentum along the (body-fixed) z-axis. I_b and I_c are equal. Since the energy depends on K^2, there will only be J+1 sublevels, although there are 2J+1 values of K.

The above equation describes a rigid symmetric top, but since molecules are not rigid, the change in molecular energy due to stretching has been taken into account by Slawsky and Dennison[16,17], who obtained the following:

$$G(J,K) = BJ(J+1) + (A-B)K^2 - D_J J^2(J+1)^2 - D_{JK} J(J+1)K^2 - D_K K^4, \quad (11)$$

where J, K, A, and B are defined above, and D_J, D_{JK}, and D_K are the centrifugal stretching constants.

It is obvious that the symmetric top approximation gives simpler expressions than that of the asymmetric top. Therefore, since HCOF and DCOF are nearly symmetrical, we shall use the symmetric top equation to approximate the energy levels of these molecules. Essentially we shall be using Wang's equation with the approximation that $W_\tau = K^2$.

Selection Rules

If a molecule has a permanent dipole moment, it will have a pure rotational spectrum. For a molecule with a component of its dipole moment along (parallel to) the

---

[16] Z. I. Slawsky and D. M. Dennison, J. Chem. Phys. 7, 509 (1939).

[17] Herzberg, p. 26.

unique axis, transitions are allowed for the following changes in the quantum numbers (selection rules)[18,19]:

$$\Delta K = 0;\ \Delta J = 0, \pm 1 \quad \text{if } K \neq 0; \tag{12}$$

$$\Delta K = 0;\ \Delta J = \pm 1 \quad \text{if } K = 0.$$

Naturally, for pure rotational absorption spectra $J = 0, -1$ have no meaning. For a molecule with a component of its dipole moment perpendicular to the unique axis (possible only for an accidentally symmetric top), the selection rules are:

$$\Delta K = \pm 1;\ \Delta J = 0, \pm 1, \tag{13}$$

where again transitions resulting in no change or in a decrease of energy have no meaning for pure rotational absorption spectrum.

Vibration-Rotation

In a real molecule, both rotational and vibrational transitions may take place together; hence, the rotational and vibrational energies must be considered together. If there were no interactions between rotation and vibration, the energy of the molecule (neglecting electronic energy) would be the sum of the vibrational and rotational energies:

$$T = G(v_1, v_2, --) + F(J,K). \tag{14}$$

---

[18] Dennison, p. 313.

[19] Herzberg, pp. 29,32.

We may retain this form and still account for the interaction between rotation and vibration if we consider the rotational constants, A and B, as having a particular value when the molecule is in a given vibrational state, which is the average value of A or B in that particular vibrational state. That is, we consider A and B as functions of the vibrational quantum numbers[20]:

$$A_v = A_e - \sum \alpha_i^A (v_i + \tfrac{1}{2} d_i) + \cdots \qquad (15)$$

$$B_v = B_e - \sum \alpha_i^B (v_i + \tfrac{1}{2} d_i) + \cdots$$

where A_e and B_e indicate the values in the equilibrium state, v_i are the vibrational quantum numbers, α_i^A and α_i^B are constants, and d_i is the degeneracy ($d_i = 1$ for HCOF and DCOF). We may then write:

$$T = G(v_1, v_2, \cdots) + F_v(J,K), \qquad (16)$$

with
$$F_v(J,K) = B_v J(J+1) + (A_v - B_v)K^2 - D_J^v J^2 (J+1)^2 \qquad (17)$$

$$- D_{JK}^v J(J+1)K^2 - D_K^v K^4,$$

where the D^v are small centrifugal stretching constants which may differ in different vibrational states. The above formulas are for a symmetric top molecule. It can be shown that the selection rules for rotation and vibration together are the same as they are separately (to a good approximation)[21].

---

[20] Herzberg, p. 400.

[21] Herzberg, p. 414.

The Appearance of Infrared Absorption Bands

That part of the infrared spectrum which interests us is that part between about 500 cm^{-1} and 5000 cm^{-1}. The spectrum in this region (for HCOF and DCOF at least) consists entirely of vibration-rotation bands. It will be advantageous, therefore, to examine the appearance of these bands.

For convenience we adopt the usual notation[22] that the initial state values be indicated by double primes (as A", B", J") and that the final state values be indicated by a single prime (as A', B', J'); the difference in the vibrational terms alone, the band origin, is indicated by ν_o cm^{-1}.

$$\nu_o = G(v_1', v_2', --) - G(v_1'', v_2'', --) = G' - G'' \qquad (18)$$

When there is a vibrational transition the rotational energy may increase, remain unchanged, or it may decrease. The rotational selection rules will depend on the direction of change of the dipole moment in the vibrational transition. If the vibrational transition results in a change in the component of the dipole moment parallel to the unique axis,

---

[22] Herzberg, pp. 19, 381.

the rotational selection rules will be those given in equation (12):

$$\Delta K = 0;\ \Delta J = 0, \pm 1 \quad \text{if } K \neq 0 \qquad (12)$$
$$\Delta K = 0;\ \Delta J = \pm 1 \quad \text{if } K = 0$$

and the resulting band will be a "parallel band." If the vibrational transition results in a change in the component of the dipole moment perpendicular to the unique axis, the rotational selection rules will be those given in equation (13):

$$\Delta K = \pm 1;\ \Delta J = 0, \pm 1, \qquad (13)$$

and the resulting band will be a "perpendicular band." These two types of bands are essentially different in appearance.

Parallel Bands[23]

A parallel band is observed to have three absorption maxima. The one on the low wave number side is called the P branch, the rather sharper one in the center is called the Q branch, and the one on the high wave number side is called the R branch. These three branches correspond to the allowed changes in J: $\Delta J = -1, 0, +1$ respectively. In a parallel band ΔK is always zero.

If one neglects the interaction between rotation and vibration, and also neglects the centrifugal stretching

---

[23]Herzberg, p. 416.

terms (the D's), one finds that the P and R branches are composed of a series of equally spaced lines. The frequencies corresponding to the branches are (from equations 11 and 14):

$$\text{P branch} \quad P_J = \nu_o - 2BJ \qquad J = 1,2,3,\cdots \qquad (19\text{-A})$$

$$\text{Q branch} \quad Q = \nu_o \qquad (19\text{-B})$$

$$\text{R branch} \quad R_J = \nu_o + 2B(J+1) \qquad J = 0,1,2,\cdots \qquad (19\text{-C})$$

where P_J and R_J stand for the lines originating from the transitions whose initial state has the rotational quantum number J. A line P_o is not possible since the P branch corresponds to $\Delta J = -1$.

With the above approximations the transitions from $J = J''$ in the ground state to $J = J'$ in the elevated state gives the same frequency regardless of the value of K, but when the interaction of vibration and rotation is included there is a different frequency for every $|K|$. Each "line" in the P and R branches will, therefore, consist of a series of lines; the separation for different K's is small, however, so that a series of discrete lines is still observed. The Q branch will also consist of a group of lines, close together; one line for ever value of J,K. The frequencies are now (inserting the D's also):

$$P_J = \nu_o + F'(J-1,K) - F''(J,K) \qquad (20\text{-A})$$

$$= \nu_o - (B'+B'')J + (B'-B'')J^2 + \left[(A'-B')-(A''-B'')\right]K^2$$
$$-D'_J(J-1)^2J^2 + D''_J(J+1)^2J^2 - D'_{JK}(J-1)JK^2$$
$$+D''_{JK}(J+1)JK^2 - (D'_K - D''_K)K^4$$

$$R_J = \nu_o + F'(J+1,K) - F''(J,K) \qquad (20\text{-}B)$$

$$= \nu_o + (3B'-B'')J + (B'-B'')J^2 + 2B'$$

$$+ \left[(A'-B')-(A''-B'')\right]K^2 - D'_J(J+1)^2(J+2)^2 + D''_J J^2(J+1)^2$$

$$- D'_{JK}(J+1)(J+2)K^2 + D''_{JK} J(J+1)K^2 + (D'_K - D''_K)K^4$$

and where the Q branch frequencies are $\nu_o + F(J,K)$ as given in equation (17) with every constant replaced with the difference in constants. Strictly speaking, P_J and R_J above should be written as $P_{J,K}$ and $R_{J,K}$, but, since the K's will be neglected in the analysis, this is not done.

If the experimentally determined lines had to be fitted directly to the above equations in order to determine the constants, a very great deal of work would be involved. The analysis is made much easier by the use of the following combination relations:

$$R_{J-1} - P_{J+1} = (2J+1)\left[2B'' - 4D''_J(J^2+J+1)\right], \qquad (21\text{-}A)$$

or

$$\frac{R_{J-1}-P_{J+1}}{2J+1} = 2B'' - 4D''_J(J^2+J+1); \qquad (21\text{-}B)$$

$$R_J - P_J = (2J+1)\left[2B' - 4D'_J(J^2+J+1)\right], \qquad (21\text{-}C)$$

or

$$\frac{R_J-P_J}{2J+1} = 2B' - 4D'_J(J^2+J+1); \qquad (21\text{-}D)$$

$$R_{J-1}+P_J = 2\left[\nu_o + (B'-B'')J^2 + \left\{(A'-B')-(A''-B'')\right\}K^2\right]. \qquad (21\text{-}E)$$

It has been assumed throughout that $D_{JK} = 0$; in equation

(21-E) it is also assumed that $D' = D''$. In the analysis it is usually assumed that the terms involving K may be neglected. In the analysis of a band equations (21-A) and (21-C) were used only to check the assignment. The intercepts of equations (21-B), (21-D), and (21-E) give B'', B', and ν_o; the slopes of these same equations give D''_J, D'_J, and $(B'-B'')$.

Perpendicular Bands[24]

A perpendicular band is considerably more complicated. Since it involves changes in both J and K, there are six possibilities: $\Delta K = \pm 1$; $\Delta J = -1, 0, +1$. If we again neglect the interaction of rotation and vibration and also neglect the D's, we may write (using equation 10):

$$\nu(\Delta K = +1, \Delta J = +1) = \nu_o + F(J+1, K+1) - F(J,K) \qquad (22\text{-A})$$
$$= \left[\nu_o + 2(A-B)(K+\tfrac{1}{2})\right] + 2B(J+1),$$

with $J = 0,1,2,\cdots$; $K = -J,\cdots,-1,0,+1,\cdots J$;

$$\nu(\Delta K = +1, \Delta J = 0) = \left[\nu_o + 2(A-B)(K+\tfrac{1}{2})\right], \qquad (22\text{-B})$$

with $J = 0,1,\cdots$; $K = -J,\cdots,+J$;

$$\nu(\Delta K = +1, \Delta J = -1) = \left[\nu_o + 2(A-B)(K+\tfrac{1}{2})\right] - 2BJ, \qquad (22\text{-C})$$

with $J = 1,2,3,\cdots$; $K = -J,\cdots,+J$;

$$\nu(\Delta K = -1, \Delta J = +1) = \left[\nu_o - 2(A-B)(K-\tfrac{1}{2})\right] + 2BJ(J+1), \qquad (22\text{-D})$$

with $J = 0,1,\cdots$; $K = -J,\cdots,J$;

---

[24] Herzberg, p. 424.

$$\nu(\Delta K = -1, \Delta J = 0) = \left[\nu_o - 2(A-B)(K-\tfrac{1}{2})\right], \qquad (22\text{-E})$$

with $J = 0,1,2,\cdots$; $K = -J+1, -J+2, \cdots, J$;

$$\nu(\Delta K = -1, \Delta J = -1) = \left[\nu_o - 2(A-B)(K-\tfrac{1}{2})\right] - 2BJ \qquad (22\text{-F})$$

with $J = 1,2,3,\cdots$; $K = -J+1, \cdots, J$.

An examination indicates that these are a series of sub-bands, each centered around a $\nu_{o,sub} = \nu_o \pm 2(A-B)(K \pm \tfrac{1}{2})$. It is stated in Herzberg (p. 424) that the P and R branches of such a sub-band are always of the same order of intensity (together) as the Q branch of the sub-band. Further, the lines of the P and R branches of different sub-bands do not coincide, and hence, these weak lines do not reinforce one another, but rather tend to form an unresolved "background." Therefore, in most cases, we need only consider the Q branches of the sub-bands:

$$\nu_{o,sub} = \nu_o \pm 2(A-B)(K \pm \tfrac{1}{2}). \qquad (23)$$

These Q branches or Q lines are usually referred to as $^{P}Q_{K}$ and $^{R}Q_{K}$, where the K indicates the initial state, $^{P}Q_{K}$ and $^{R}Q_{K}$ refer to the Q branches on the low and high wave number side of ν_o, respectively. If we now consider the interaction of rotation and vibration, we may write (still omitting the centrifugal stretching terms):

$$^{P}Q_{K} = \nu_o + (A'-B') - 2(A'-B')K + \left[(A'-B') - (A''-B'')\right]K^2, \qquad (24)$$

$$^{R}Q_{K} = \nu_o + (A'-B') + 2(A'-B')K + \left[(A'-B') - (A''-B'')\right]K^2. \qquad (25)$$

Again a great deal of work can be avoided by using the following combination relations (which do include the centrifugal stretching terms, except that D_{JK} is assumed to be zero):

$$R_{Q_{K-1}} - P_{Q_{K+1}} = 4K\left[(A''-B'') - D''_K(2K^2+2)\right] \qquad (26\text{-A})$$

or

$$\frac{R_{Q_{K-1}} - P_{Q_{K+1}}}{4K} = (A''-B'') - 2D''_K(K^2+1); \qquad (26\text{-B})$$

$$R_{Q_K} - P_{Q_K} = 4K\left[(A'-B') - D'_K(2K^2+2)\right], \qquad (26\text{-C})$$

or

$$\frac{R_{Q_K} - P_{Q_K}}{4K} = (A'-B') - 2D'_K(K^2+1); \qquad (26\text{-D})$$

$$R_{Q_{K-1}} + P_{Q_K} = 2\nu_o + 2(B'-B'')J(J+1) + \left[(A'-B')-(A''-B'')\right](2K^2-2K+1); \qquad (26\text{-E})$$

$$R_{Q_K} - P_{Q_K} = 2\nu_o + 2(B'-B'')J(J+1) + 2(A'-B') - 2D_K + \left[\{(A'-B')-(A''-B'')\} - 6D_K\right]2K^2. \qquad (26\text{-F})$$

In equations (26-E) and (26-F) it is assumed that $D'=D''$. Equations (26-A) and (26-C) were used only to check the assignment. The intercept of equations (26-B), (26-D), and (26-E) give $(A''-B'')$, $(A'-B')$, and ν_o; their slopes give D''_K, D'_K, and $\left[(A'-B')-(A''-B'')\right]$. Equation (26-F) was sometimes used to determine ν_o also. In analysis the terms in J were neglected.

Spectra of HCOF and DCOF

The dipole moments of HCOF and DCOF have components

along both the a and b axes, and a given vibration may result in a change in the components of the dipole moment along both axes. The observed absorption bands, therefore, often appear as a perpendicular band superposed over a parallel band. This gives one two equations to use in determining ν_o, but it tends to make the assignment of the lines in the parallel band more difficult.

Effects of Asymmetry

While we have treated HCOF and DCOF as symmetric tops, they are in reality asymmetric tops. We must consider, at least briefly, the justification for and the accuracy of this treatment.

In order to find the molecular constants using Wang's energy relation it is necessary to solve for the quantum number W_τ. But the W_τ's, themselves, depend on the molecular constants. The algebraic equations for W involve the constant $b = (C-B)/2\left[A-\frac{1}{2}(B+C)\right]$. These equations need not be solved if the approximation $W_\tau = K^2$ is used. The approximation does not appear to be too inaccurate, and serves as a useful ordering of the lines.

As a measure of the accuracy of the symmetric top approximation we may compare the W_τ's with the K^2's. If

we use the electron diffraction data mentioned earlier[25] and assume a C-H bond length of 1.08 Å, we find the results given in Table I. Using these values we can calculate the values of W_2. The calculated values of W are given in Table II for J = 0, 1, and 2. Comparison shows that K^2 is a fair approximation for W.

---

[25] M. E. Jones, K. Hedberg, and V. Schomaker, J. Amer. Chem. Soc. 77, 5278 (1955).

TABLE I

CALCULATED VALUES OF THE RECIPROCAL MOMENTS OF INERTIA

Moment	HCOF $_{cm^{-1}}^{-1}$	DCOF $_{cm^{-1}}^{-1}$
A	2.885	2.104
B	0.390	0.389
C	0.344	0.329
$\overline{B}$	0.367	0.359
b	-0.0175	-0.0338

TABLE II

CALCULATED VALUES OF W_τ

J	K	K^2	W_τ for HCOF	W_τ for DCOF	τ
0	0	0	0	0	0
1	0	0	0	0	-1
	-1	1	0.9825	0.9662	0
	+1	1	1.0175	1.0338	+1
2	0	0	-0.000918	-0.00342	-2
	-1	1	0.9475	0.8986	-1
	+1	1	1.0525	1.1014	0
	-2	4	4	4	+1
	2	4	4.000918	4.00342	+2

CHAPTER III

EXPERIMENTAL DETAILS

The Spectrometer

The spectra of HCOF and DCOF were observed and measured with the University of Tennessee automatically-recording grating spectrometer which has been described elsewhere by A. H. Nielsen[1]. Figure 2 is a ray diagram of the spectrometer. A Nernst glower was used as a source of continuous radiation. The cell containing the sample was placed near the focus between mirrors M-2 and M-3. The beam is chopped either just before or just after passing through slit S-1. Chopping modulates the beam at the frequency to which the amplifier is tuned. The beam is dispersed by a prism monochromator before passing through slit S-2 so that the grating sees only a narrow range of wave numbers, thus eliminating unwanted orders. After passing through slit S-2, the beam strikes an off-axis parabolic mirror, and is sent to the grating as a parallel beam. The light diffracted back in the direction of the paraboloid is sent through slit S-3 to the detector system. The output of the detector system is then amplified and fed into a

---

[1] A. H. Nielsen, J. Tenn. Acad, Sci. 22, 241 (1947).

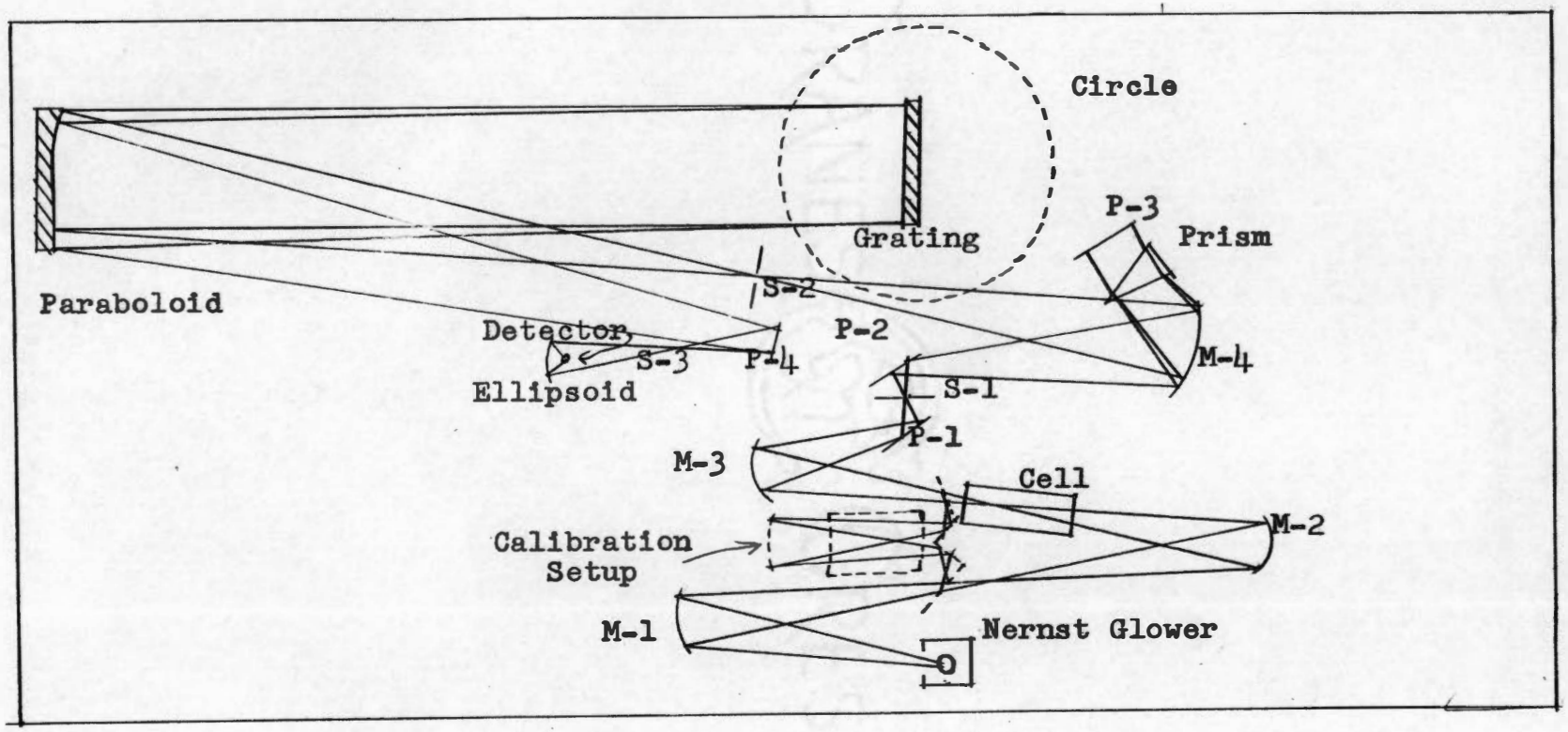

Figure 2. Ray diagram of the spectrometer

Leeds and Northrup, Type G, speedomax recorder.

Four detectors were used in the course of the work. They were a Perkin-Elmer thermocouple, and a Golay detector (both of which are sensitive throughout the entire spectral range considered here), a lead sulfide photoconductive cell (sensitive above about 3300 cm^{-1}), and a cooled lead telluride photoconductive cell (sensitive above about 1900 cm^{-1}, and used to about 3800 cm^{-1}). The energy from slit S-3 was focused on the thermocouple, the lead sulfide cell, and sometimes on the Golay detector by an elliptical mirror with the slit at one focus, and the detector at the other focus. The lead telluride cell was installed in a box with its own mirror system. At the beginning of the work reported here a silver chloride lens was used to focus the radiation from slit S-3 onto the Golay detector.

Five gratings were used. They were: a 1200 lines-per-inch original ruled at the University of Michigan, a 3600 lines-per-inch replica by R. W. Wood, 4500 lines-per-inch and 7500 lines-per-inch Bausch and Lomb replicas, and a 15,000 lines-per-inch Bausch and Lomb original.

The prism monochromator, which consisted of a 15° KBr prism, a 15° NaCl prism, or a 60° NaCl prism, allowed only a narrow band of frequencies to reach the grating. It was necessary to reset the prism during the recording of a

band (except at the high wave number limit of a prism); with practice this adjustment could be made so as to be undetectable on the finished record.

All of the detectors, except the lead telluride cell, used a 13 cycle-per-second half disk chopper immediately after slit S-1. The lead telluride cell used an 800 cycles-per-second chopper; in this case the plane mirror P-1 was replaced with a plane mirror which was forced to oscillate about a vertical axis at 400 cycles per second. The amplitude of the oscillations could be controlled.

The grating and a Gaertner circle were mounted on a motor driven shaft. The position of the circle, and hence of the grating, can be read to 5 seconds of arc by means of a micrometer microscope. These angles were marked directly onto the chart paper, at intervals of one minute of arc on records that were to be measured, by a pen activated by a manually operated solenoid.

Atmospheric Absorption

The spectrometer has an air tight sheet metal cover which fits into a slot around the base of the spectrometer. Apiezon (type Q) wax is packed into this slot, and into any other openings. Once the spectrometer is sealed, it is only necessary to remove the water and carbon dioxide

already inside of the spectrometer.

To some extent this may be accomplished by flushing the spectrometer with dry nitrogen from a cylinder. This was often done.

Originally trays of P_2O_5 and Ascarite were placed on the floor of the spectrometer to remove the H_2O and CO_2 respectively. This method works rather well, especially when coupled with N_2 flushing.

Later the air inside the spectrometer was re-cycled continuously through a column of activated alumina by means of a small centrifugal blower. By changing to a fresh column frequently at the start it was possible to obtain a very low background even in regions of strong atmospheric absorption. At times trays of P_2O_5 and Ascarite were used in conjunction with this method; the results were no better than could be obtained without the chemicals. A background record was made for every band, for comparison.

The Gas

The samples of HCOF and DCOF used in this study, together with a great deal of useful information about handling these compounds, were very kindly supplied by H. W. Morgan, and P. A. Staats of the Oak Ridge National Laboratory. As the properties of HCOF and DCOF are virtually identical (with regard to handling), only HCOF will be dis-

cussed.

HCOF is a relatively stable compound which boils at about -26°C, decomposes into HF and CO in the absence of water, and hydrolyzes to formic acid (H_2CO_2) and HF. At room temperature a container of the gas decomposes completely in about 24 hours, but at dry ice temperatures (-78°C) it can be (and was) stored in the liquid phase for months without excessive decomposition.

For the absorption spectrum of HCOF, the gas was put into a glass cell 15 cm long and about 2 inches in diameter, closed with either NaCl or KBr windows. The pressure used varied from about 1 mm to about 500 mm of mercury. Because of decomposition, it was necessary to remove the gas from the cell at the end of each day's work. Otherwise, the sample would decompose and attack the cell, especially the windows. Since HCOF has a vapor pressure of 2 or 3 cm of mercury even at -78°C, it was not found practical to save the sample after a run; it was pumped into the air.

It was necessary to seal the spectrometer to be able to eliminate atmospheric absorption. Thus it was necessary to be able to fill the cell with the spectrometer sealed. In order to do this a glass tube was run through the base of the spectrometer from the sample storage tube to the absorption cell inside of the spectrometer.

The decomposition of the sample resulted in CO and

CO_2 being present in the absorption cell as an internal background when some of the bands were examined. The CO resulted directly from decomposition; the CO_2 resulted from oxidization of some of the CO by oxygen in the air that leaked into the container over a long period of time. No absorption due to HF was observed since this gas reacted with the glass of the system soon after it was formed. It was possible to remove most of the CO and CO_2 by pumping on the sample while it was at dry ice temperatures. There was a considerable loss of HCOF in this case. The CO_2 did not present a problem except in samples that had been stored for a relatively long time, and then only in one band of DCOF (the high wave number side of the R branch of ν_1). The decomposition could be observed directly by noting the increase in the absorption of CO if several runs were made over this region at intervals of several hours.

The particular grating, detector, gas pressure, and background conditions for each band are given in Table III.

Wave Number Measurements

The final result of a run over a band was a strip of chart paper with a continuously drawn graph of absorption versus angle (and hence, indirectly, wave number). The fiducial marks were spaced at intervals of one minute of arc. A pencil line was drawn from the absorption peak to the base

line, and the angle was read with a special eyepiece, since the fiducial marks were not always equally spaced. The difference between the recorded angle and the angle of the central image was designated the angle θ, used to calculate the wave number. The central image, i.e., the position in which the grating acted as a reflecting mirror, was recorded several times before and after each band. The wave number was determined by the equation

$$\nu\ (cm^{-1}) = nK/\sin\theta,$$

where n is the order, K (cm^{-1}) is the instrument constant, and θ is the angle.

Calibration

To find the wave number of a particular peak, it was necessary to know the grating or instrument constant, K. This could be found by finding the angle corresponding to a known frequency. Any absorption or emission lines whose frequencies are accurately known could have been used. In this investigation the fundamental[2] and first overtone[3] of carbon monoxide were used. At the beginning of each run four

---

[2]E. K. Plyler, L. R. Blaine, and W. S. Conner, J. Opt. Soc. Am. 45, 104 (1955).

[3]E. K. Plyler, W. S. Benedict, and S. Silverman, J. Chem. Phys. 20, 180 (1952).

to six lines from the center of one of these bands were recorded. This allowed the calculation of the grating constant for that particular run. The variations of the grating constant were small, but significant.

This work was done in air, while the wave numbers of the CO lines were vacuum wave numbers. If the value of the index of refraction of air does not vary from the wave number of the CO lines to that of the band being measured, the results will automatically be reduced to vacuum. Calculations from a formula given by Edlen[4] indicate that the index of refraction of air changes by about 7 parts in 10^8 from 4.5 microns to 15 microns, which may be neglected. Therefore it was unnecessary to correct the wave numbers, as they were already vacuum wave numbers.

For low wave numbers it was necessary to use the CO in second or third order. The fundamental was used with all bands below 3000 cm^{-1}, and the overtone with both bands over 3000 cm^{-1}.

The cell containing the CO was usually placed in the spectrometer between the sample cell and the mirror M-3. It was mounted on a shaft so that it could be lowered out of the beam during a run. A few times a special mirror system, shown in Figure 2, was used. In that case it was the mirrors which were moved out of the beam.

---

[4] B. Edlen, J. Opt. Soc. Am. 43, 339 (1953).

Discussion of Errors

Any error in the determination of the wave number of an absorption peak must result from error in either the angle, θ, or from error in calibration, or from both.

Except for errors in the circular scale, which are small, errors in the angle θ will be random errors and will arise from errors in placing the fiducial marks, errors in marking the lines, and errors in reading the angle. The latter can easily be done to $\pm\frac{1}{2}$ second of arc. The errors in placing the fiducial marks should be rather uniform, but errors in marking the lines will depend on the sharpness of the line. Where about six central images were recorded, the average deviation was about ± 2 seconds of arc. Where about three records were made of a sharp absorption line, the average deviation was about ± 4 seconds of arc (as determined from ν_1 in HCOF). When the absorption peaks were not sharp, the deviations were larger.

Errors in the calibration will result from errors in the angle of the central image, errors in the circle angle of the calibration lines, errors in the calibration lines themselves, and from changes of the grating constant with time and angle. It is difficult to estimate these errors, but when the same band has been recorded using two different gratings, the results have, on the average, agreed to within 0.2 cm^{-1} or better.

The molecular constants, other than ν_0, depend on differences between the lines, and systematic error will not affect them, while random error will. The results indicate that the values of B" are accurate to about ± 0.001 cm^{-1}, and that A"-B" is accurate to about ± 0.005 cm^{-1}.

CHAPTER IV

EXPERIMENTAL RESULTS AND ANALYSIS

Introduction and Methods of Analysis

The observed bands and their interpretations are presented in this chapter with corresponding bands of HCOF and DCOF being presented together. Tables III and IV give a summary of the observed bands and the conditions under which they were observed. The figures depicting observed bands were taken from intermediate speed records made at six degrees per hour with fiducial marks every ten to twenty minutes of arc.

Every band reported here was observed at least three times at one degree per hour, which was the normal speed for records which were to be measured. Quite often more than three records were made. The circle angles of a given absorption peak were then averaged and subtracted from the average central image. From this the wave number was calculated. The same method was used for both the calibration lines and the lines being measured, except that for the calibration lines it was the grating constant rather than the wave number which was found. This method was quicker than, and gave the same results as, the method in which the angle θ is obtained for each record of a given peak and then averaged.

TABLE III

A SUMMARY OF THE OBSERVED BANDS AND THE CONDITIONS OF OBSERVATION
HCOF

Assignment	Band Center[a] (cm^{-1})	Type[b]	Grating Lines/Inch	Detector[c]	Pressure cm of Mercury	Slit Width (cm^{-1})	Background Conditions	Remarks
ν_1	2981.0	hybrid	7500	PbTe	5.0	0.25	water in R branch quickly removed	
ν_2	1836.9	hybrid	4500 7500	Golay	0.4-0.8	0.4 0.35	water largely removed	perpendicular component observed only in R branch; best results with about 6 cm pressure
ν_3	1342.5	⊥	3600 4500	Golay	26-45	0.4	water greatly reduced	very weak
ν_4	1064.8	hybrid	3600	Golay	0.2-0.3	0.3	clean	
ν_5	662.5	hybrid	1200	Golay T.C.	2.8-4.6	0.45 0.75	CO_2 almost completely removed	parallel component not resolved
$2\nu_2$	3651.8	∥	15000	PbS	10.0	0.15	H_2O and CO_2 partly removed	

TABLE III (continued)

A SUMMARY OF THE OBSERVED BANDS AND THE CONDITIONS OF OBSERVATION
HCOF

Assignment	Band Center[a] (cm^{-1})	Type[b]	Grating Lines / Inch	Detector[c]	Pressure cm of Mercury	Slit Width (cm^{-1})	Background Conditions	Remarks
$2\nu_4$	2115.6	∥	7500	PbTe	5.0-6.5	0.15	CO in R branch sometimes	
$\nu_3+\nu_4$	2412	-	7500	PbTe	32	0.2	CO on low wave number edge	very poor results
$\nu_4+\nu_5$	1719.3	∥	7500	Golay	9.0	0.3	not all water removed	partly resolved

[a]The quoted band center is the estimated band center, except where combination relations were applied to the band; in that case the results quoted are the result of the combination relations.

[b]Parallel bands are designated ∥; perpendicular bands are designated ⊥.

[c]PbS indicates the lead sulfide photoconductive cell; PbTe indicates the lead telluride photoconductive cell; T.C. indicates the thermocouple.

TABLE IV

A SUMMARY OF THE OBSERVED BANDS AND THE CONDITIONS OF OBSERVATION
DCOF

Assignment	Band Center[a] (cm^{-1})	Type[b]	Grating Lines / Inch	Detector[c]	Pressure cm of Mercury	Slit Width (cm^{-1})	Background Conditions	Remarks
ν_1	2261.7	hybrid	7500	PbTe	3.8-5.5	0.15	CO_2 at edge of R branch	
ν_2	1796.8	‖	7500 (4500)	Golay (T.C.)	1.2-2.0	0.4 (0.7)	water largely removed	unresolved with 4500 lines per inch grating
ν_3	967.9	hybrid	3600	Golay	2.2	0.4	clean	
ν_4	1073.2	hybrid	3600	Golay	0.4-0.7	0.3	clean	
ν_5	657.5	hybrid	1200	Golay T.C.	4.0-8.0	0.45 0.75	CO_2 almost completely removed	parallel component not resolved
ν_6	857.4	-	3600	Golay	10.2	0.25	clean	
$2\nu_2$	3579.4	‖	15000	PbTe	3.5	0.25	water and CO_2 removed; clean	
$2\nu_3$	1930.6	‖	7500	PbTe	15-20	0.2	clean	

TABLE IV (continued)

A SUMMARY OF THE OBSERVED BANDS AND THE CONDITIONS OF OBSERVATION
DCOF

Assignment	Band Center[a] (cm^{-1})	Type[b]	Grating Lines / Inch	Detector[c]	Pressure cm of Mercury	Slit Width (cm^{-1})	Background Conditions	Remarks
$2\nu_4$	2137.8	∥	7500	PbTe	7.5	0.15	CO in R branch	
$\nu_3+\nu_4$	2028.6	hybrid	7500	PbTe	23.0	0.2	clean	parallel unresolved
$\nu_3+\nu_5$	1624.5	hybrid?	4500	Golay	45.0	0.4	water reduced but still excessive	unresolved
$\nu_4+\nu_5$	1705.8	∥	7500	Golay	4.5	0.4	water reduced	
$\nu_4+\nu_6$	1928.4	-	7500	PbTe	15-20	0.2	clean	central Q branch only

[a]The quoted band center is the estimated band center, except where combination relations were applied to the band; in that case the results quoted are the result of the combination relations.

[b]Parallel bands are designated ∥; perpendicular bands are designated ⊥.

[c]PbTe indicates the lead telluride photoconductive cell; T.C. indicates the thermocouple.

After the wave numbers were obtained, it was necessary to assign an initial quantum state to each absorption peak. In most cases the wave numbers were plotted against a running number so as to give an approximately straight line. Then a center was chosen, thus automatically assigning all of the absorption peaks. The center was picked by noting the position and shape of the central Q branch, by the shape of the band in general, and by the intensity of nearby lines. For a perpendicular band the band center must lie halfway between two of the running numbers, and for a parallel band the band center must lie on one of the running numbers. Because of the relatively wide spacing of the Q lines in formyl fluoride, the center was rather easy to choose for a perpendicular band, so that if a perpendicular component were present it was assigned and analyzed before the parallel component. Where only a parallel component was present, the assignment of a band center was more difficult. The presence of strong Q lines tended to make the assignment of the lines of the parallel component more difficult, however, since each Q line obscures one or two lines of the parallel component. One way to check the assignment was to plot $R_{Q_{K-1}}-P_{Q_{K+1}}$ or $R_{Q_K}-P_{Q_K}$ versus K for a perpendicular component and $R_{J-1}-P_{J+1}$ or R_J-P_J versus 2J+1 for a parallel component. If the assignment were correct, the result would be a straight line passing through the origin. The slope would

be 4(A-B) for a perpendicular component and 2B for a parallel component. Unfortunately, any of a series of assignments will always meet these conditions. In addition, those lines nearest to the band center often deviate from a straight line more than those lines farther from the band center.

After a seemingly satisfactory assignment was made the lines were listed in a table. The sums and differences used in the combination relations were listed also if the band was to be analyzed. When the combination relations were plotted, they served as a check on the assignment. The molecular constants were obtained from either the graphs of the combination relations or from a least squares treatment in most cases.

In plotting $(R_{J-1}-P_{J+1})/2J+1$ and $(R_J-P_J)/2J+1$ versus (J^2+J+1), the slope was approximately zero, so that the average value was often used instead of the intercept. This was more accurate than the drawn intercept, much easier, and only slightly less accurate than a least squares treatment.

The line positions quoted in the tables are given to two decimal places even though the errors for some bands are thought to be about ± 0.2 cm^{-1} or perhaps more. This is done because it is thought that the errors in the spacings between lines of a given band are about 0.08 cm^{-1} or less on the average.

With the exception of $\nu_4+\nu_6$ in DCOF, which was not

reported by Morgan, Staats, and Goldstein[1], the assignments reported in their paper have been found to be in agreement with our work, and are accepted as correct.

The Fundamentals

ν_1

By reference to Figure 1, one might expect that the vibration associated with the C-H stretch would result only in a change of the dipole moment perpendicular to the a axis, the "almost unique" axis, and hence would be associated with a perpendicular band. However, the only observed bands which can reasonably be assigned to the C-H stretching vibration are hybrid bands at 2981 cm^{-1} in HCOF and 2262 cm^{-1} in DCOF. The parallel and perpendicular components appear to have about equal intensities and are both well resolved. Figures 3 and 4 show these bands.

HCOF. When the wave numbers of the Q lines were plotted against a running number, they lay very close to a straight line after two of the Q lines were dropped. The assignment of the remaining Q lines was straightforward, and the constants obtained seemed to be satisfactory. The two unassigned Q lines lie at 2970.71 cm^{-1} (between $^PQ_2$ and $^PQ_3$)

---

[1] H. W. Morgan, P. A. Staats, and J. H. Goldstein, J. Chem. Phys. 25, 337 (1956).

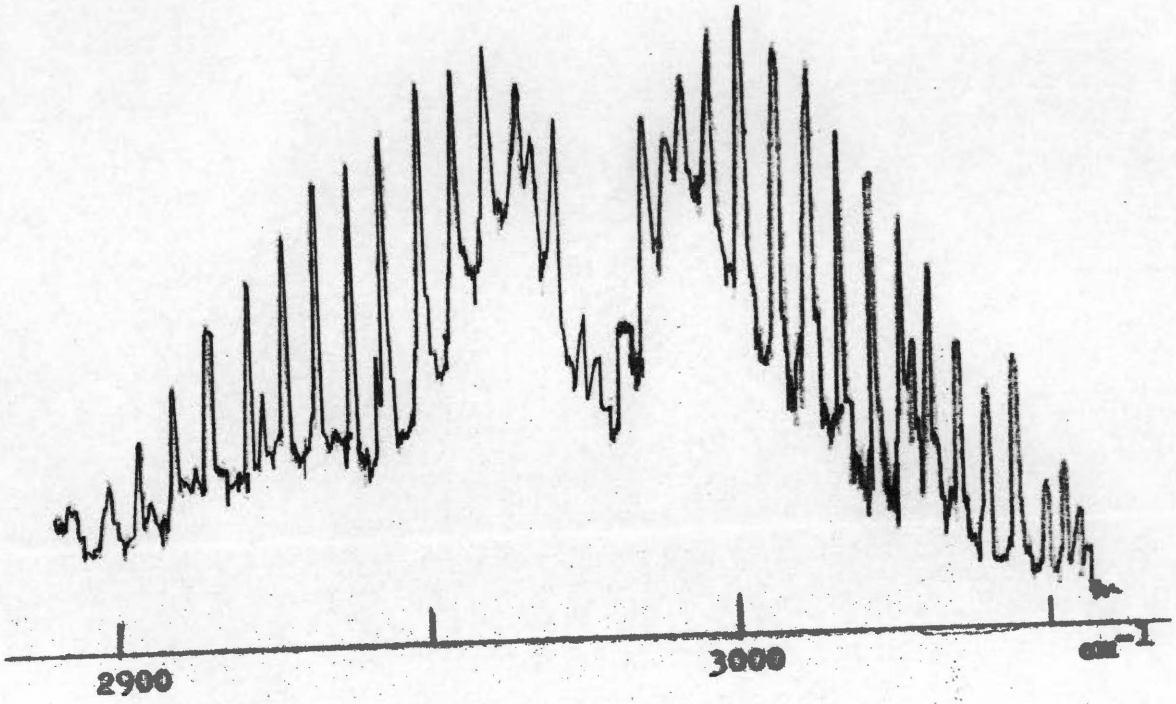

Figure 3. The ν_1 vibration-rotation band of HCOF

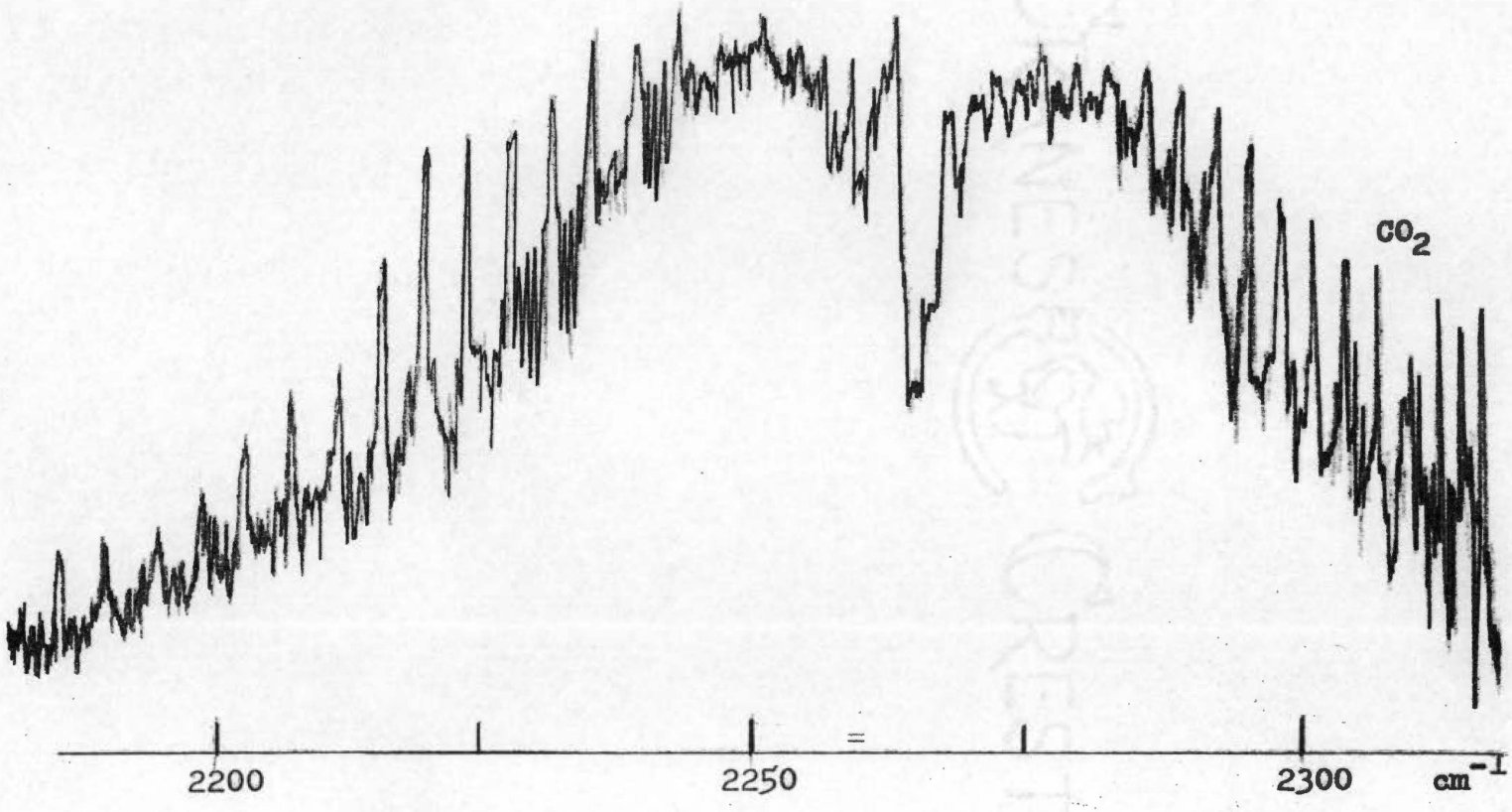

Figure 4. The ν_1 vibration-rotation band of DCOF

and 2991.13 cm^{-1} (between $^{R}Q_1$ and $^{R}Q_2$). The average of these two lines (2980.92 cm^{-1}) lies between the values of ν_o as determined from the parallel and perpendicular components of the band and only 0.13 cm^{-1} from their average.

The parallel component does not have a strong central Q branch; a relatively weak absorption line at 2980.77 cm^{-1} was tentatively assigned as being the Q branch. Assignment of the lines of the parallel component would have been expected to be more difficult because of the interruption of the Q lines. The assignment was straightforward, however.

Tables V and VI list the observed lines and their assignments for the parallel and perpendicular components, respectively. Figures 5 and 6 are graphs of the combination relations for the parallel component, and Figures 7 and 8 are graphs of the combination relations for the perpendicular component.

DCOF. Assignment of the perpendicular component was unambiguous and left no unassigned lines.

Assignment of the parallel component was, however, difficult, and was made by comparing calculated line positions with observed lines. The first assignment, which seemed to be the most natural, resulted in a B value which was much too small. The final assignment seems to be quite satisfactory and does not appear to be forced or artificial.

It must be pointed out that the lines P(3) and P(4)

TABLE V

WAVE NUMBERS OF THE OBSERVED LINES OF THE PARALLEL COMPONENT OF ν_1 OF HCOF

J	R(J) (cm^{-1})	P(J) (cm^{-1})
0	2981.61	-
1	2982.36	-
2	2983.43	2979.80
3	-	2978.88
4	-	-
5	2985.04	2977.35
6	2986.06	2976.21
7	2986.89	2975.47
8	-	-
9	-	-
10	2988.88	2973.30
11	2989.86	2972.93
12	2990.56	2972.21
13	2991.66	2971.62
14	2992.13	-
15	2992.83	2969.95
16	2993.41	2969.16
17	-	2968.35
18	2994.86	-
19	2995.72	2967.36
20	2996.47	2966.56
21	2996.95	2965.84
22	2997.88	2965.08
23	2998.91	2964.25
24	-	2963.20
25	-	-
26	3000.62	-
27	3001.53	2961.07
28	3002.16	2960.14
29	3002.56	2959.39

TABLE V (continued)

WAVE NUMBERS OF THE OBSERVED LINES OF THE PARALLEL COMPONENT OF ν_1 OF HCOF

J	R(J) (cm^{-1})	P(J) (cm^{-1})
30	3003.10	2958.34
31	-	2957.63
32	-	-
33	3005.34	2956.53
34	3005.93	2955.93
35	3006.61	2955.10
36	3007.62	2954.44
37	3008.54	2953.62
38	-	2952.84
39	-	-
40	3010.54	-
41	3011.38	2950.68
42	3012.19	2949.93
43	3012.75	2949.06
44	3013.77	2948.26
45	-	2947.22
46	-	2946.81
47	3016.04	-
48	3016.65	-
49	3017.34	2944.78
50	3017.90	2944.23
51	3018.64	2943.46
52	-	2942.88
53	-	2942.28
54	3020.74	2941.15
55	3021.53	-
56	3022.48	2939.56
57	3023.22	2938.80
58	3023.97	2938.17
59	-	2937.28

TABLE V (continued)

WAVE NUMBERS OF THE OBSERVED LINES OF THE PARALLEL COMPONENT OF ν_1 OF HCOF

J	R(J) (cm^{-1})	P(J) (cm^{-1})
60	-	2936.61
61	3026.12	2935.96
62	3026.90	-
63	3027.59	-
64	3028.34	2933.90
65	3029.11	2933.12
66	-	2932.21
67	3030.66	2931.28
68	3031.43	2930.63
69	3032.13	2929.97
70	3032.77	-
71	3033.32	2928.35
72	3034.14	2927.80
73	-	2926.97
74	3035.36	2925.99
75	3036.06	2925.19
76	3036.71	2924.71
77	3037.56	-
78	3038.37	2923.17
79	3039.12	2922.32
80	-	2921.63
81	3040.47	2920.84
82	3041.30	2920.14
83	3042.00	2919.43
84	3042.52	-
85	3043.12	-
86	3043.64	-
87	-	2916.83
88	3045.76	2915.68
89	3046.33	2915.04

TABLE V (continued)

WAVE NUMBERS OF THE OBSERVED LINES OF THE PARALLEL COMPONENT OF ν_1 OF HCOF

J	R(J) (cm^{-1})	P(J) (cm^{-1})
90	3047.19	2914.52
91	3047.98	2913.89
92	-	-
93	-	-
94	3049.62	-
95	3050.51	-
96	3051.22	-

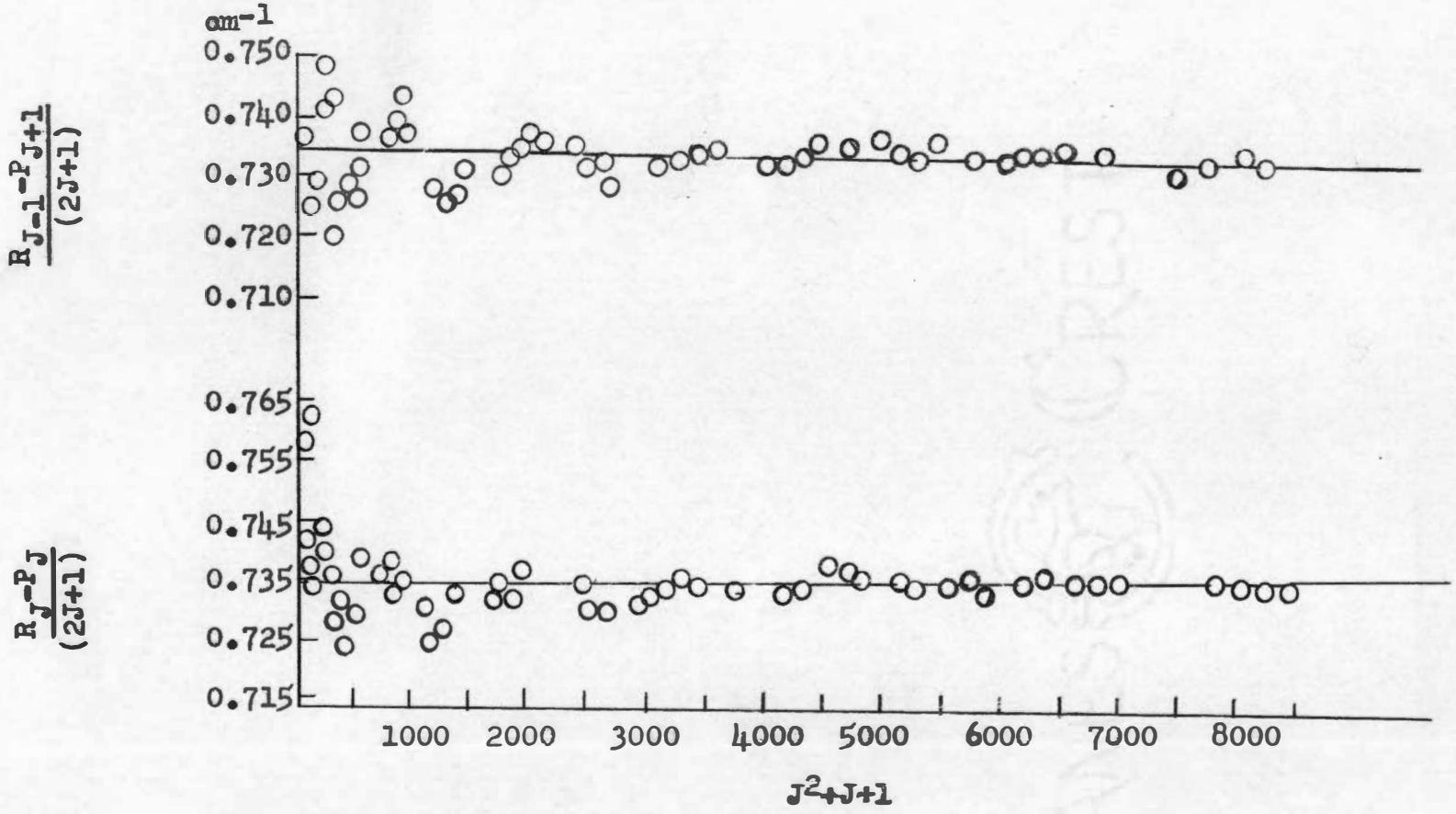

Figure 5. A plot of $(R_{J-1}-P_{J+1})/(2J+1)$ and $(R_J-P_J)/(2J+1)$ versus (J^2+J+1) for the parallel component of ν_1 of HCOF

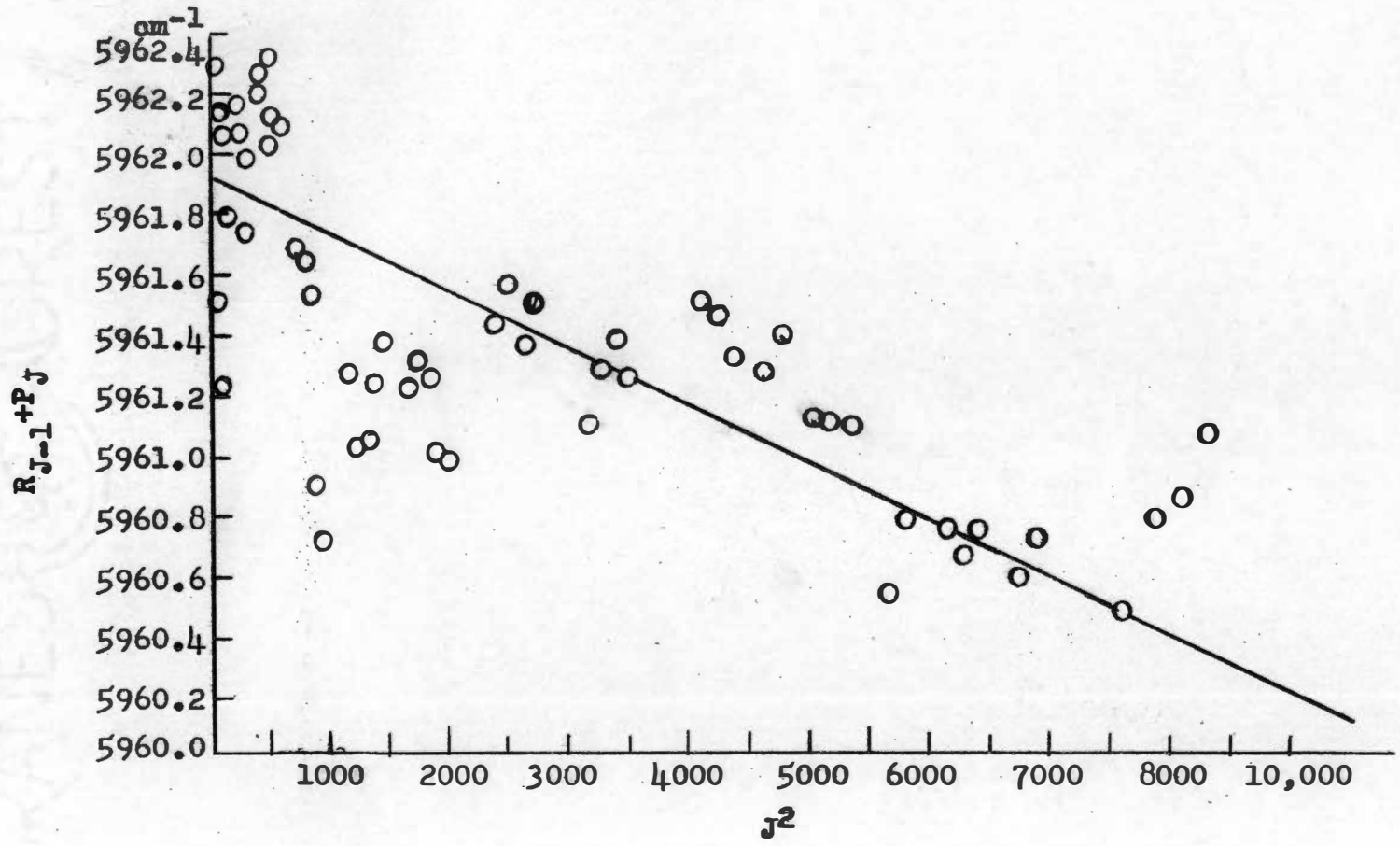

Figure 6. A plot of $(R_{J-1}+P_J)$ versus J^2 for the parallel component of ν_1 of HCOF

TABLE VI

WAVE NUMBERS OF THE OBSERVED Q LINES IN ν_1 OF HCOF

K	$^{R}Q_{K}$ (cm^{-1})	$^{P}Q_{K}$ (cm^{-1})
0	2984.32	-
1	2987.78	2978.19
2	2994.21	2974.06
3	2999.67	2967.86
4	3004.43	2962.37
5	3009.75	2957.14
6	3014.97	2951.65
7	3019.74	2945.80
8	3025.02	2940.64
9	3030.06	2934.98
10	3034.71	2929.23
11	3039.64	2923.90
12	3044.61	2918.23
13	3049.02	2912.92
14	3053.66	2907.16
15	3058.31	2901.46
16	3062.82	-

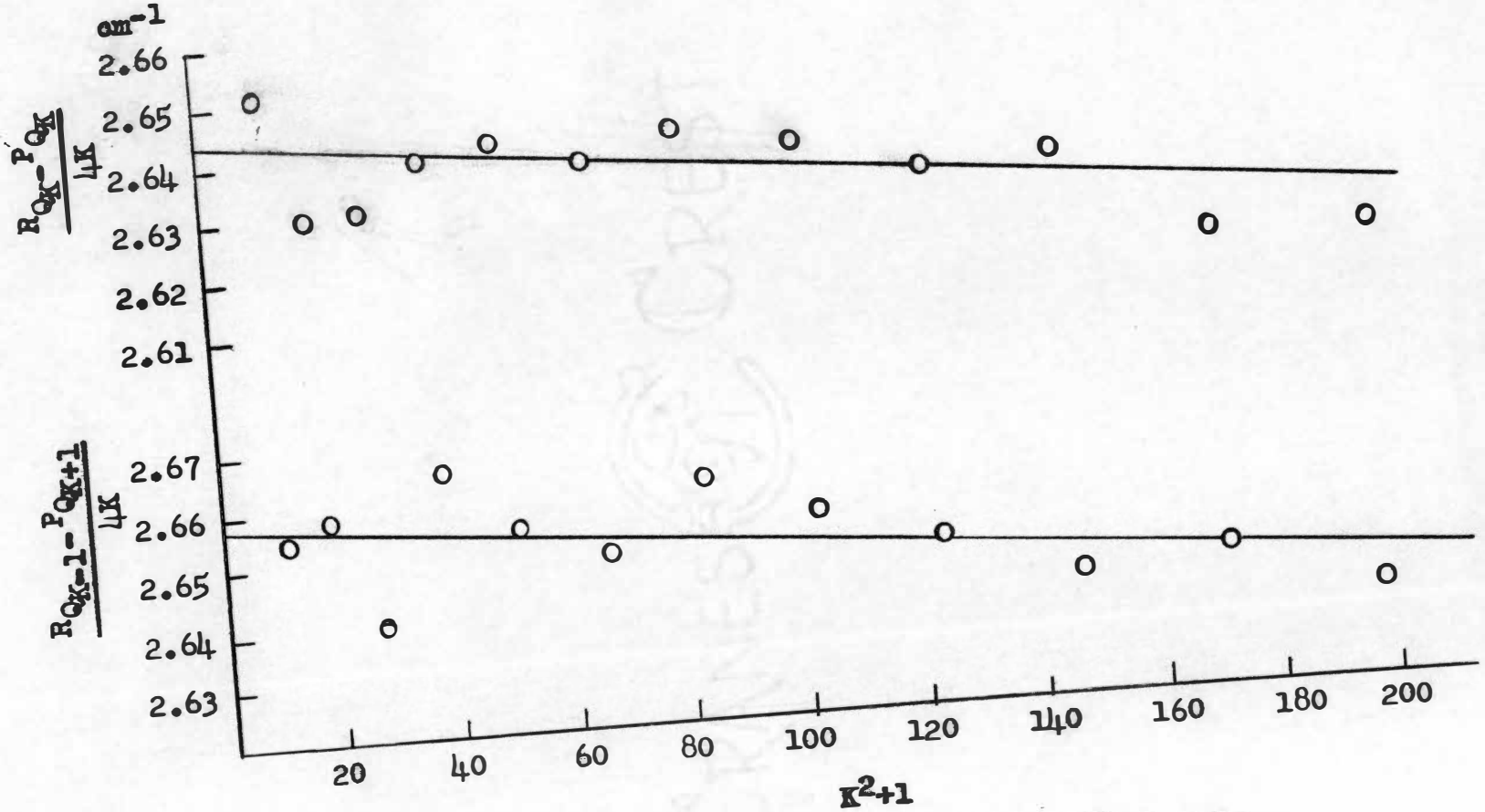

Figure 7. A plot of $(R_{Q_K}-P_{Q_K})/4K$ and $(R_{Q_{K-1}}-P_{Q_{K+1}})/4K$ versus K^2+1 for the Q lines of ν_1 of $HCOF^{18}$

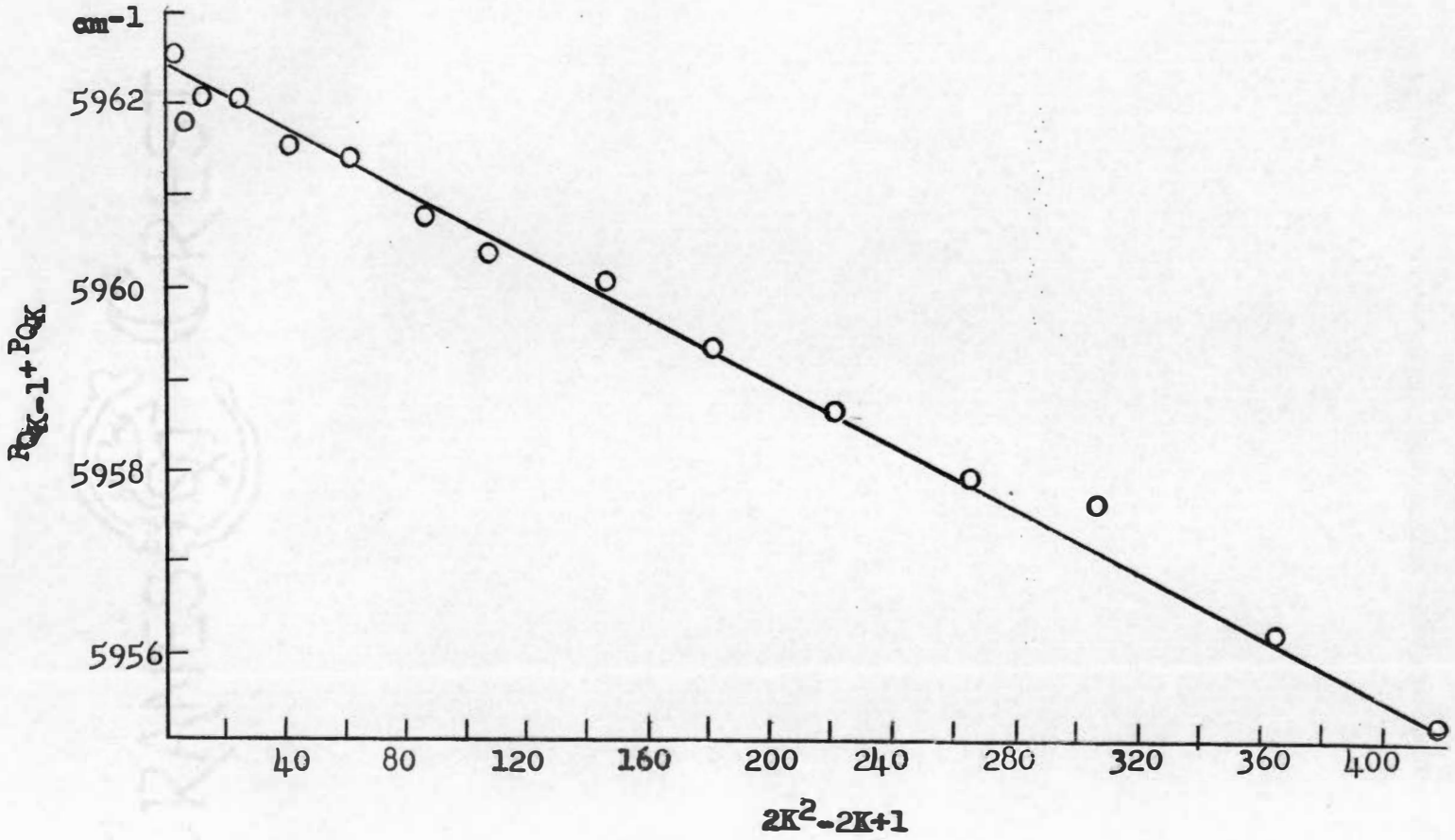

Figure 8. A plot of $(R_{Q_{K-1}}+P_{Q_K})$ versus $(2K^2-2K+1)$ for the Q lines of ν_1 of HCOF

actually appear to be double in all of the records that show them. P(3) at 2259.69 cm^{-1} is made up of lines at 2259.81 cm^{-1} and 2259.57 cm^{-1}. P(4) at 2258.96 cm^{-1} is composed of lines at 2259.15 cm^{-1} and 2258.78 cm^{-1}.

Tables VII and VIII list the observed lines and their assignments for the parallel and perpendicular components, respectively. Figures 9 and 10, and 11 and 12 are graphs of the combination relations of the parallel and perpendicular components, respectively.

ν_2

The C=O stretching vibrations of both molecules appear as ordinary parallel-type bands. Figures 13 and 14 show ν_2 for HCOF and DCOF, respectively.

HCOF. When ν_2 in HCOF was measured with the 4500 lines-per-inch grating, the P branch was resolved, but only the first eight to twelve lines in the R branch were resolved. The R branch and part of the P branch were repeated with good resolution using the 7500 lines-per-inch grating. The assignment presented no unexpected difficulty. The observed lines and their assignments are listed in Table IX, and the graphs of the combination relations are shown in Figures 15 and 16.

A few Q lines of the perpendicular component were observed in the R branch. These lines, listed in Table X, are better observed at a higher pressure than that used for the parallel component.

TABLE VII

WAVE NUMBERS OF THE OBSERVED LINES OF THE PARALLEL COMPONENT OF ν_1 OF DCOF

J	R(J) (cm^{-1})	P(J) (cm^{-1})
0	2262.25	-
1	2263.05	-
2	2264.00	-
3	2264.65	2259.69
4	2265.40	2258.96
5	-	2258.27
6	2266.84	2257.80
7	2267.38	2256.73
8	2267.94	2256.23
9	-	2255.56
10	2269.41	2254.79
11	-	2253.46
12	-	2252.79
13	-	2252.27
14	-	2251.44
15	-	2250.59
16	-	2249.82
17	2274.66	2248.96
18	2275.18	2248.01
19	2275.73	2247.28
20	2276.35	2246.60
21	-	2245.91
22	2278.27	2245.28
23	2278.85	2244.56
24	2279.58	2243.81
25	2280.36	2243.14
26	-	2242.47
27	2281.56	-
28	2282.19	2241.07
29	2282.79	2240.35

TABLE VII (continued)

WAVE NUMBERS OF THE OBSERVED LINES OF THE PARALLEL COMPONENT OF γ_1 OF DCOF

J	R(J) (cm^{-1})	P(J) (cm^{-1})
30	2283.34	2239.58
31	-	2238.91
32	2285.20	2238.22
33	2285.84	2237.10
34	2286.48	2236.40
35	2287.08	2235.60
36	-	2234.86
37	2288.32	-
38	2289.07	2233.35
39	2289.67	2232.64
40	2290.36	2231.82
41	-	2231.18
42	2291.81	2230.54
43	2292.49	-
44	2293.19	2229.10
45	2293.97	2228.41
46	-	2227.63
47	2295.22	2226.92
48	2295.96	-
49	2296.79	2225.27
50	-	2224.61
51	2297.93	2224.14
52	2298.58	2223.64
53	2229.30	2222.96
54	2300.07	-
55	2301.09	2221.44
56	2301.62	2220.69
57	2302.35	2220.03
58	2302.85	2219.07
59	-	-

TABLE VII (continued)

WAVE NUMBERS OF THE OBSERVED LINES OF THE PARALLEL COMPONENT OF ν_1 OF DCOF

J	R(J) (cm^{-1})	P(J) (cm^{-1})
60	2304.98	2217.59
61	2305.65	2216.92
62	2306.29	2216.19
63	2306.70	2215.48
64	-	-
65	-	-
66	-	2213.20
67	-	2212.37
68	-	2211.52
69	-	-
70	-	-
71	-	2209.58
72	-	2208.56
73	-	2207.77
74	-	2206.95
75	-	2206.10
76	-	2205.53
77	-	2205.04
78	-	2204.44
79	-	2203.66
80	-	2203.14

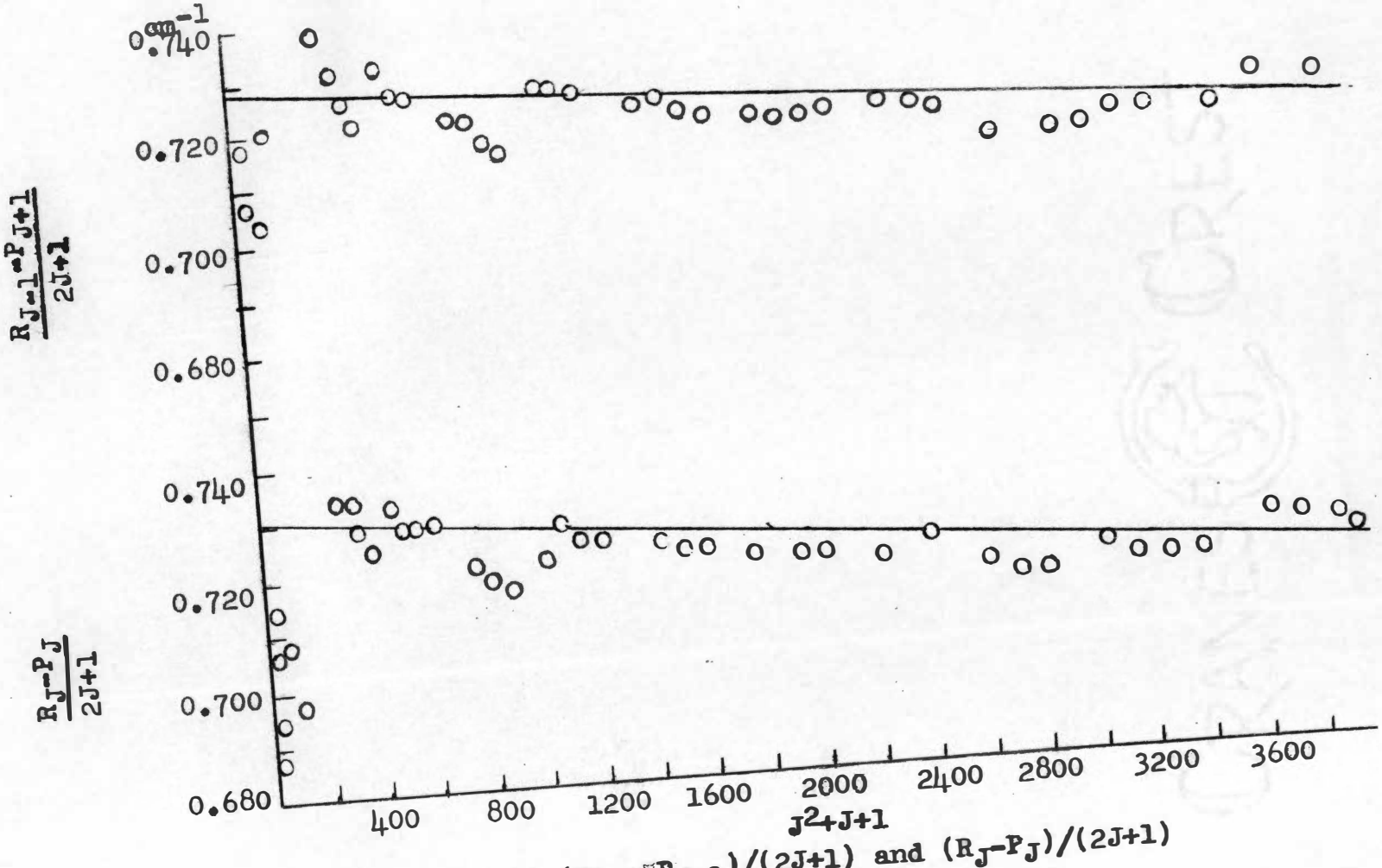

Figure 9. A plot of $(R_{J-1}-P_{J+1})/(2J+1)$ and $(R_J-P_J)/(2J+1)$ versus J2+J+1 for the parallel component of ν_1 of DCOF

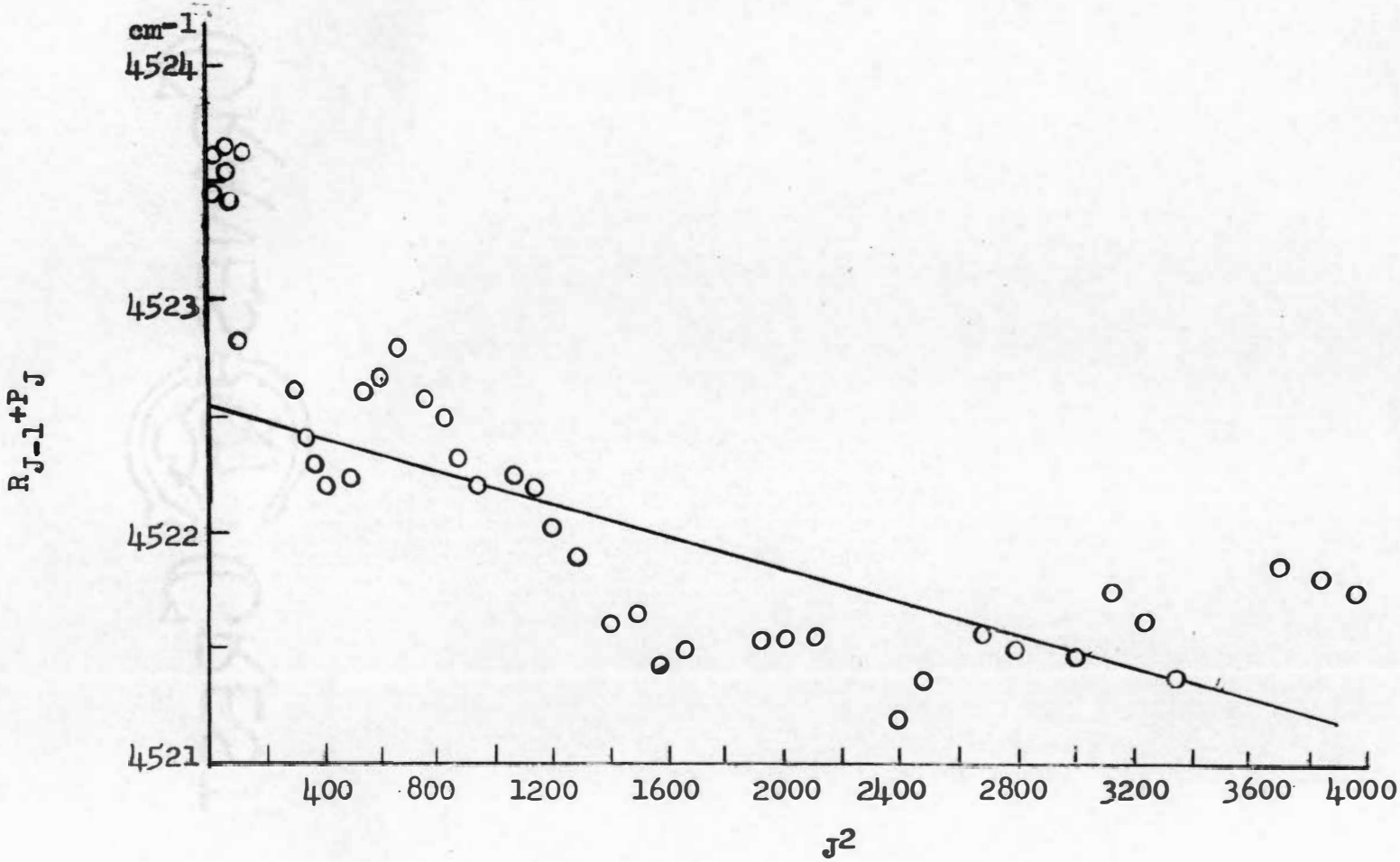

Figure 10. A plot of $R_{J-1}+P_J$ versus J^2 for the parallel component of ν_1 of DCOF

TABLE VIII

WAVE NUMBERS OF THE OBSERVED Q LINES IN ν_1 OF DCOF

K	R_{Q_K} (cm^{-1})	P_{Q_K} (cm^{-1})
0	2266.52[a]	-
1	2268.64[a]	2259.72[a]
2	2270.94	2257.14[a]
3	2274.25	2254.43[a]
4	2277.44	2249.00
5	2280.90	2245.42
6	2284.24	2241.64
7	2287.70	2237.76
8	2290.94	2233.87
9	2294.28	2229.96
10	2297.52	2226.08
11	2300.74	2222.24
12	2304.04	2218.24
13	2306.99	2214.46
14	2310.25	2210.45
15	2313.30	2206.44
16	2316.19	2202.52
17	-	2198.55
18	-	2193.62

[a]These lines were not used in calculations.

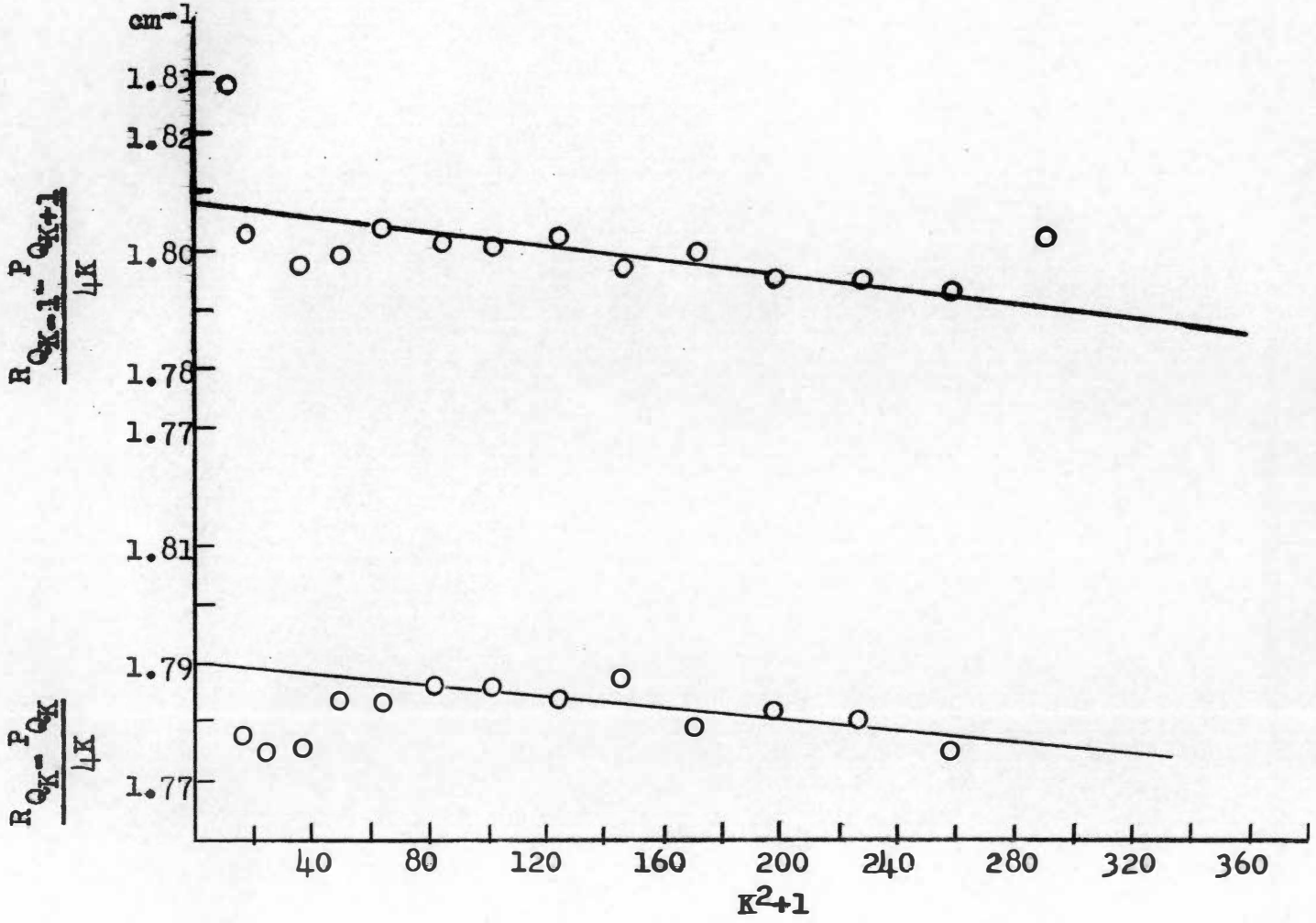

Figure 11. A plot of $(^{R}Q_{K-1}-{}^{P}Q_{K+1})/4K$ and $(^{R}Q_{K}-{}^{P}Q_{K})/4K$ versus K^2+1 for the Q lines of ν_1 of DCOF

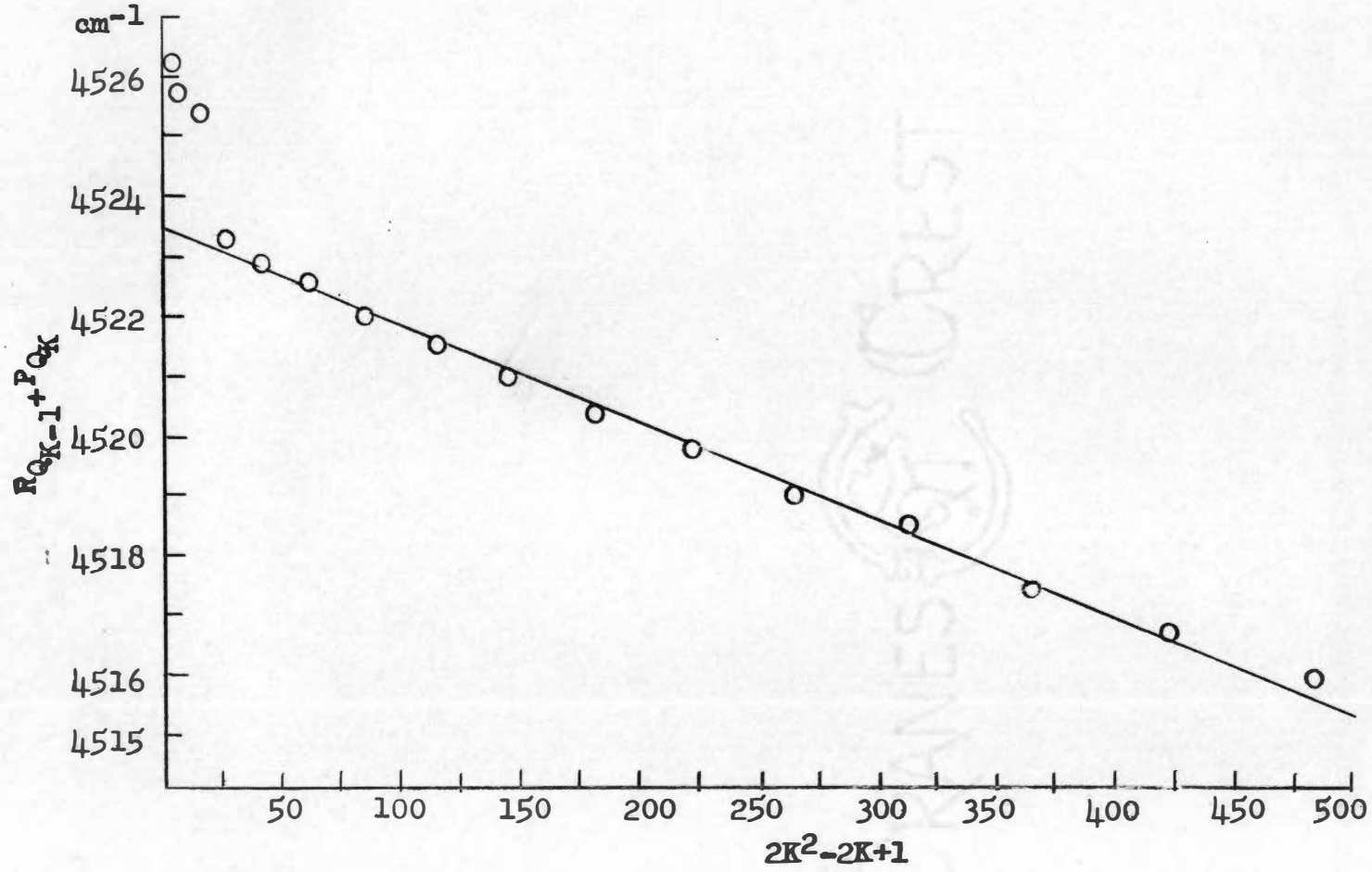

Figure 12. A plot of ($R_{Q_{K-1}}+P_{Q_K}$) versus ($2K^2-2K+1$) for the Q lines of ν_1 of DCOF

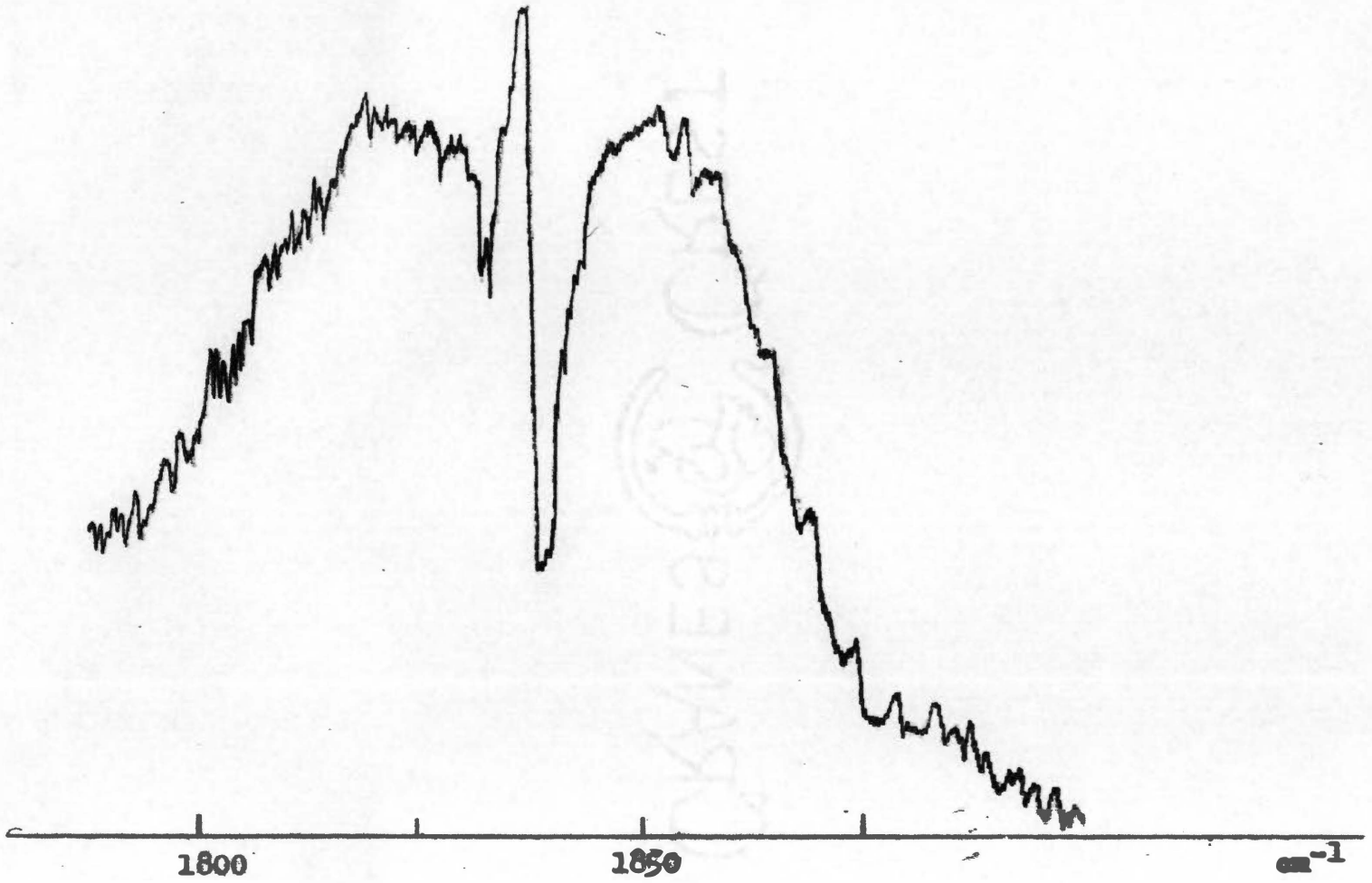

Figure 13. The ν_2 vibration-rotation band of HCOF

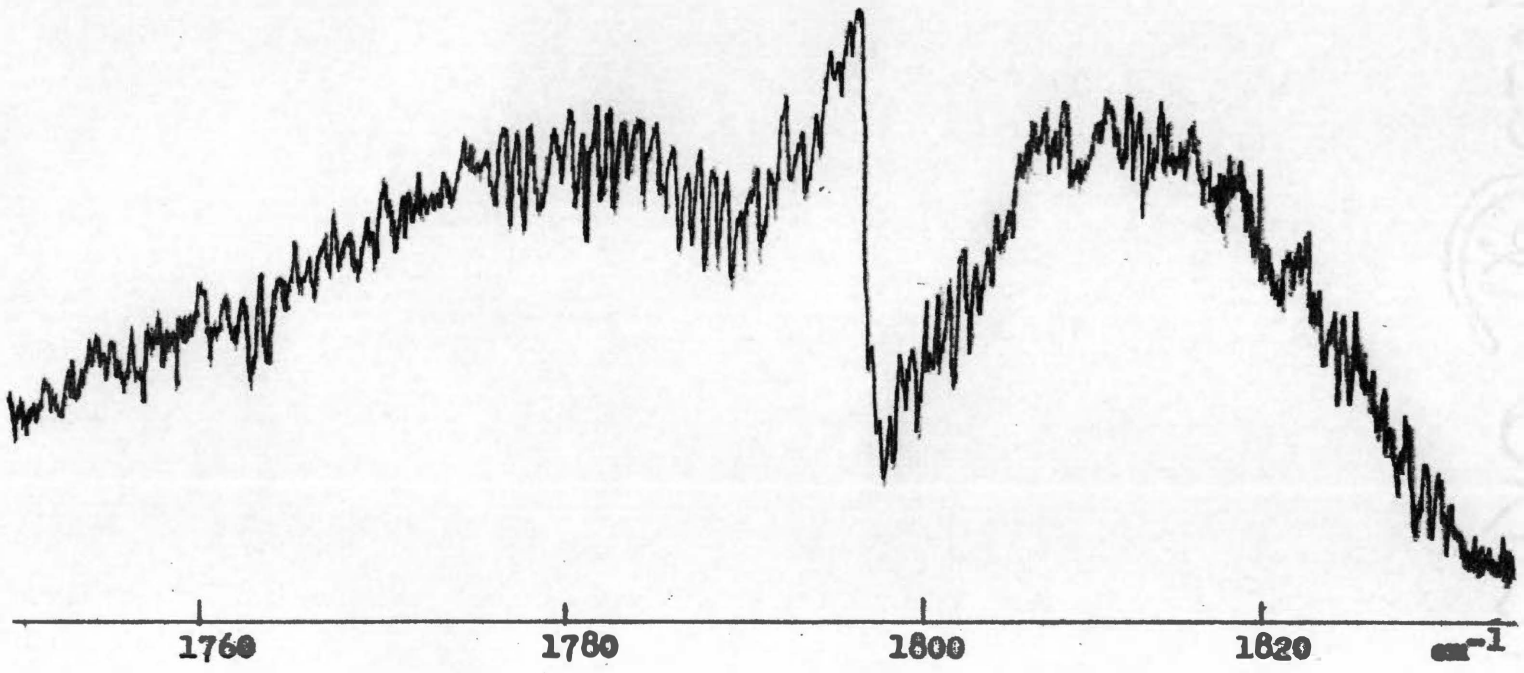

Figure 14. The ν_2 vibration-rotation band of DCOF

TABLE IX

WAVE NUMBERS OF THE OBSERVED LINES OF THE PARALLEL COMPONENT OF ν_2 OF HCOF

J	R(J) (cm^{-1})	P(J) (cm^{-1})
0	1837.51	-
1	1838.32	-
2	1839.06	1835.52
3	1839.80	1834.70
4	1840.50	1833.89
5	1841.12	1833.13
6	1841.82	1832.26
7	1842.50	1831.52
8	1843.23	1830.85
9	1844.02	1830.12
10	1844.64	1829.23
11	1845.33	1828.44
12	1845.95	1827.66
13	1846.67	1826.82
14	1847.43	1826.02
15	1847.97	1825.29
16	1848.78	1824.40
17	1849.32	1823.62
18	1849.94	1822.86
19	1850.34	1822.14
20	1851.06	1821.38
21	1851.67	1820.62
22	1852.31	1819.85
23	1853.00	1818.91
24	1853.66	1818.08
25	1854.32	1817.24
26	1854.90	1816.35
27	1855.49	1815.40
28	1856.17	1814.59
29	1856.81	1813.88

TABLE IX (continued)

WAVE NUMBERS OF THE OBSERVED LINES OF THE PARALLEL COMPONENT OF ν_2 OF HCOF

J	R(J) (cm^{-1})	P(J) (cm^{-1})
30	1857.49	1813.10
31	1858.10	1812.39
32	1858.74	1811.58
33	1859.29	1810.76
34	1859.82	1809.90
35	1860.36	1809.14
36	1861.00	1808.19
37	1861.57	1806.94
38	1862.16	1806.16
39	1862.84	1805.24
40	1863.40	1804.50
41	1863.97	1803.72
42	1864.57	1802.88
43	1865.31	1801.94
44	1865.70	1801.14
45	1866.30	1800.41
46	-	1799.60
47	-	1798.70
48	-	1797.82

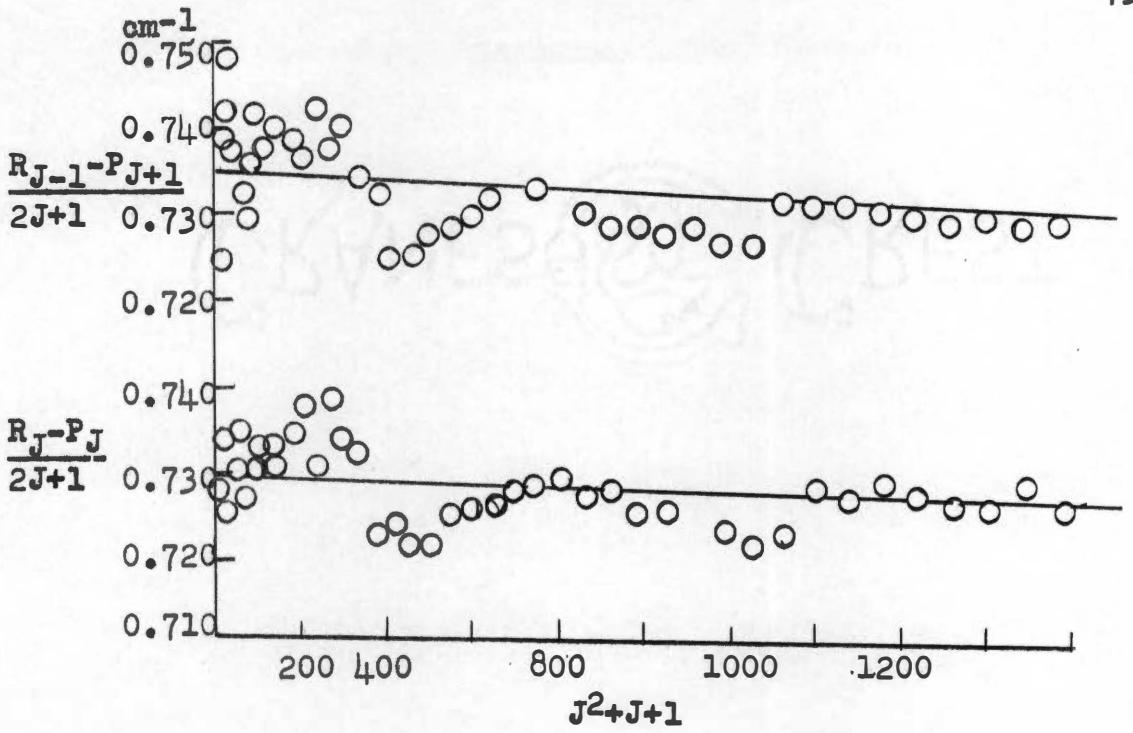

Figure 15. A plot of $(R_{J-1}-P_{J+1})/(2J+1)$ and $(R_J-P_J)/(2J+1)$ versus (J^2+J+1) for the parallel component of ν_2 of HCOF

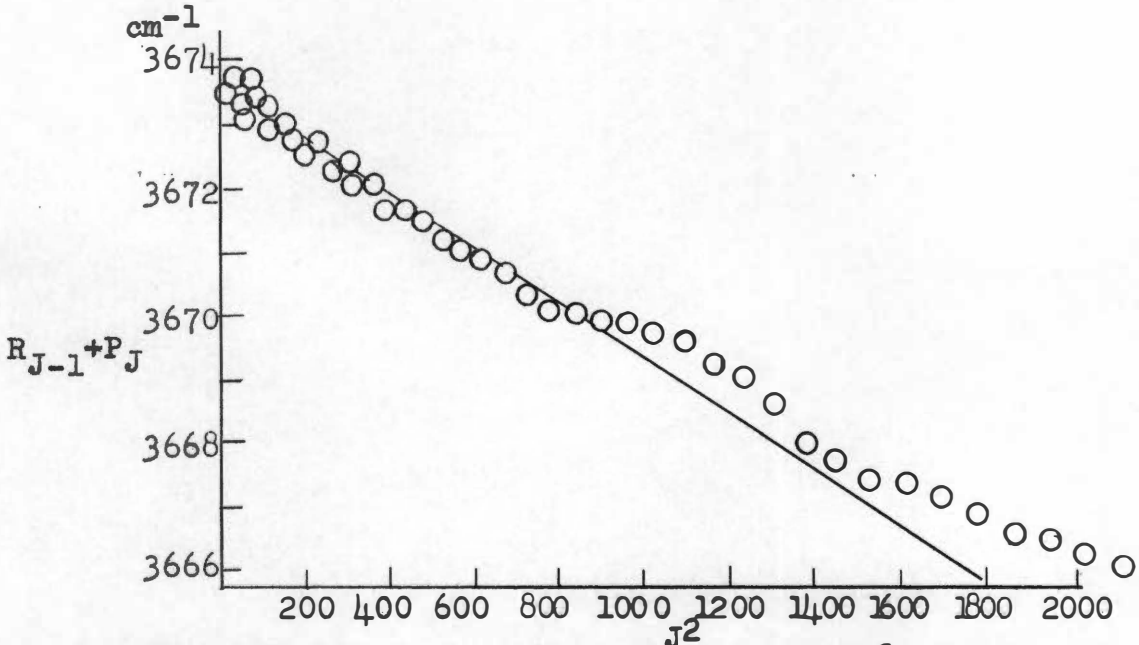

Figure 16. A plot of $(R_{J-1}+P_J)$ versus J^2 for the parallel component of ν_2 of HCOF

TABLE X

WAVE NUMBERS OF THE OBSERVED Q LINES IN ν_2 OF HCOF

Chart Number	Wave Number
50	1870.17
60	1875.50
70	1880.64
80	1885.54
90	1890.58
100	1895.47
110	1900.38
120	1904.96
130	1910.17

DCOF. Measurement of ν_2 in DCOF using the thermocouple and the 4500 lines-per-inch grating was useless because the individual lines were not resolved. The band was, however, well resolved with the 7500 lines-per-inch grating and the Golay detector. There were regions where the lines faded into unresolved absorption. The general appearance of these regions was that of a region where absorption lines interfere with one another. These regions presented no real difficulty, and the constants obtained appeared to be quite satisfactory. The observed lines are listed in Table XI; the combination relations are shown in Figures 17 and 18.

There were no observed Q lines.

ν_3

The planar C-H bending vibrations in the two molecules differ more than any other corresponding pair of observed bands. In HCOF ν_3 is observed as a weak perpendicular band with only a suggestion of a parallel component; in DCOF it is a strong hybrid band in which the Q lines do not stand out, but rather are observed as humps under the lines with $\Delta J = \pm 1$. Figures 19 and 20 show these bands.

HCOF. Although the background was largely removed, some of the water lines were of about the same order of intensity as the HCOF lines being measured. For this reason there was some question of identification. The lines were

TABLE XI

WAVE NUMBERS OF THE OBSERVED LINES OF THE PARALLEL COMPONENT OF ν_2 OF DCOF

J	R(J) (cm^{-1})	P(J) (cm^{-1})
0	1797.87	-
1	-	-
2	1799.46	-
3	1800.04	-
4	1800.68	1794.33
5	1801.40	1793.53
6	1802.10	1792.73
7	1802.78	1791.96
8	1803.39	1791.03
9	1804.01	1790.30
10	-	1789.56
11	-	1788.80
12	-	1788.06
13	-	1787.32
14	-	1786.52
15	1807.75	1785.47
16	1808.62	1784.66
17	1809.43	1783.88
18	1810.16	1783.06
19	1810.64	1782.29
20	1811.30	1781.51
21	1812.02	1780.87
22	1812.65	1779.82
23	1813.27	1778.80
24	1813.96	1778.09
25	1814.88	1777.21
26	-	-
27	1816.43	-
28	1817.04	1775.10
29	1817.67	1774.34

TABLE XI (continued)

WAVE NUMBERS OF THE OBSERVED LINES OF THE PARALLEL COMPONENT OF ν_2 OF DCOF

J	R(J) (cm^{-1})	P(J) (cm^{-1})
30	1818.19	1773.53
31	1818.69	1772.77
32	1819.30	1771.92
33	1819.84	1771.10
34	1820.39	1770.13
35	1820.97	1769.48
36	1821.45	1768.60
37	1822.21	1767.81
38	1822.85	1767.29
39	1823.60	1766.52
40	1824.33	1765.66
41	1824.96	1764.76
42	1825.42	1763.92
43	1825.96	1763.11
44	1826.68	1761.90
45	-	1761.19
46	-	1760.28
47	-	1759.41

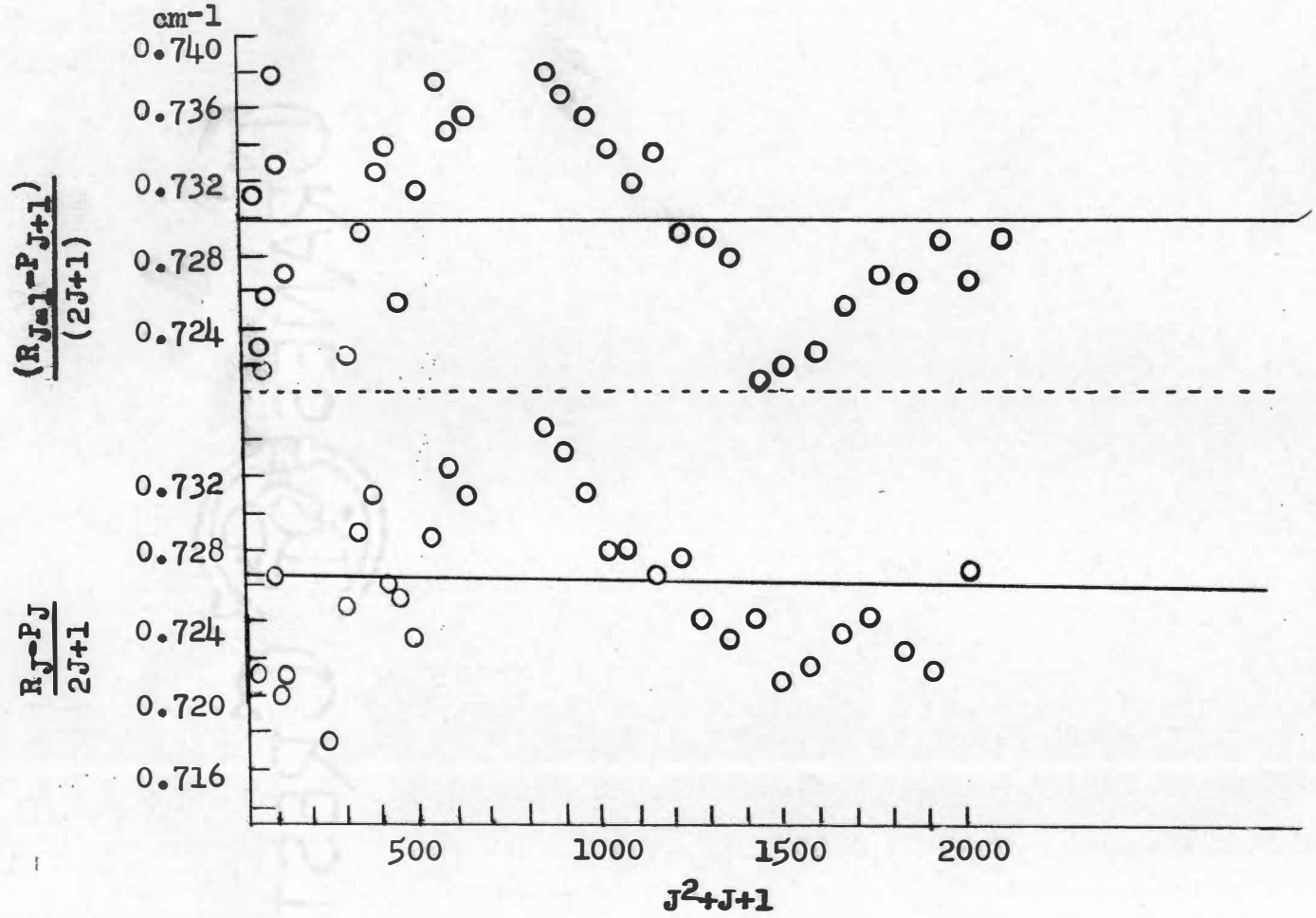

Figure 17. A plot of $(R_{J-1}-P_{J+1})/(2J+1)$ and $(R_J-P_J)/(2J+1)$ versus J^2+J+1 for ν_2 of DCOF

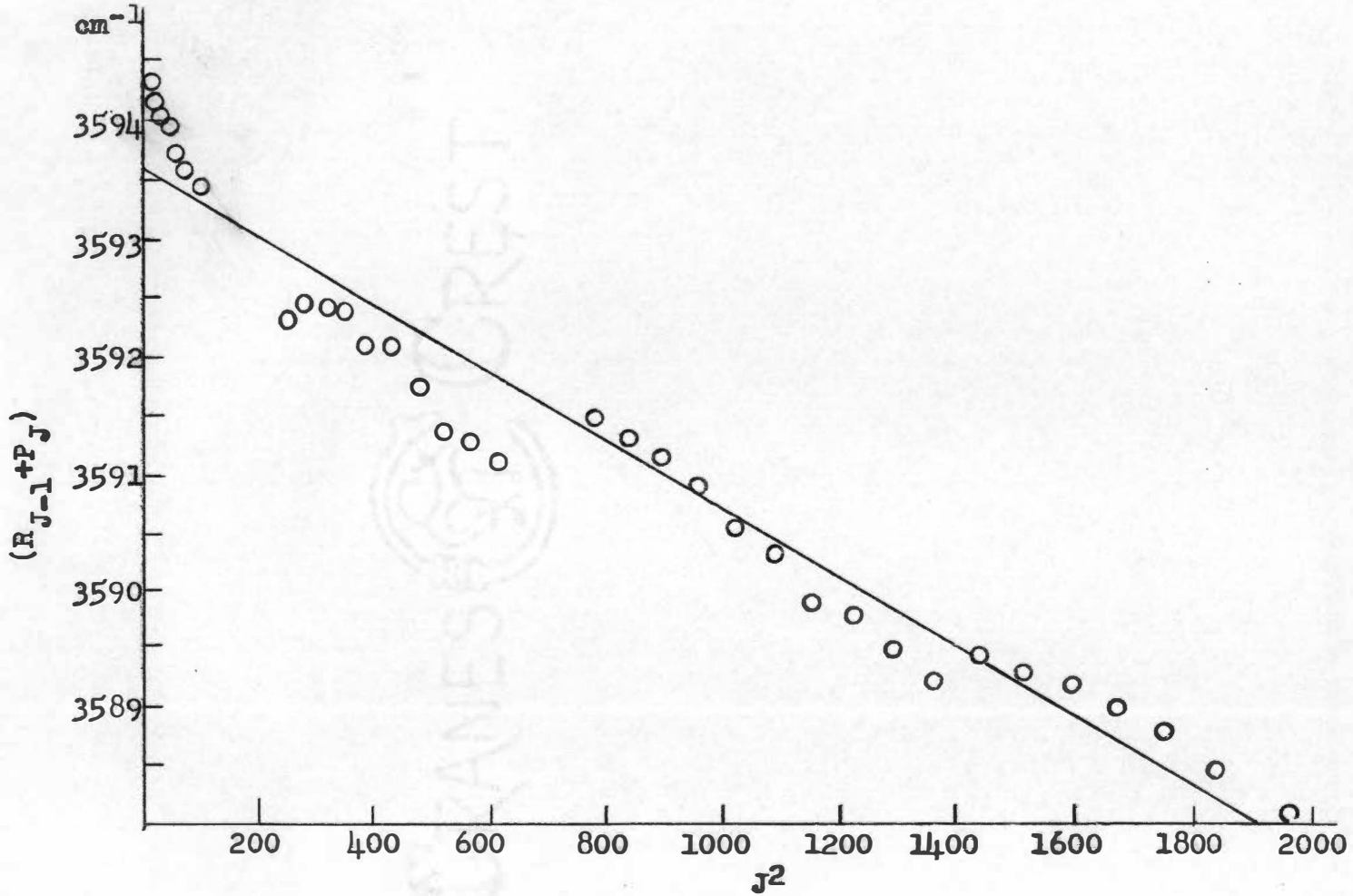

Figure 18. A plot of $(R_{J-1}+P_J)$ versus J^2 for ν_2 of DCOF

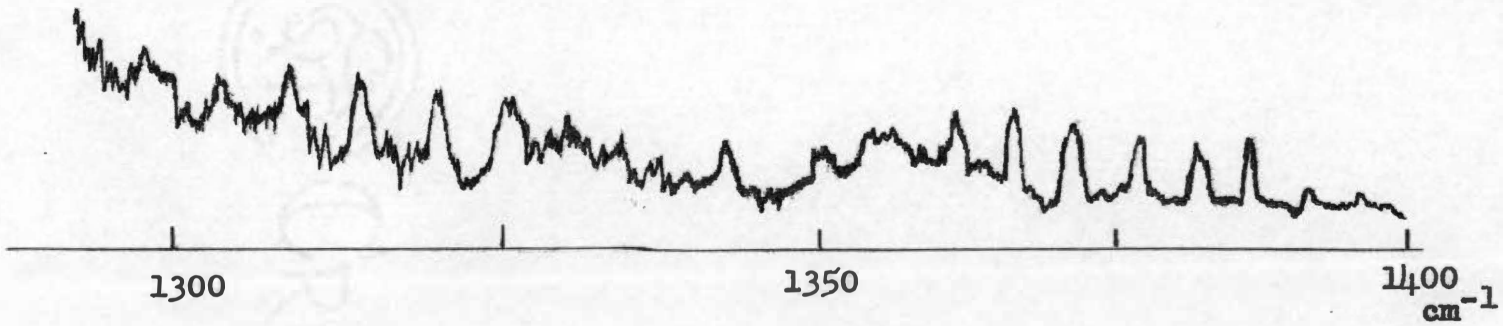

Figure 19. The ν_3 vibration-rotation band of HCOF

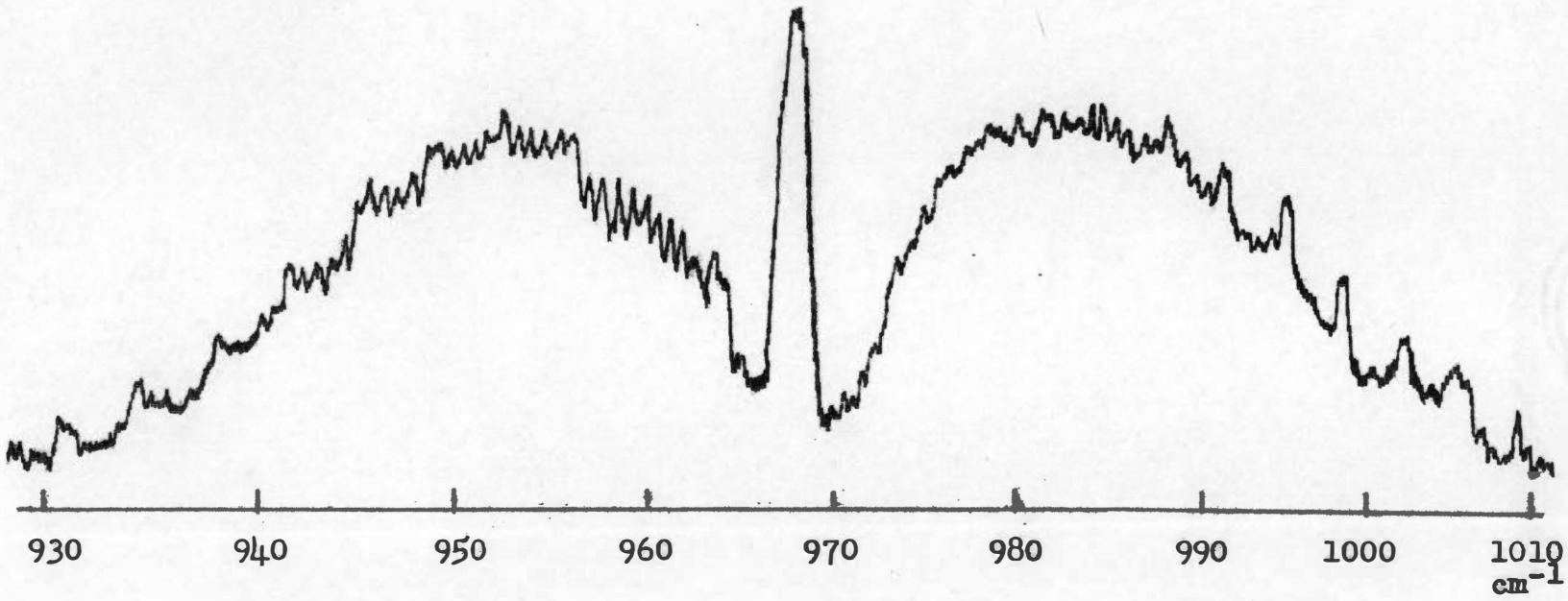

Figure 20. The ν_3 vibration-rotation band of DCOF

measured with the 3600 lines-per-inch grating, and then with the 4500 lines-per-inch grating; the results were averaged. The assignment was unambiguous and gave constants in agreement with those obtained from other bands.

The observed lines are listed in Table XII. Figures 21 and 22 show the combination relations.

DCOF. This band is strong. The author believes that there is an interaction between this band (ν_3) and the C-F stretching vibration (ν_4). This is discussed in a later paragraph under the heading ν_4 DCOF.

The assignment of the parallel component was reasonably simple, except for the high frequency side of the R branch. There the spacing was such that one could assume that lines were missing in two places, or one could assume that the spacing was merely different (or apparently different) at these two points. Finally it was assumed that there were no missing lines. The lines that appear to be too widely spaced are R(18) and R(19), and R(26) and R(27). The plots of the combination relations (Figures 23 and 24) show definite groupings which do not seem to fit together very well. The results are more consistent, however, than they would be if it were assumed that the lines were missing. Table XIII lists the observed lines.

TABLE XII

WAVE NUMBERS OF THE OBSERVED Q LINES IN ν_3 OF HCOF

K	$^{R}Q_K$ (cm^{-1})	$^{P}Q_K$ (cm^{-1})
0	-	-
1	1349.54	1340.50
2	1355.39	1335.72
3	1360.94	1328.99
4	1366.02	1323.65
5	1371.48	1318.54
6	1376.66	1313.05
7	1381.71	1307.59
8	1386.83	1302.09
9	1392.02	1296.77
10	-	1291.21
11	-	1285.86

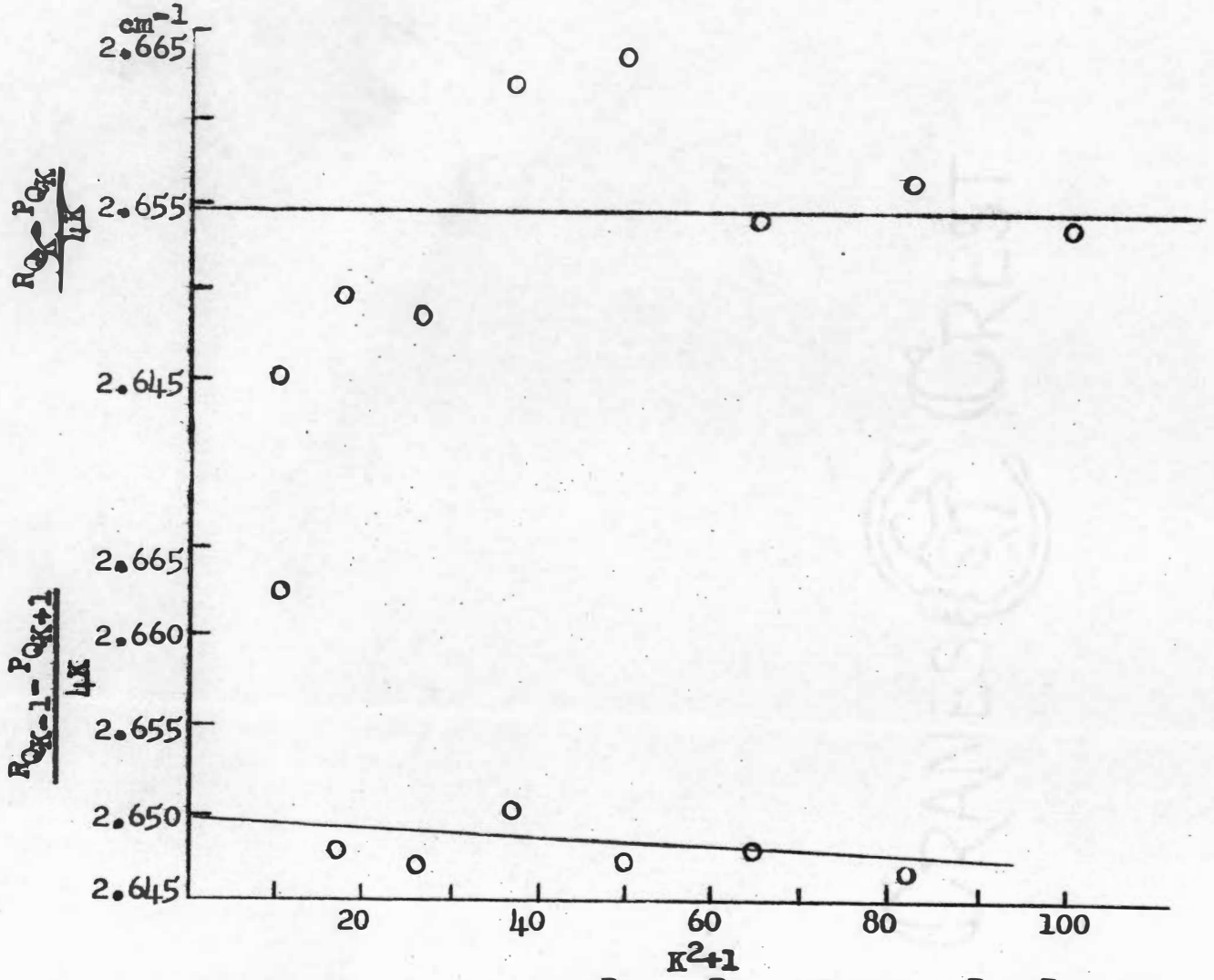

Figure 21. A plot of $(R_{Q_{K-1}} - P_{Q_{K+1}})/4K$ and $(R_{Q_K} - P_{Q_K})/4K$ versus K^2+1 for the Q lines of ν_3 of HCOF

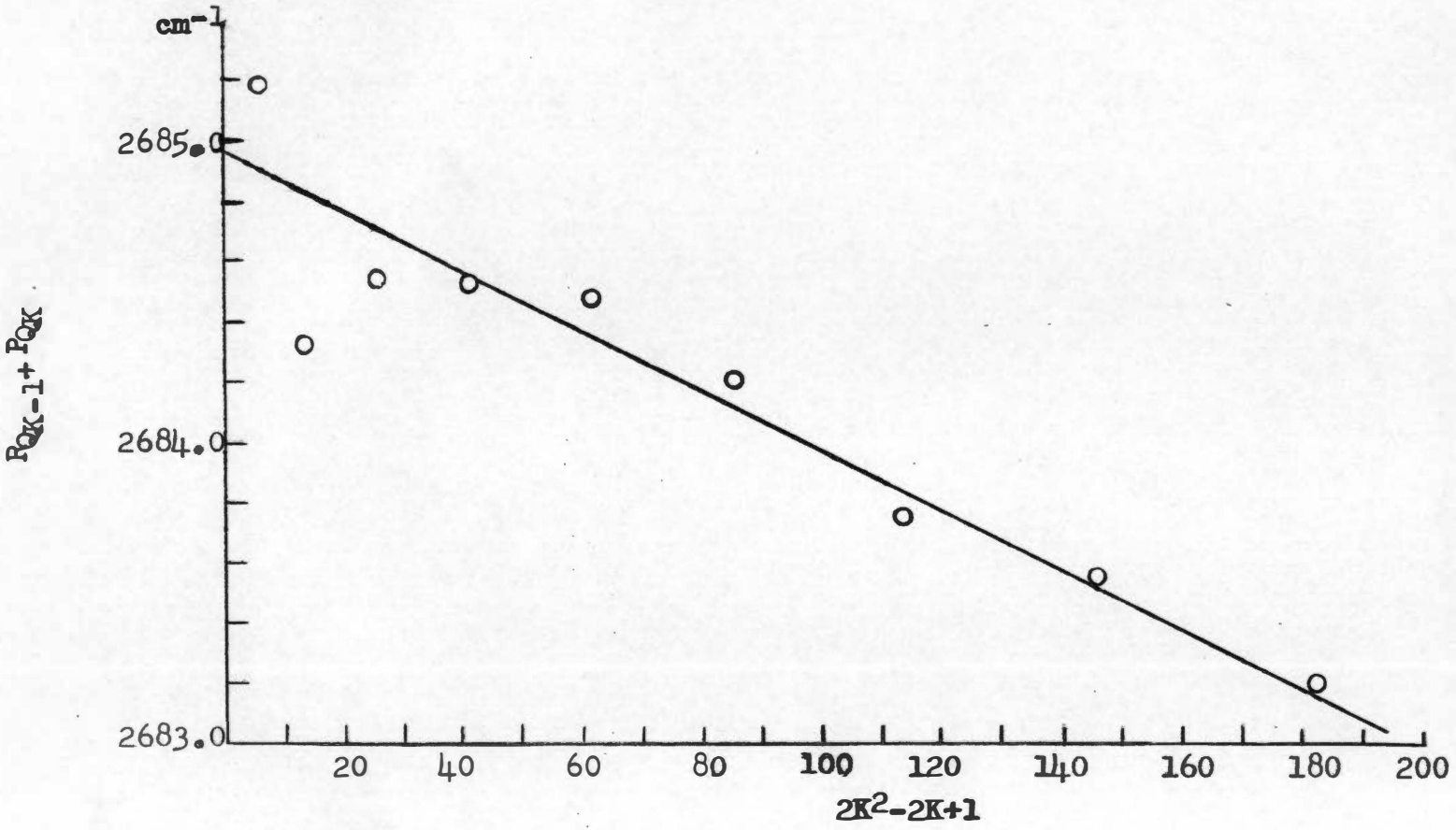

Figure 22. A plot of ($R_{Q_{K-1}} + P_{Q_K}$) versus ($2K^2-2K+1$) for the Q lines of ν_3 of HCOF

TABLE XIII

WAVE NUMBERS OF THE OBSERVED LINES OF THE PARALLEL COMPONENT OF ν_3 OF DCOF

J	R(J) (cm^{-1})	P(J) (cm^{-1})
0	-	-
1	969.31	-
2	970.03	-
3	970.74	965.79
4	971.47	964.95
5	972.17	964.22
6	972.87	963.44
7	973.61	962.75
8	974.31	962.00
9	975.06	961.22
10	975.76	960.49
11	976.61	959.71
12	977.35	959.02
13	978.00	958.32
14	978.75	957.61
15	979.44	956.88
16	980.24	956.19
17	980.90	955.47
18	981.68	954.77
19	982.60	954.13
20	983.25	953.42
21	984.04	952.64
22	984.76	951.86
23	985.49	951.12
24	986.20	950.45
25	986.89	949.72
26	987.66	949.08
27	988.70	948.36
28	989.45	947.70
29	990.25	947.03

TABLE XIII (continued)

WAVE NUMBERS OF THE OBSERVED LINES OF THE PARALLEL COMPONENT OF ν_3 OF DCOF

J	R(J) (cm^{-1})	P(J) (cm^{-1})
30	991.14	946.28
31	991.75	945.60
32	992.49	944.90
33	993.21	944.28
34	993.91	943.57
35	994.76	942.87
36	-	942.15
37	-	941.51
38	-	940.76
39	-	940.09
40	-	939.44
41	-	938.73
42	-	938.06
43	-	937.35

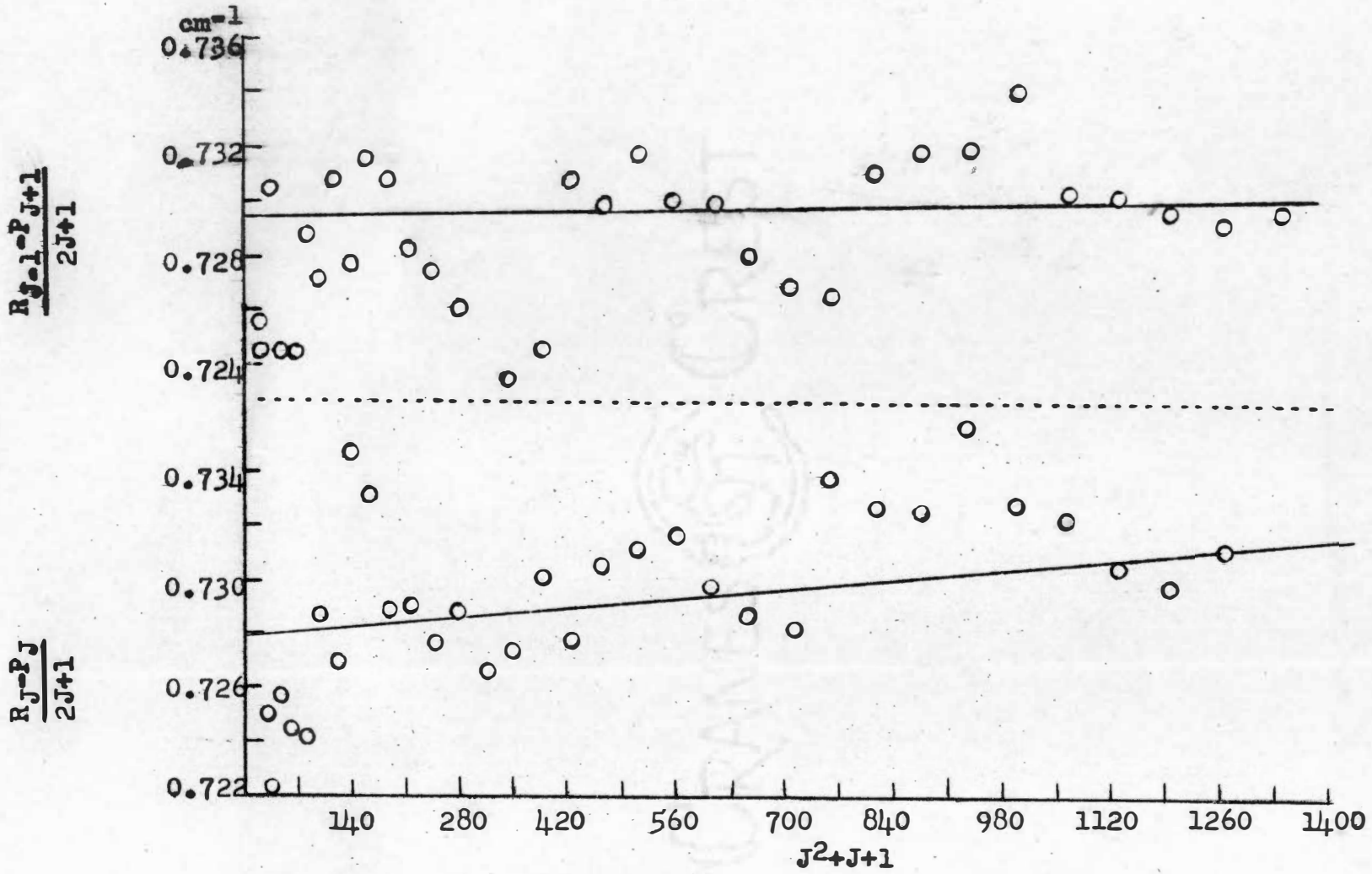

Figure 23. A plot of $(R_{J-1}-P_{J+1})/(2J+1)$ and $(R_J-P_J)/(2J+1)$ versus J2+J+1 for the parallel component of ν_3 of DCOF

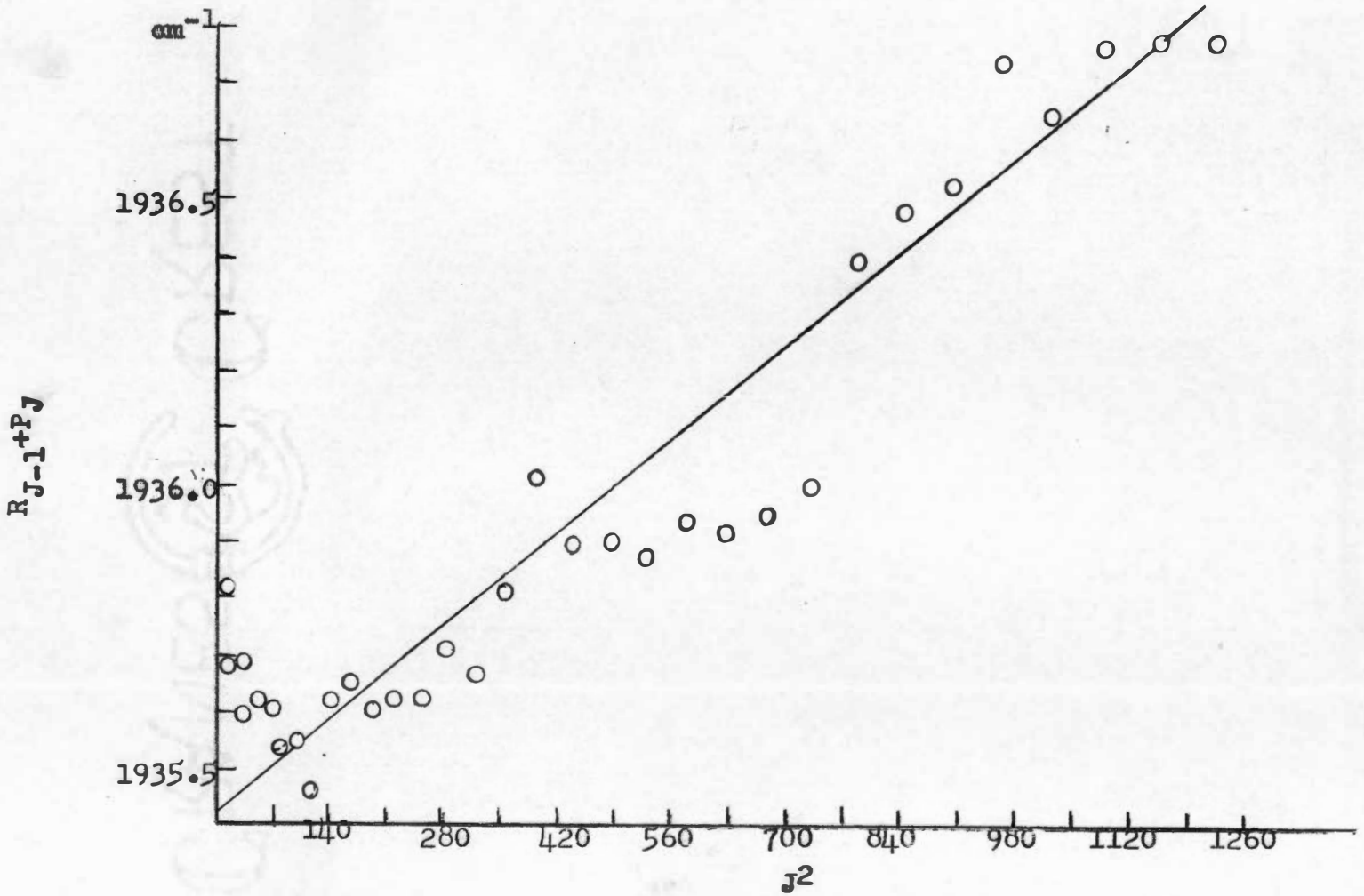

Figure 24. A plot of $(R_{J-1}+P_J)$ versus J^2 for the parallel component of ν_3 of DCOF

When the wave numbers of the Q lines were plotted against a running number, they fell very close to a straight line. The assignment presented no difficulty after an initial error involving the band center was corrected. Table XIV lists the observed Q lines, and Figures 25 and 26 give the combination relations.

ν_4

The C-F stretching vibration is the most intense band for each molecule. Both are hybrid bands with the parallel component stronger than the perpendicular component. These bands are shown in Figures 27 and 28.

HCOF. The parallel component of this band was the first parallel band analyzed in HCOF. The results appeared to be quite satisfactory, but they agreed with neither ν_1 nor ν_2, which were the next two bands having parallel components that were analyzed. A careful re-analysis resulted in constants which agreed very well with those obtained from the other bands. A comparison of the two assignments with their combination relations, without reference to the other bands, leaves little to choose between them. The plots of $R_{J-1}-P_{J+1}$ and R_J-P_J versus J^2+J+1 are slightly more satisfactory in the final assignment, and the plot of $R_{J-1}+P_J$ is considerably more satisfactory. These, by themselves, however, would not have been sufficient to decide between the

TABLE XIV

WAVE NUMBERS OF THE OBSERVED Q LINES IN ν_3 OF DCOF

K	R_{Q_K} (cm^{-1})	P_{Q_K} (cm^{-1})
0	-	-
1	-	-
2	-	-
3	980.63	-
4	984.04	955.21
5	987.66	951.76
6	991.16	948.23
7	994.76	944.58
8	998.45	940.76
9	1001.82	937.35
10	1005.30	933.29
11	1008.78	929.80

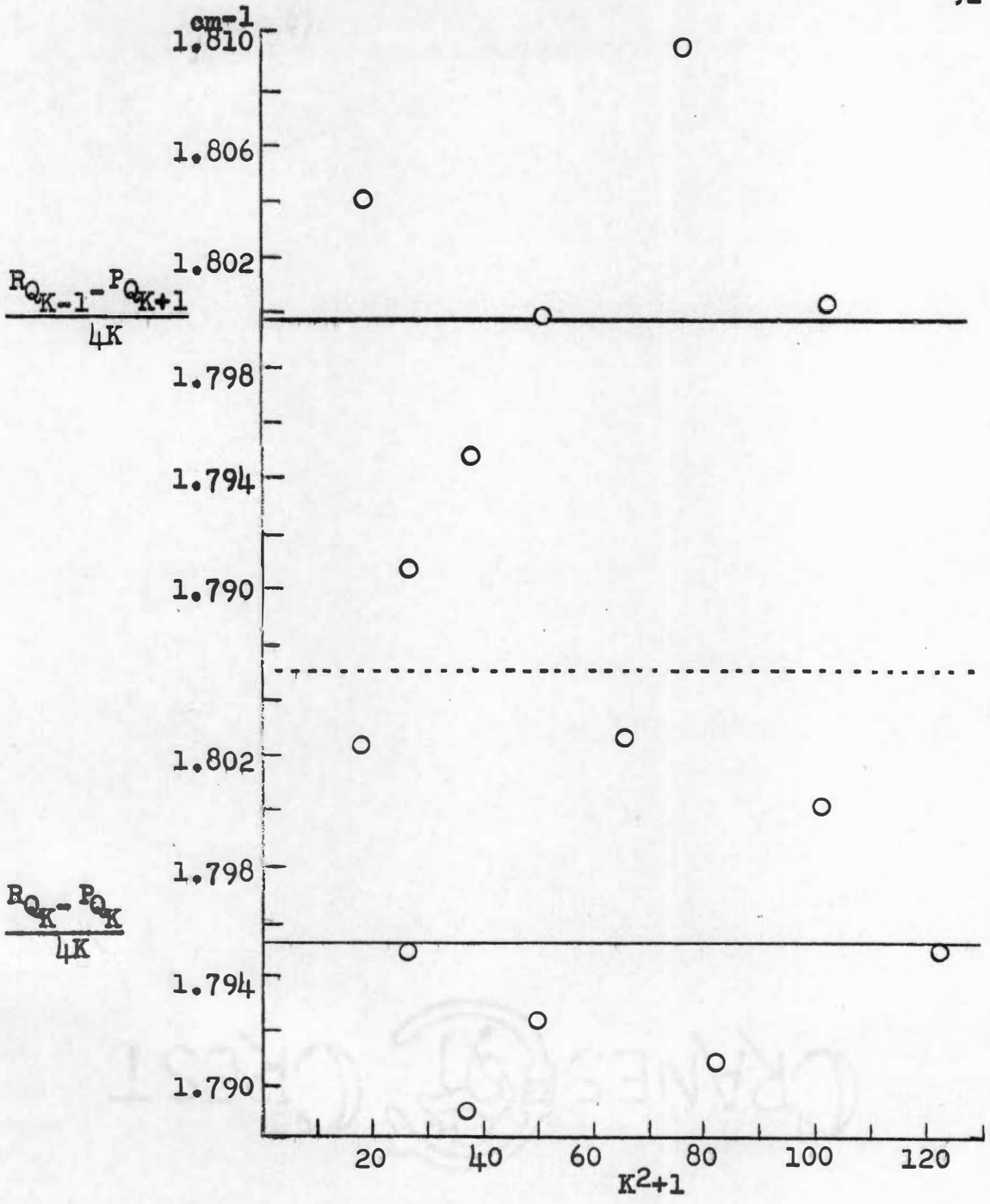

Figure 25. A plot of $(RQ_{K-1}-PQ_{K+1})/4K$ and $(RQ_K-PQ_K)/4K$ versus K^2+1 for the Q lines of ν_4 of DCOF

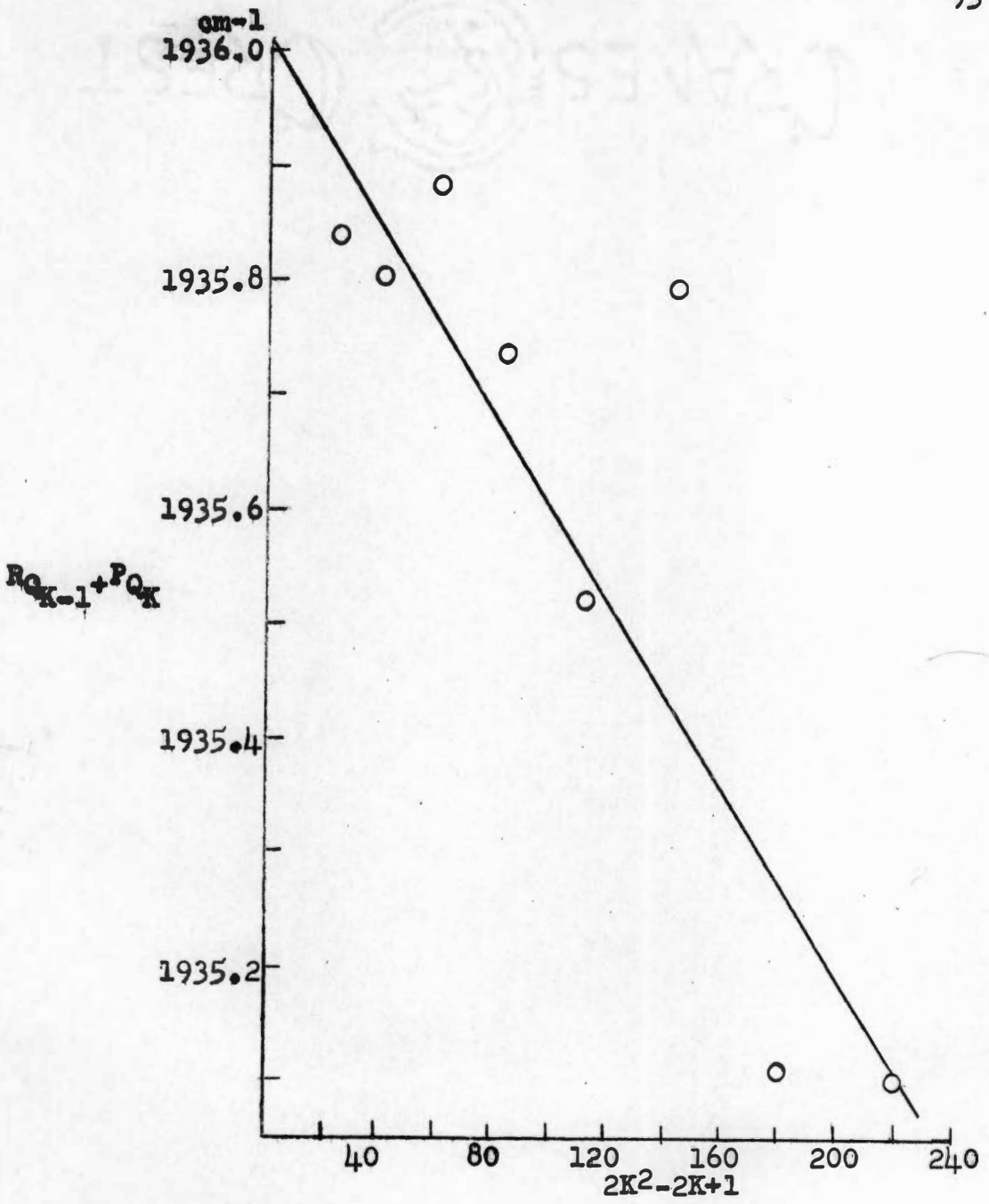

Figure 26. A plot of $(^{R}Q_{K-1}+^{P}Q_{K})$ versus $2K^2-2K+1$ for the Q lines of ν_3 of DCOF

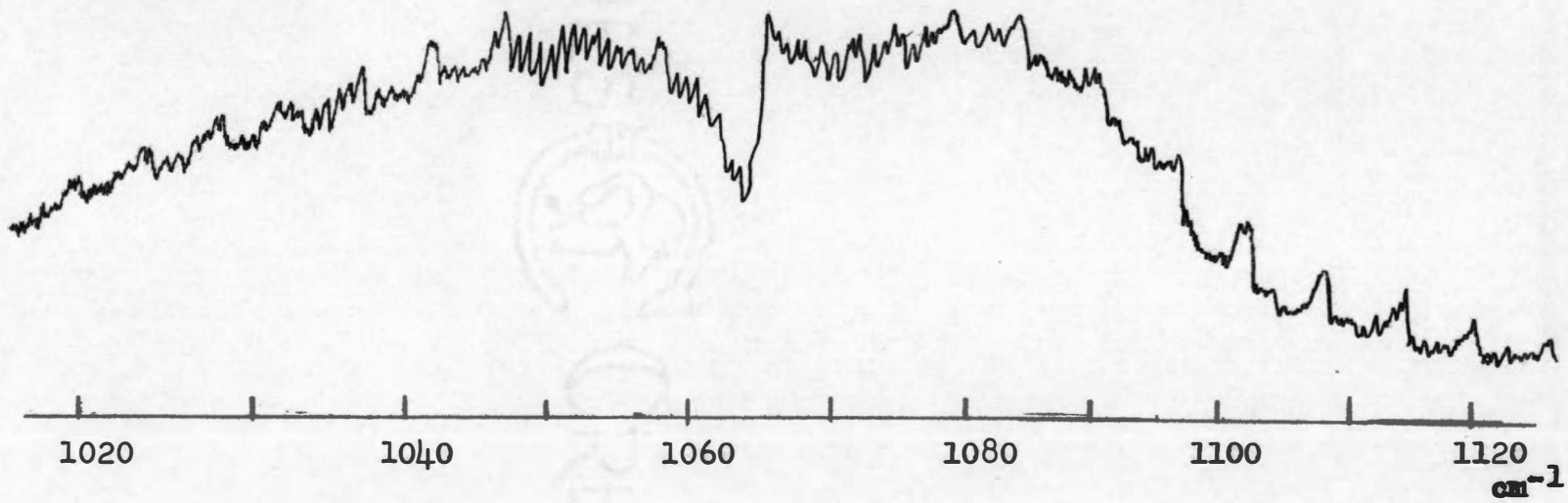

Figure 27. The ν_4 vibration-rotation band of HCOF

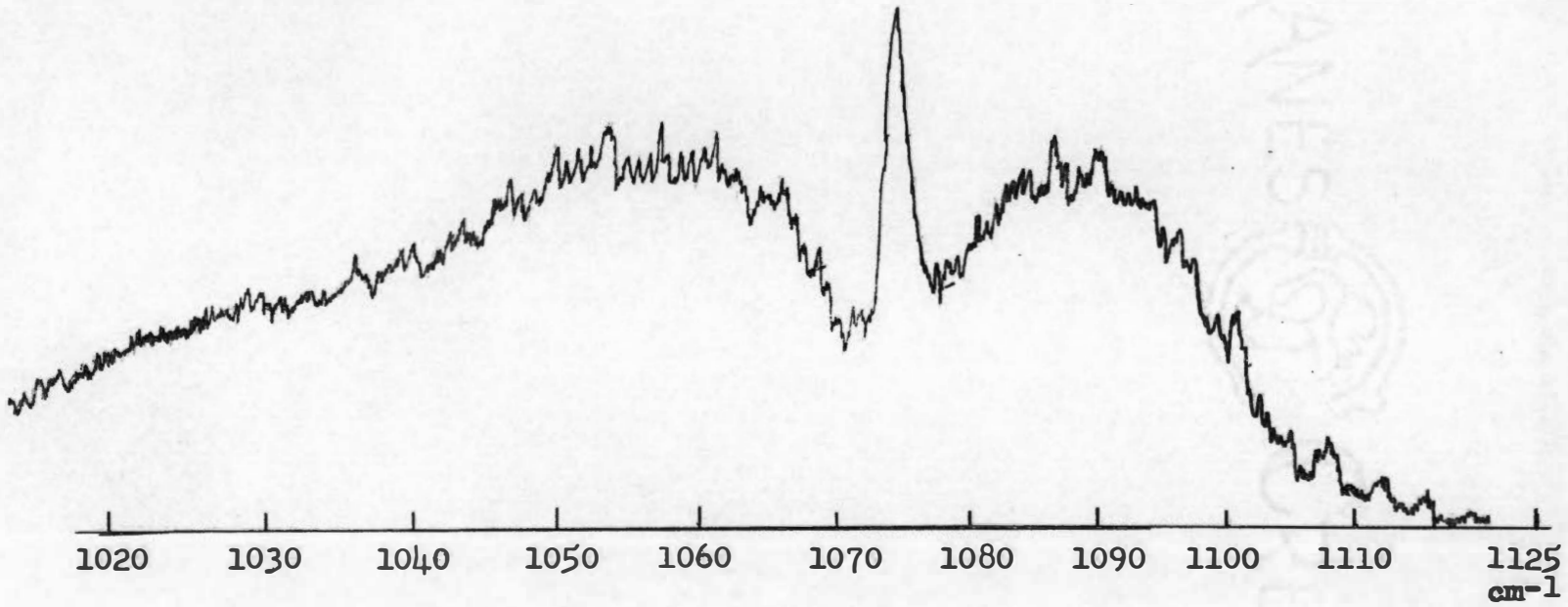

Figure 28. The ν_4 vibration-rotation band of DCOF

two assignments. Table XV lists the observed lines of the parallel component of ν_4 in HCOF. Figures 29 and 30 show the combination relations.

The perpendicular component presented no difficulty. The observed lines are listed in Table XVI, and the combination relations are shown in Figures 31 and 32.

DCOF. The analysis of this band was reasonably straightforward, and the resulting constants appeared to be satisfactory. Tables XVII and XVIII list the observed lines in the parallel and perpendicular components, respectively. Figures 33 and 34 show the combination relations for the parallel component, and Figures 35 and 36 show them for the perpendicular component.

Even though the hydrogen atom is not directly involved in the C-F stretching vibration, it is reasonable to expect ν_4 to lie at a slightly lower frequency in DCOF than in HCOF. The reverse is observed. It has already been mentioned that ν_3 in DCOF is much more intense than ν_3 in HCOF. In DCOF ν_3 and ν_4 lie close together. The author believes that there is an interaction between ν_3 and ν_4 in DCOF which causes ν_3 to be shifted to a lower frequency and ν_4 to be shifted to a higher frequency. This interaction could also account for the increased intensity of ν_3 in DCOF.

TABLE XV

WAVE NUMBERS OF THE OBSERVED LINES OF THE PARALLEL COMPONENT OF ν_4 OF HCOF

J	R(J) (cm^{-1})	P(J) (cm^{-1})
0	-	-
1	1066.32	-
2	1066.96	-
3	1067.67	-
4	1068.39	1062.03
5	1069.28	1061.20
6	-	1060.37
7	1070.15	1059.66
8	1071.12	1058.95
9	1072.08	-
10	-	-
11	1073.16	1056.67
12	1073.91	1055.64
13	1074.53	1054.75
14	1075.16	1053.92
15	1075.88	1053.18
16	1076.53	1052.32
17	1077.14	1051.62
18	1077.78	1050.74
19	-	1049.91
20	1078.74	1049.08
21	-	1048.25
22	-	1047.44
23	-	1046.53
24	-	1045.85
25	-	1045.03
26	-	-
27	-	-
28	-	1042.31
29	-	1041.45

TABLE XV (continued)

WAVE NUMBERS OF THE OBSERVED LINES OF THE PARALLEL COMPONENT OF ν_4 OF HCOF

J	R(J) (cm^{-1})	P(J) (cm^{-1})
30	-	-
31	1085.20	-
32	1085.80	-
33	-	1037.75
34	-	1036.86
35	-	1036.03
36	-	1035.18
37	-	1034.34
38	-	1033.54

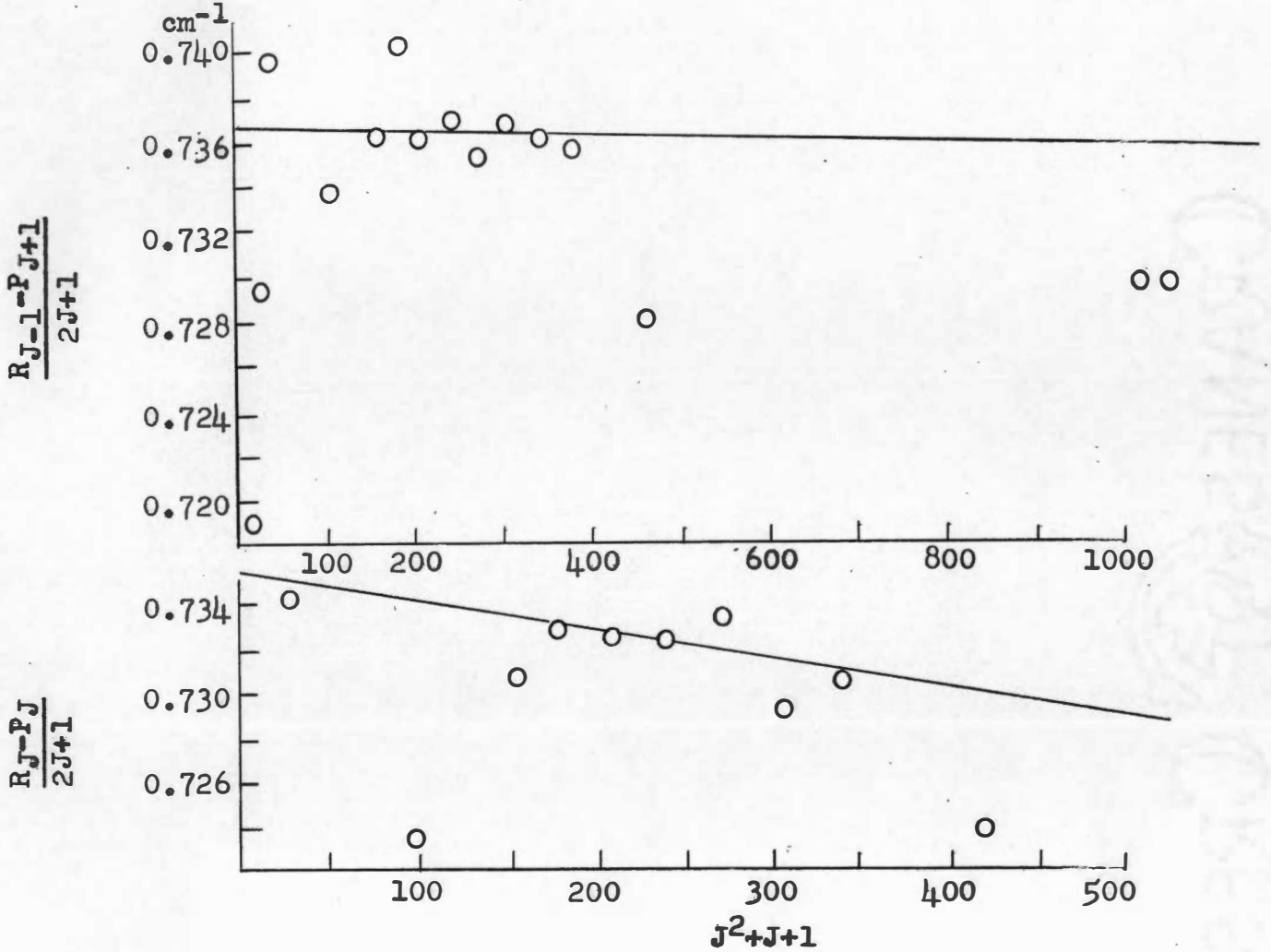

Figure 29. A plot of $(R_{J-1}-P_{J+1})/(2J+1)$ and $(R_J-P_J)/(2J+1)$ versus J^2+J+1 for the parallel component of ν_4 in HCOF

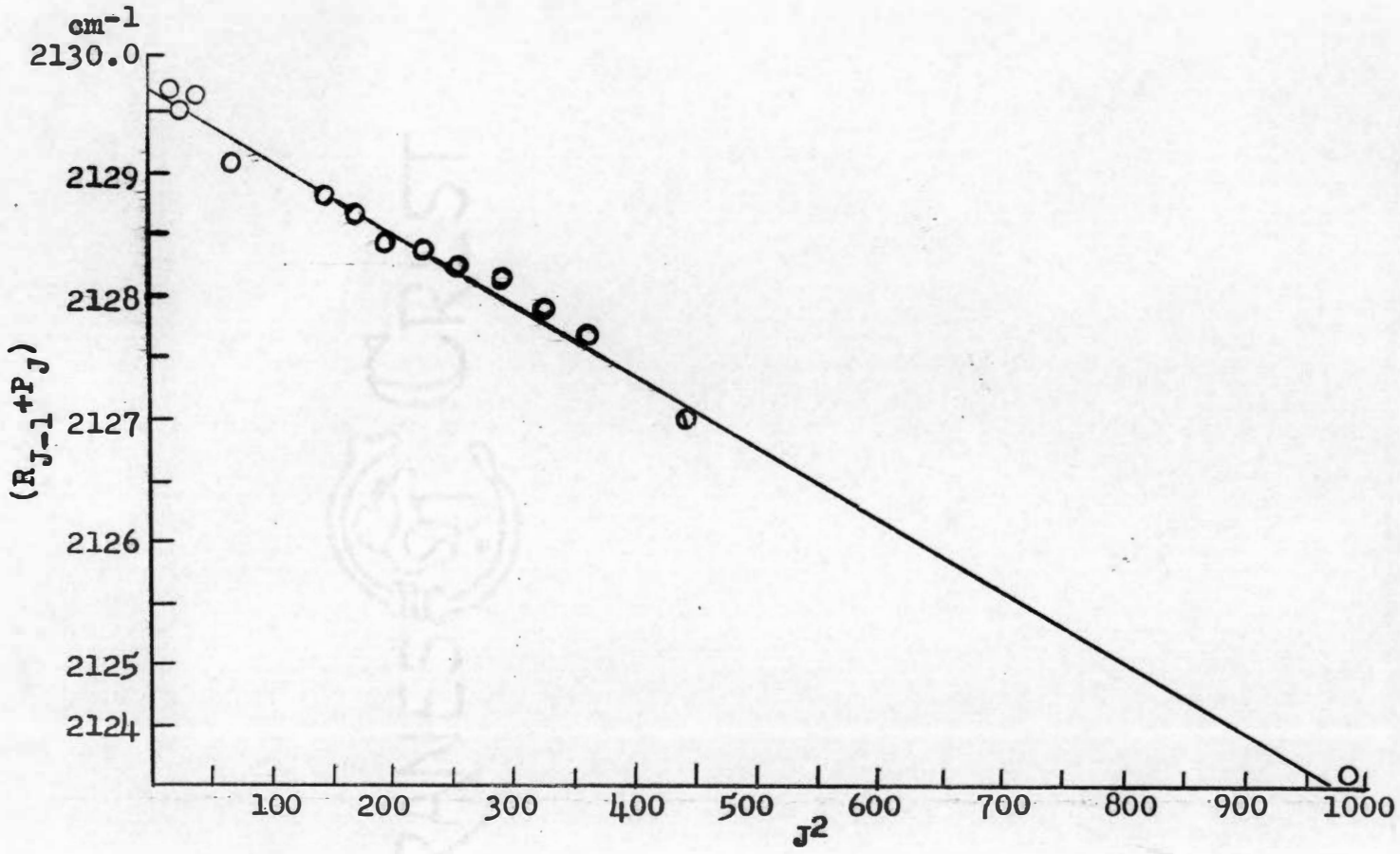

Figure 30. A plot of $R_{J-1}+P_J$ versus J^2 for the parallel component of ν_4 in HCOF

TABLE XVI

WAVE NUMBERS OF THE OBSERVED Q LINES IN ν_4 OF HCOF

K	$^{R}Q_{K}$ (cm^{-1})	$^{P}Q_{K}$ (cm^{-1})
0	-	-
1	-	-
2	1078.74	1057.79
3	1083.96	-
4	1090.06	1046.53
5	1096.52	1041.45
6	1102.00	-
7	1108.05	-
8	1114.17	1027.64
9	1120.30	1023.21
10	-	1018.71
11	-	1014.55
12	-	1010.01
13	-	1005.30

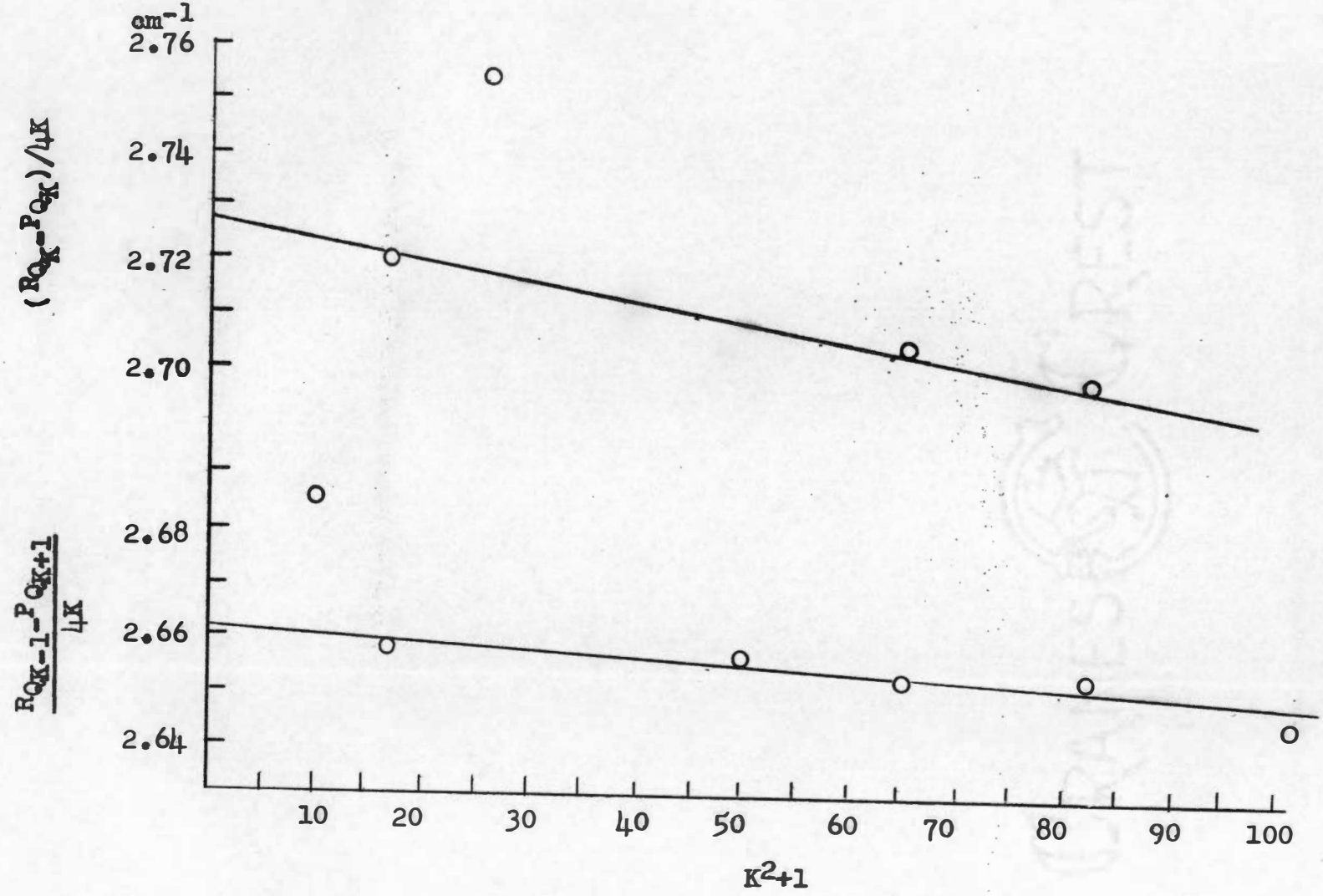

Figure 31. A plot of $(R_{Q_K}-P_{Q_K})/4K$ and $(R_{Q_{K-1}}-P_{Q_{K+1}})/4K$ versus K^2+1 for the Q lines of ν_4 of HCOF

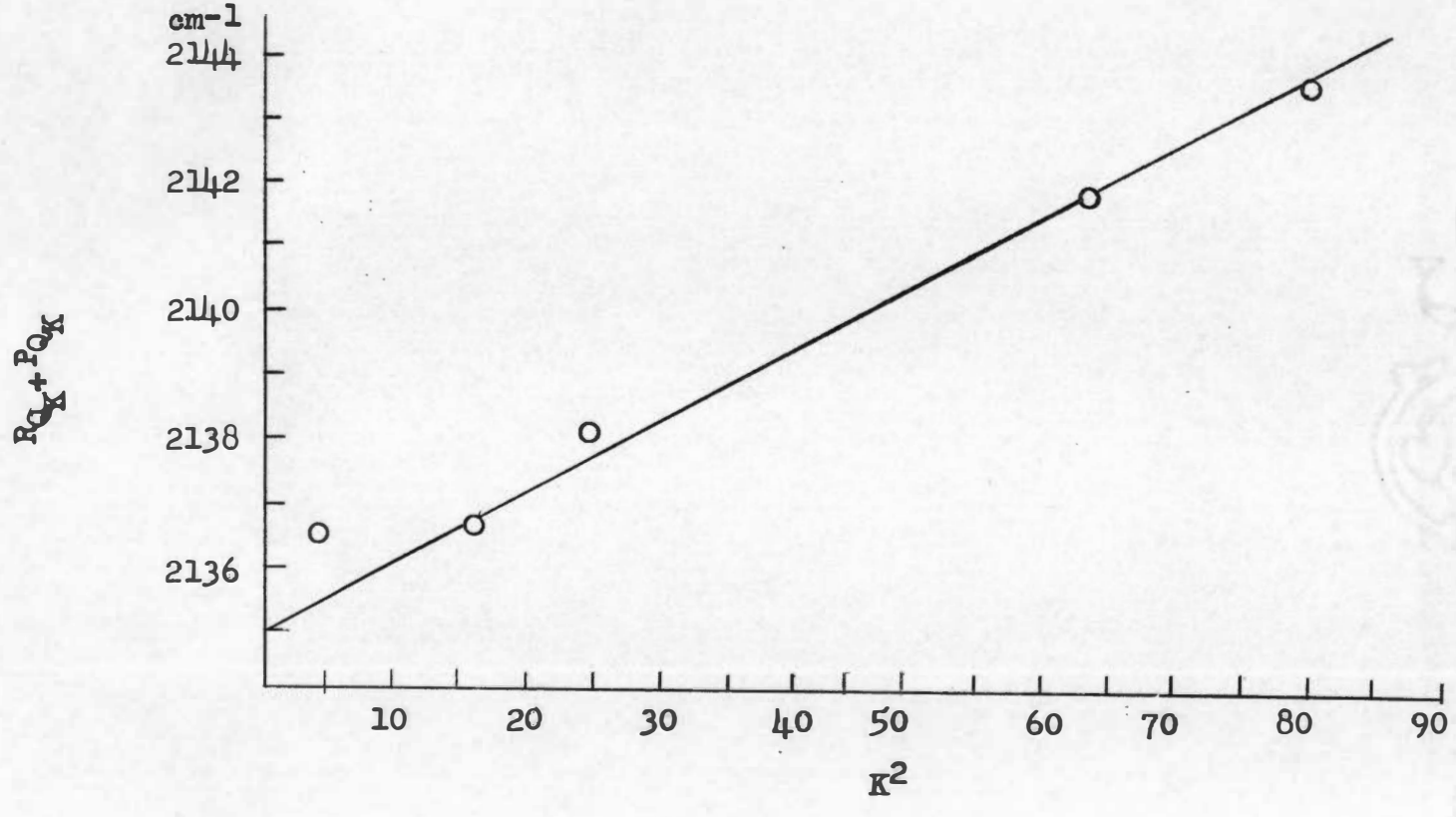

Figure 32. A plot of $R_{Q_K}+P_{Q_K}$ versus K^2 for the Q lines of ν_4 of HCOF

TABLE XVII

WAVE NUMBERS OF THE OBSERVED LINES OF THE PARALLEL COMPONENT OF ν_4 OF DCOF

J	R(J) (cm^{-1})	P(J) (cm^{-1})
0	-	-
1	-	1072.30
2	-	1071.44
3	-	1070.86
4	1076.52	1070.03
5	1077.22	1069.31
6	1078.06	1068.63
7	1078.81	1067.83
8	1079.64	1067.04
9	1080.22	1066.38
10	1081.28	1065.78
11	1081.63	1064.89
12	1082.27	1064.25
13	1082.86	1063.15
14	1083.57	1062.45
15	1084.41	1061.70
16	1085.14	1060.98
17	1085.90	1060.21
18	1086.41	1059.45
19	1087.18	1058.74
20	1088.00	1057.97
21	1088.68	1057.24
22	1089.39	1056.47
23	1089.91	1055.67
24	1090.66	1054.82
25	1091.22	1053.85
26	1091.86	1053.34
27	-	1052.47
28	-	1051.58
29	-	1050.78

TABLE XVII (continued)

WAVE NUMBERS OF THE OBSERVED LINES OF THE PARALLEL COMPONENT OF ν_4 OF DCOF

J	R(J) (cm^{-1})	P(J) (cm^{-1})
30	1094.62	1049.92
31	1095.24	1049.21
32	1095.84	1048.35
33	-	1047.50
34	-	1046.72

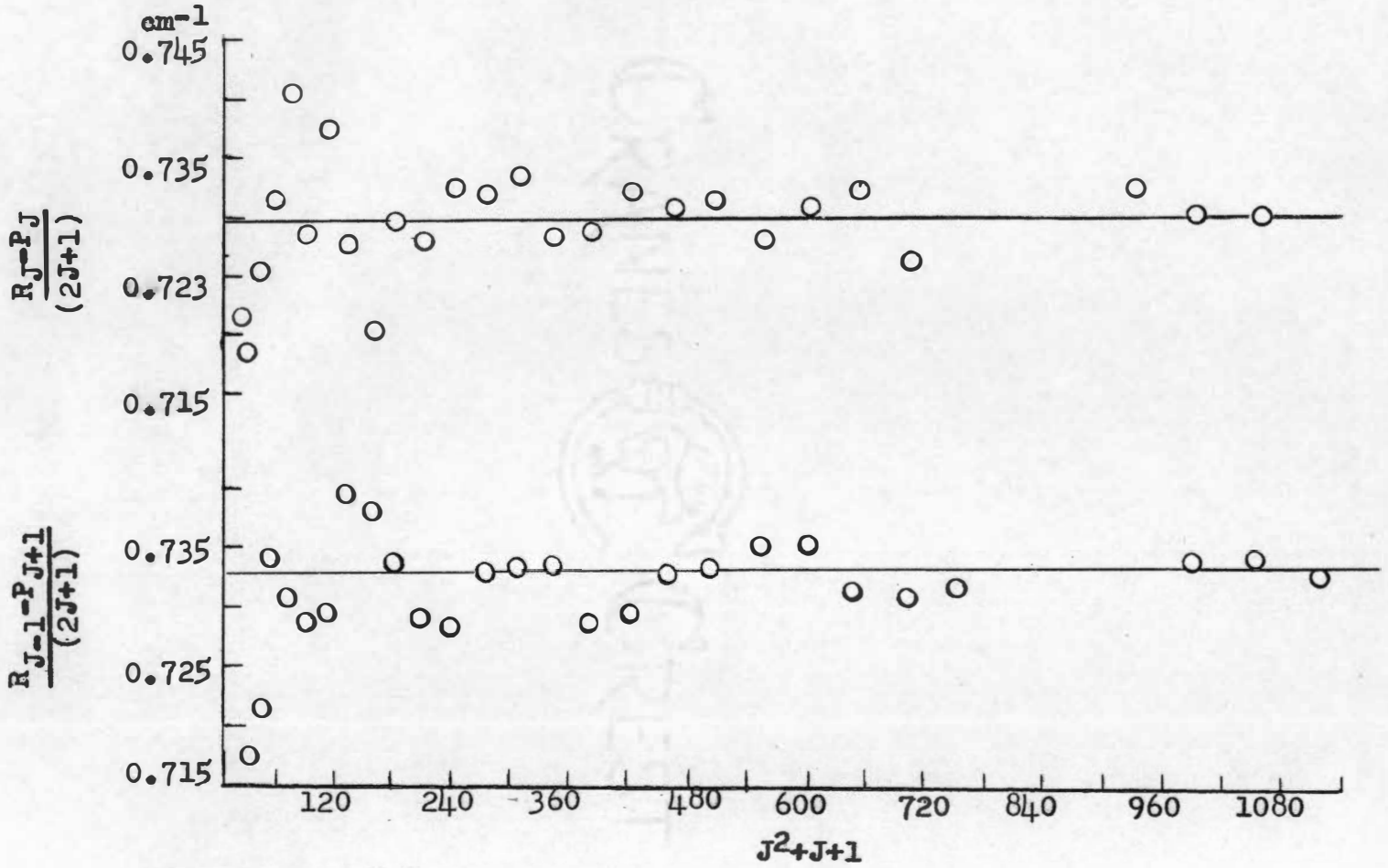

Figure 33. A plot of $(R_J-P_J)/(2J+1)$ and $(R_{J-1}-P_{J+1})/(2J+1)$ versus J^2+J+1 for the parallel component of ν_4 of DCOF

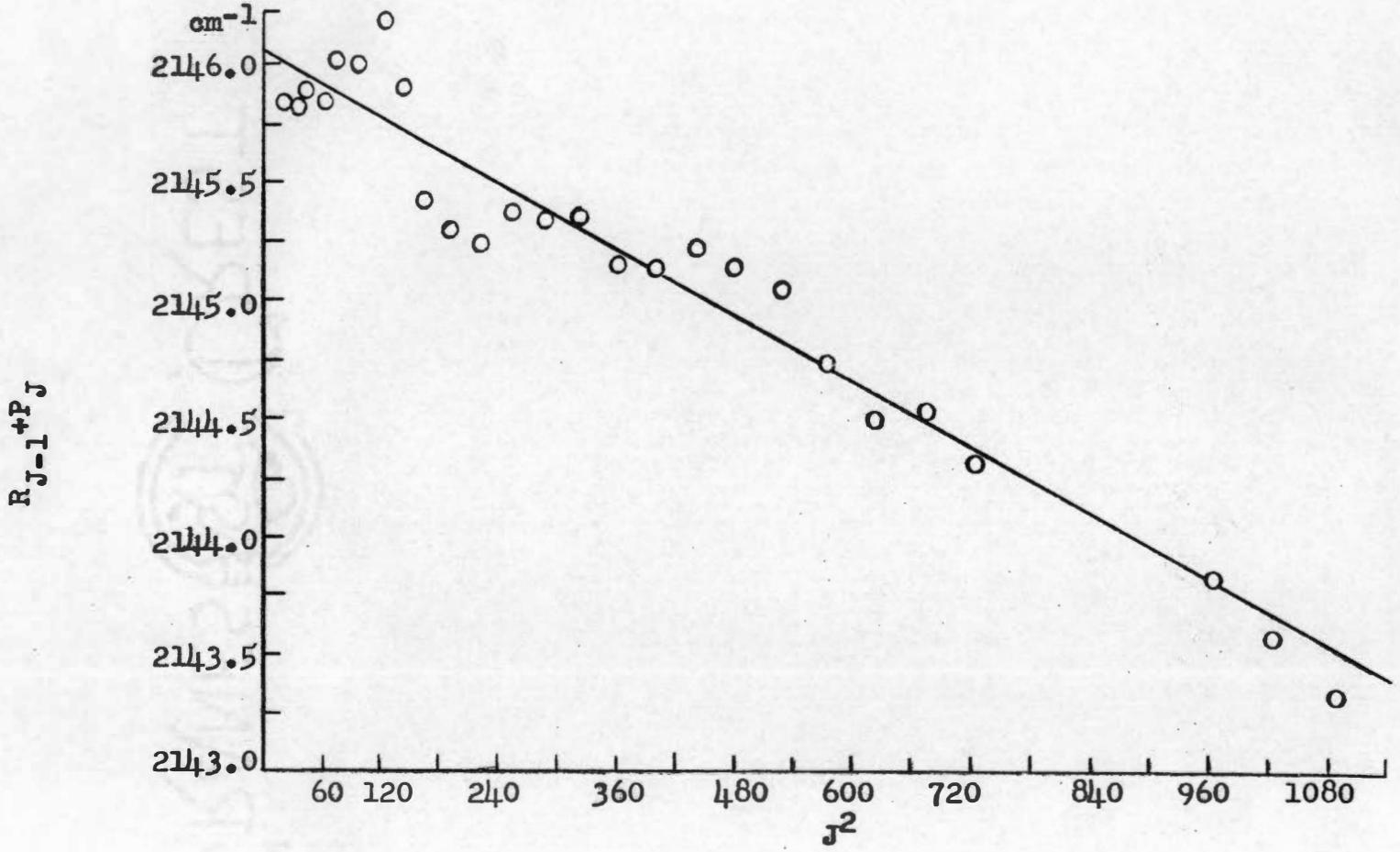

Figure 34. A plot of $(R_{J-1}+P_J)$ versus J^2 for the parallel component of ν_4 of DCOF

TABLE XVIII

WAVE NUMBERS OF THE OBSERVED Q LINES IN ν_4 OF DCOF

K	R_{Q_K} (cm^{-1})	P_{Q_K} (cm^{-1})
0	-	-
1	-	-
2	-	-
3	1086.13	-
4	1089.63	1060.98
5	1093.76	1057.24
6	1097.36	1053.67
7	1100.62	1049.92
8	1104.87	1046.72
9	1108.52	1043.28
10	1112.35	1039.95
11	1116.00	1036.52
12	1120.44	1033.16
13	1123.75	1029.90
14	1127.84	1026.57

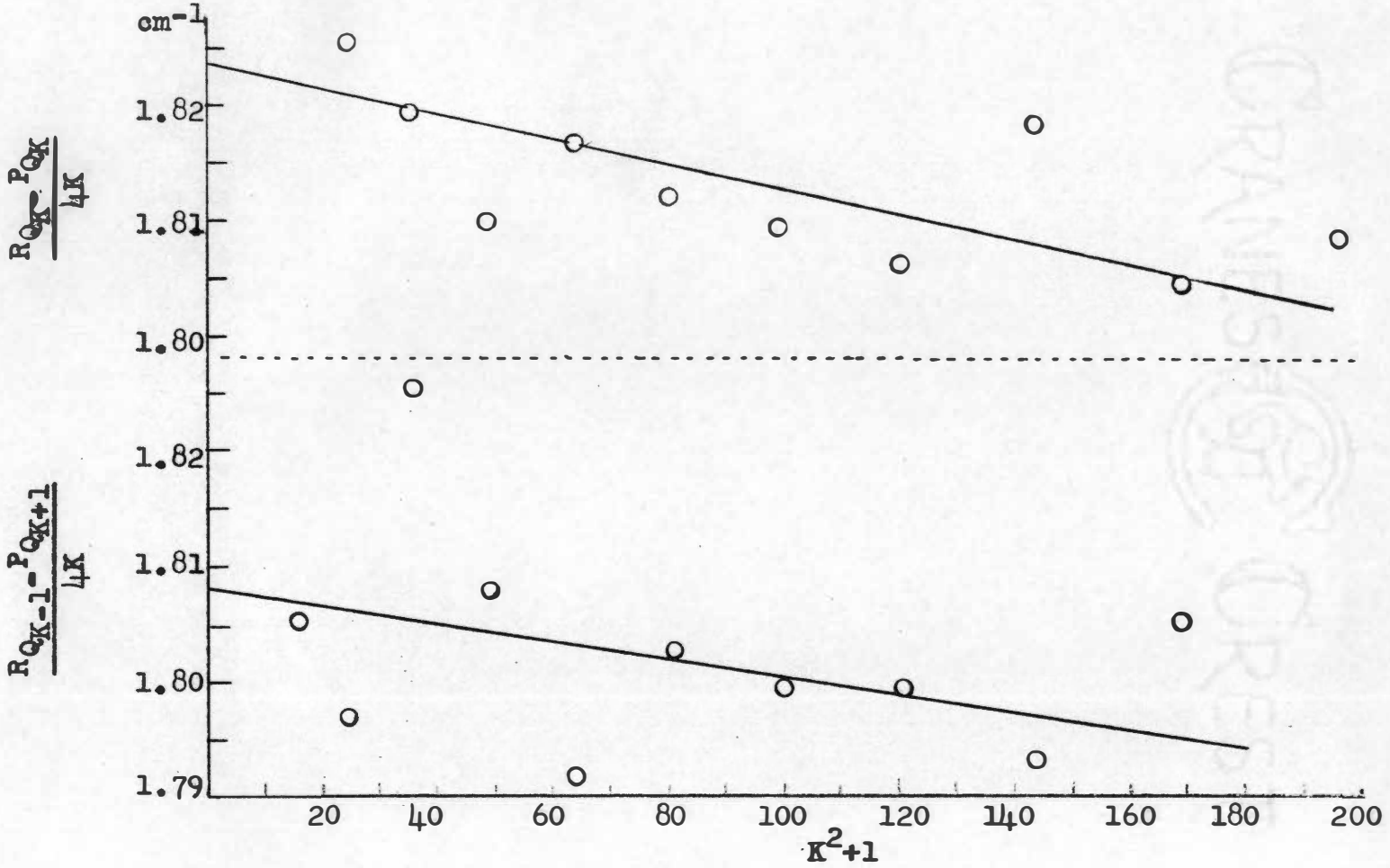

Figure 35. A plot of $(R_{Q_K} - P_{Q_K})/4K$ and $(R_{Q_{K-1}} - P_{Q_{K+1}})/4K$ versus K^2+1 for the Q lines of ν_4 of DCOF

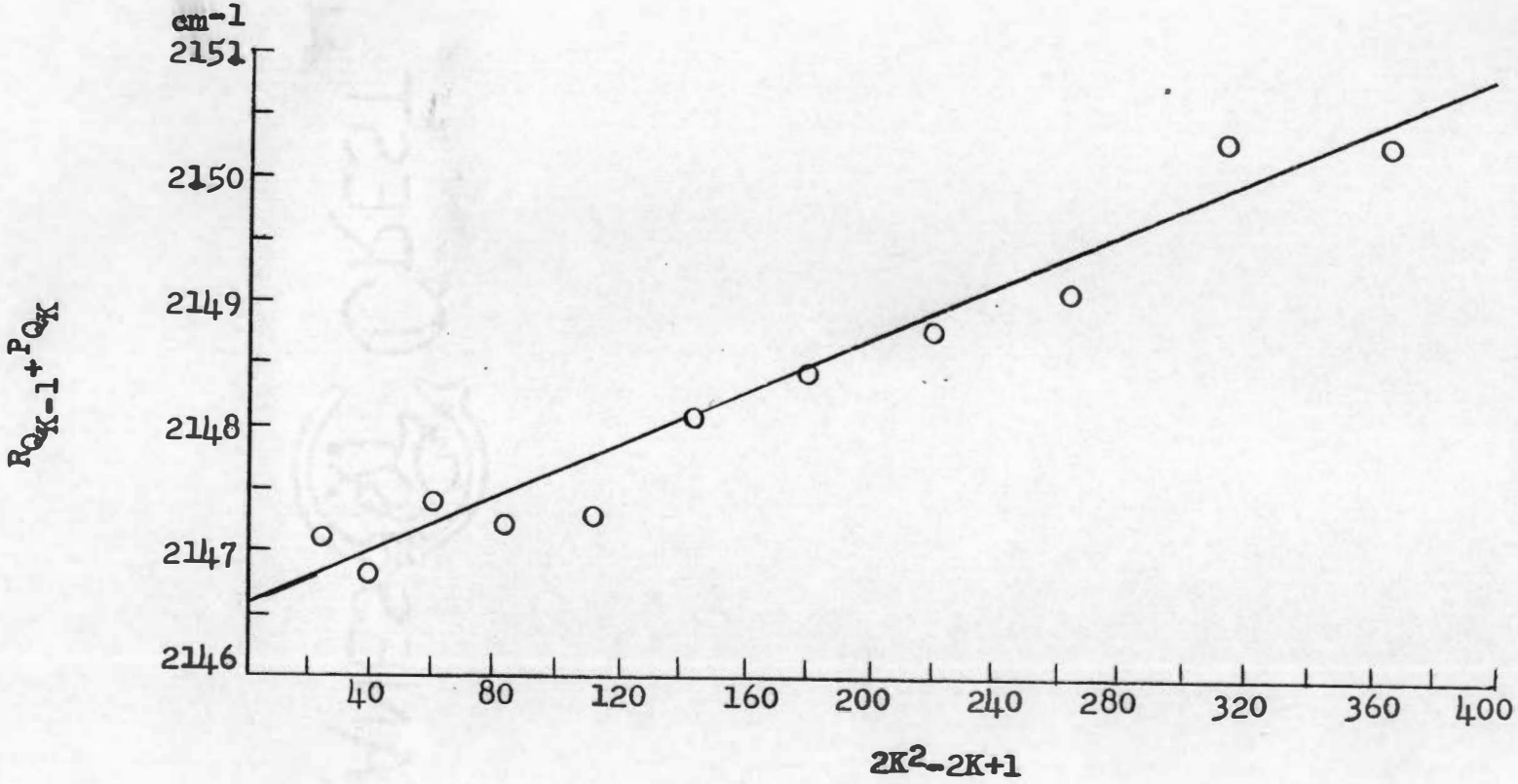

Figure 36. A plot of $({}^{R}Q_{K-1}+{}^{P}Q_{K})$ versus $(2K^2-2K+1)$ for the Q lines of ν_4 of DCOF

ν_5

The FCO bending vibration was the first fundamental to be carefully examined and the first to be analyzed. These bands were first examined using the thermocouple and then completely re-examined using the Golay detector. The perpendicular component was clearly resolved, and there was some indication of resolution in the parallel component, especially in HCOF. The results using the Golay detector were not noticeably better than those using the thermocouple.

In determining the band center for this fundamental, the combination relation involving $^{R}Q_{K}+^{P}Q_{K}$ was used, instead of the one involving $^{R}Q_{K-1}+^{P}Q_{K}$.

Figures 37 and 38 show this fundamental for HCOF and DCOF, respectively.

HCOF. A few lines were measured which appeared to be resolved lines of the parallel component. They appear on several, but not on all, of the records. Their position, if not their existence, is at least doubtful. They are not reported.

The assignment of the perpendicular component is unambiguous, and the constants obtained appear to be satisfactory. The observed Q lines are listed in Table XIX. The combination relations are given in Figures 39 and 40.

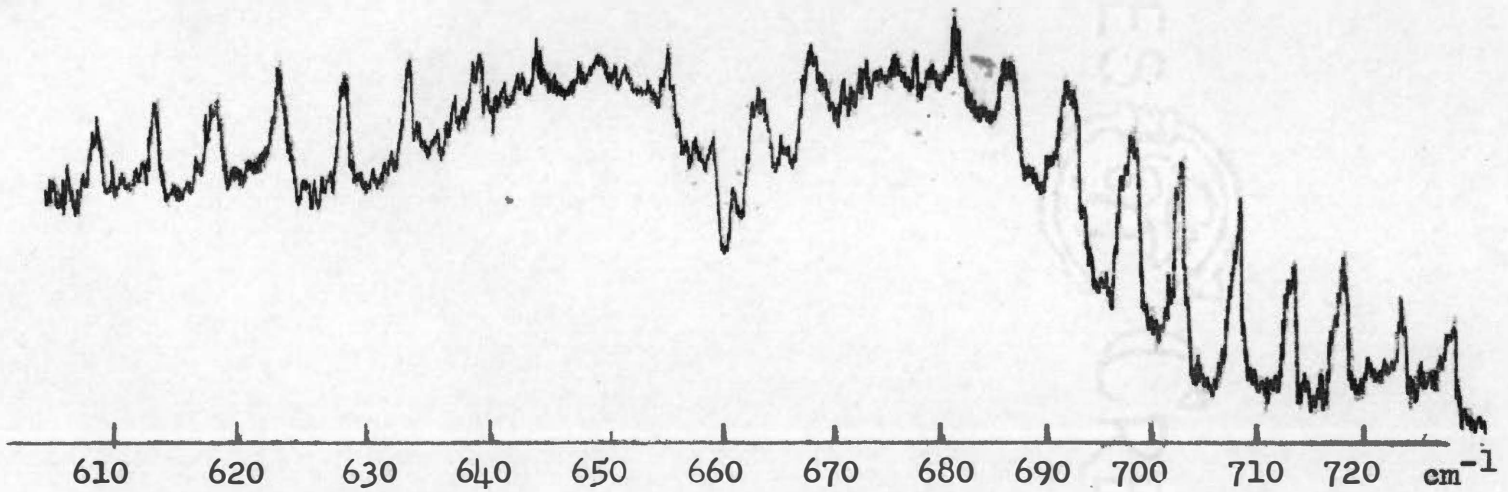

Figure 37. The ν_5 vibration-rotation band of HCOF

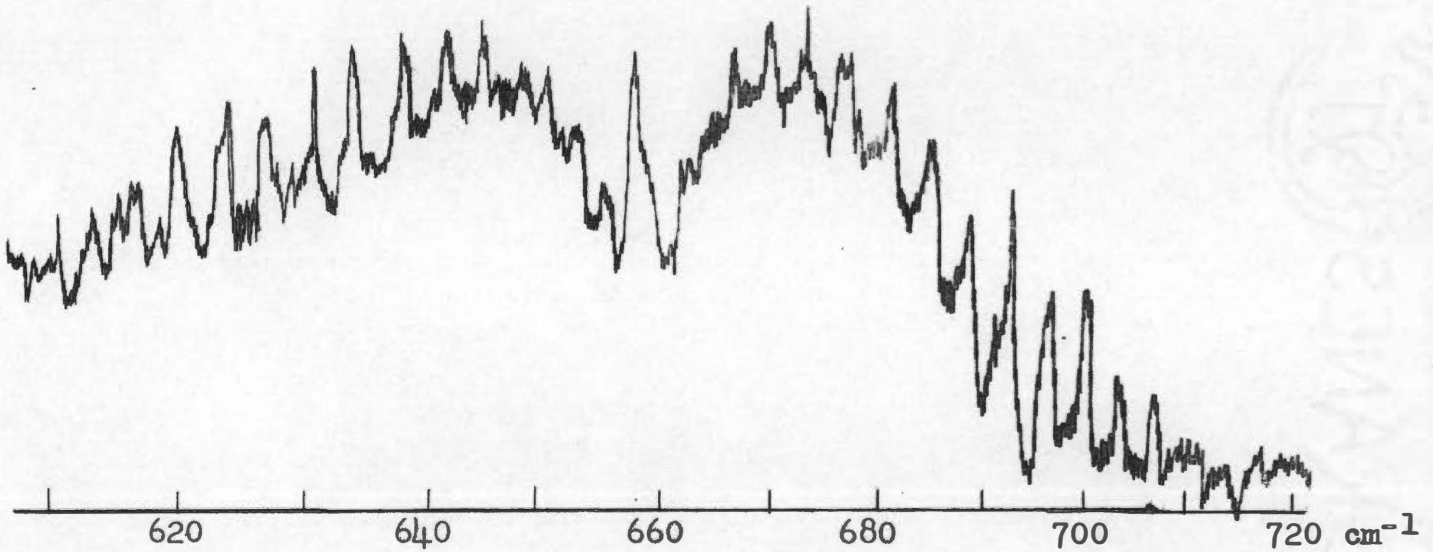

Figure 38. The ν_5 vibration-rotation band of DCOF

TABLE XIX

WAVE NUMBERS OF THE OBSERVED Q LINES IN ν_5 OF HCOF

K	R_{Q_K} (cm^{-1})	P_{Q_K} (cm^{-1})
Q Branch	663.20	
0	-	-
1	669.55	-
2	676.22	655.65
3	681.52	649.33
4	686.88	644.11
5	692.41	638.85
6	698.08	633.66
7	703.69	628.50
8	709.35	623.54
9	715.08	618.60
10	720.65	613.85
11	726.43	608.96
12	732.12	604.24
13	737.86	599.58
14	743.70	-

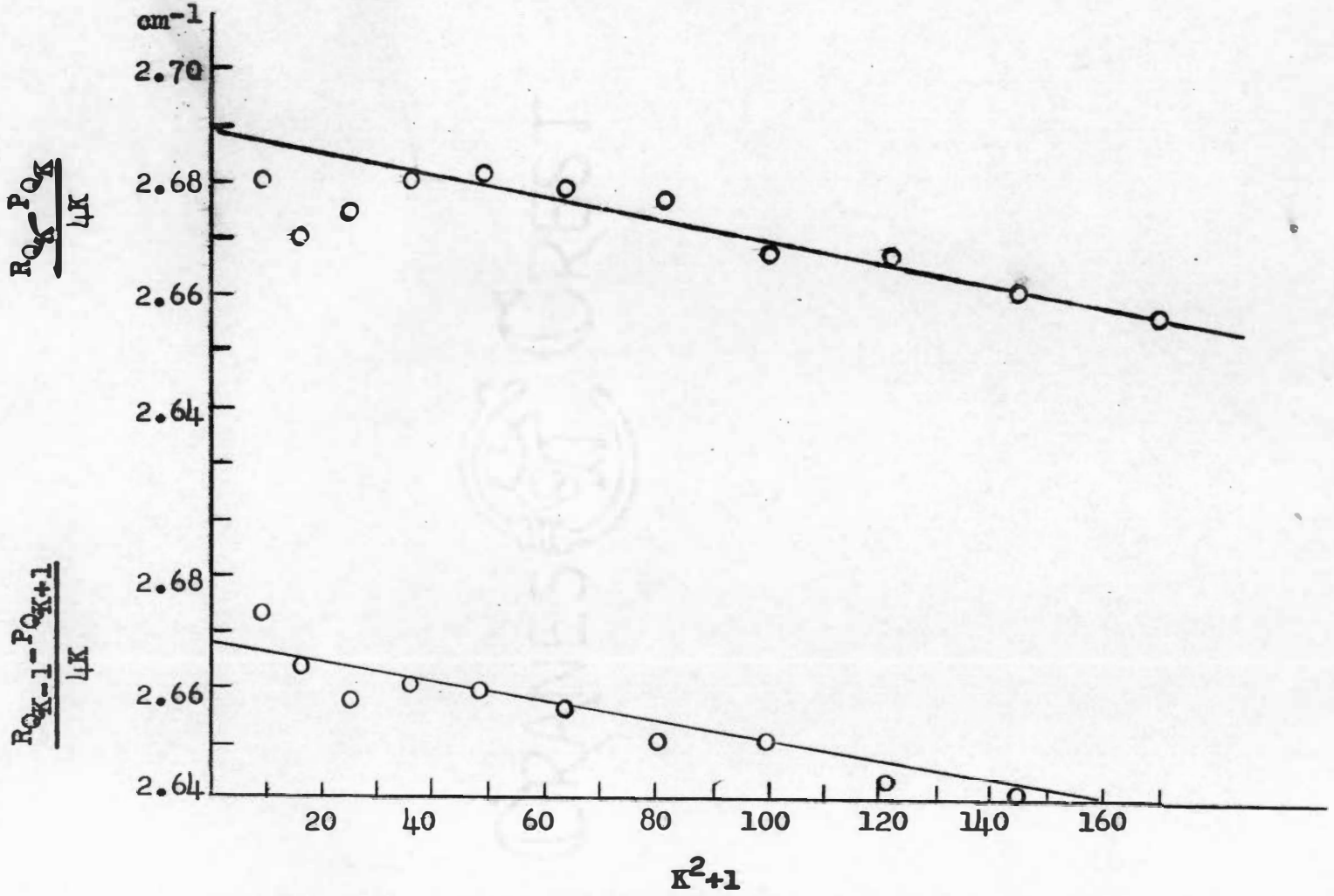

Figure 39. A plot of $(R_{Q_K} - P_{Q_K})/4K$ and $(R_{Q_{K-1}} - P_{Q_{K+1}})/4K$ versus K^2+1 for the Q lines of ν_5 of HCOF

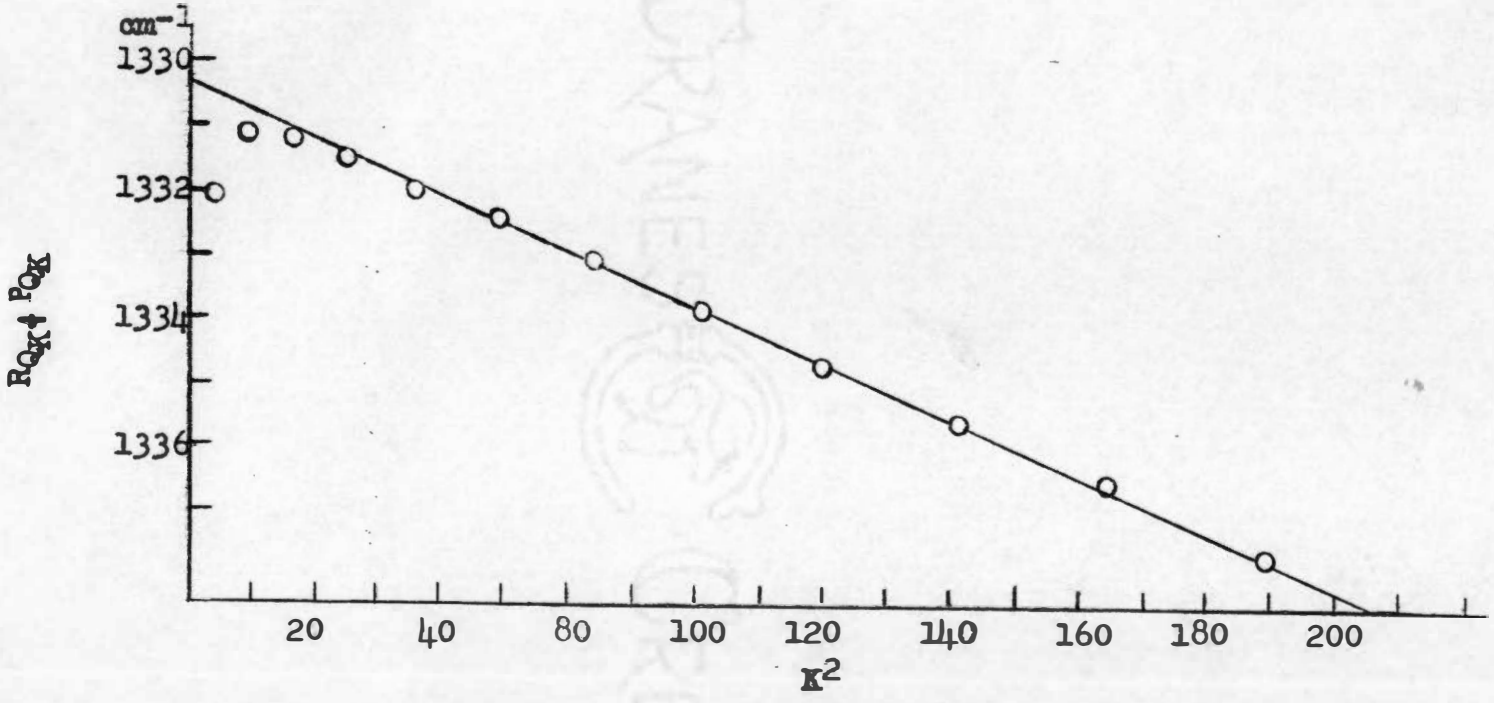

Figure 40. A plot of $(R_{Q_K} + P_{Q_K})$ versus K^2 for the Q lines of ν_5 of HCOF

DCOF. The central Q branch belonging to the parallel component is clearly defined, but, even where there was some indication of lines with $\Delta J=\pm 1$, they could not be measured.

The assignment of the perpendicular component was straightforward and appeared to give satisfactory constants. The observed lines are listed in Table XX, and the combination relations are shown in Figures 41 and 42.

ν_6

The out-of-plane C-H bending vibration in DCOF has been assigned, but no band has been observed in HCOF which can be assigned as such. It is thought[2] that if this band occured in HCOF it would lie at about the same position as ν_4. Since ν_4 absorbs totally at about one-tenth the pressure which would, by comparison with DCOF, probably be required to observe ν_6, we would expect ν_4 to obscure ν_6.

The observed band in DCOF (see Figure 43) appears to have a sharp cut off on the high frequency side. This band, which resembles no other observed band in either HCOF or DCOF, has a weak "P" branch at 856.5 cm^{-1}, a "Q" branch at 857.4 cm^{-1}, and an "R" branch at 858.0 cm^{-1}. Figure 43, unlike the other figures, is reproduced from a record made at 1° per hour and is not greatly reduced.

---

[2]Morgan, Staats, and Goldstein.

TABLE XX

WAVE NUMBERS OF THE OBSERVED Q LINES IN ν_5 OF DCOF

K	RQ_K (cm^{-1})	PQ_K (cm^{-1})
Q Branch	657.78	-
0	-	-
1	-	655.38
2	667.90	-
3	670.22	647.86
4	673.60	644.90
5	677.44	641.30
6	681.11	637.71
7	684.80	634.16
8	688.56	630.53
9	692.38	627.04
10	696.04	623.62
11	699.85	620.26
12	703.65	616.80
13	707.37	613.55
14	711.28	610.08
15	715.06	607.01
16		603.66

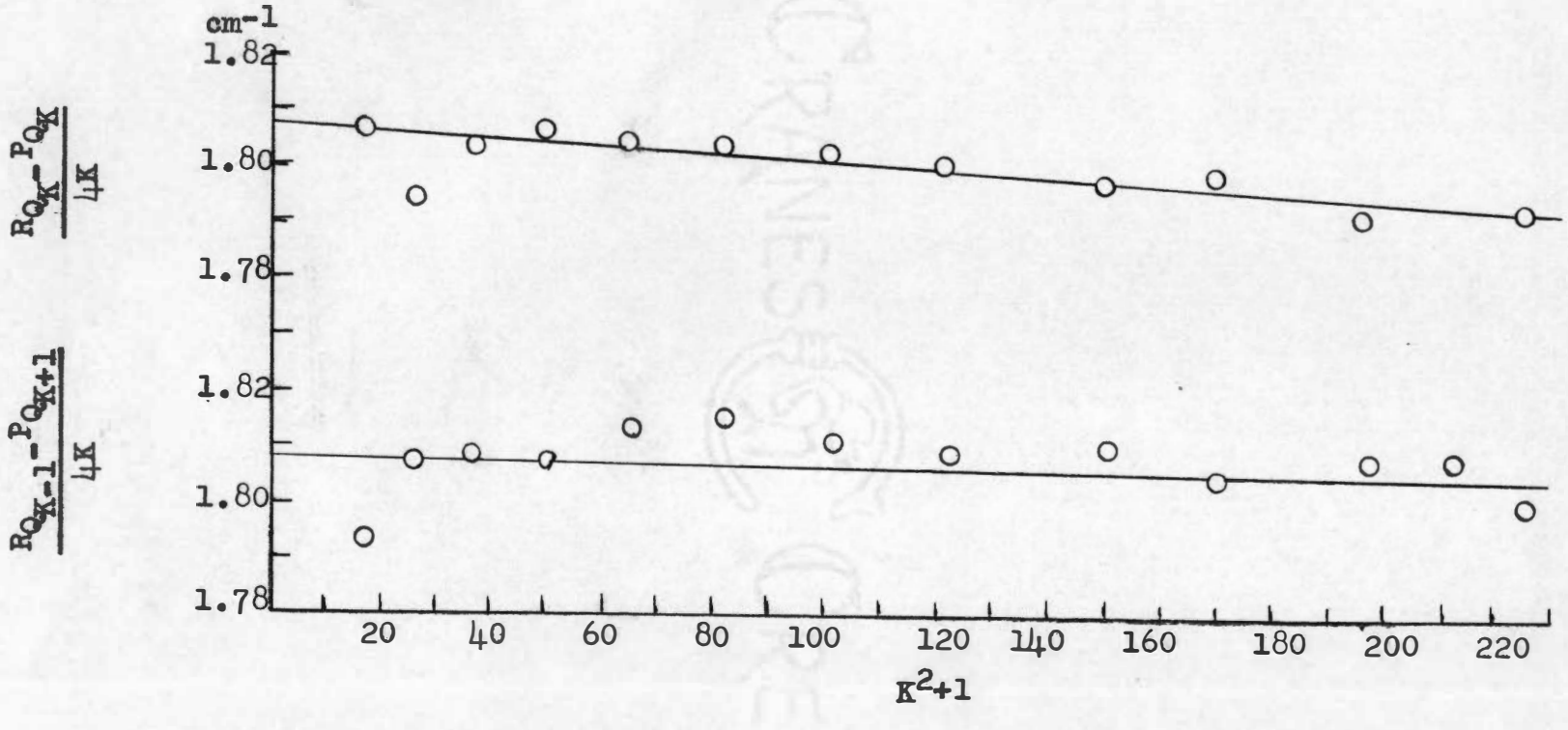

Figure 41. A plot of $(R_{Q_{K-1}}+P_{Q_{K+1}})/4K$ and $(R_{Q_K}-P_{Q_K})/4K$ versus K^2+1 for the Q lines of ν_5 of DCOF

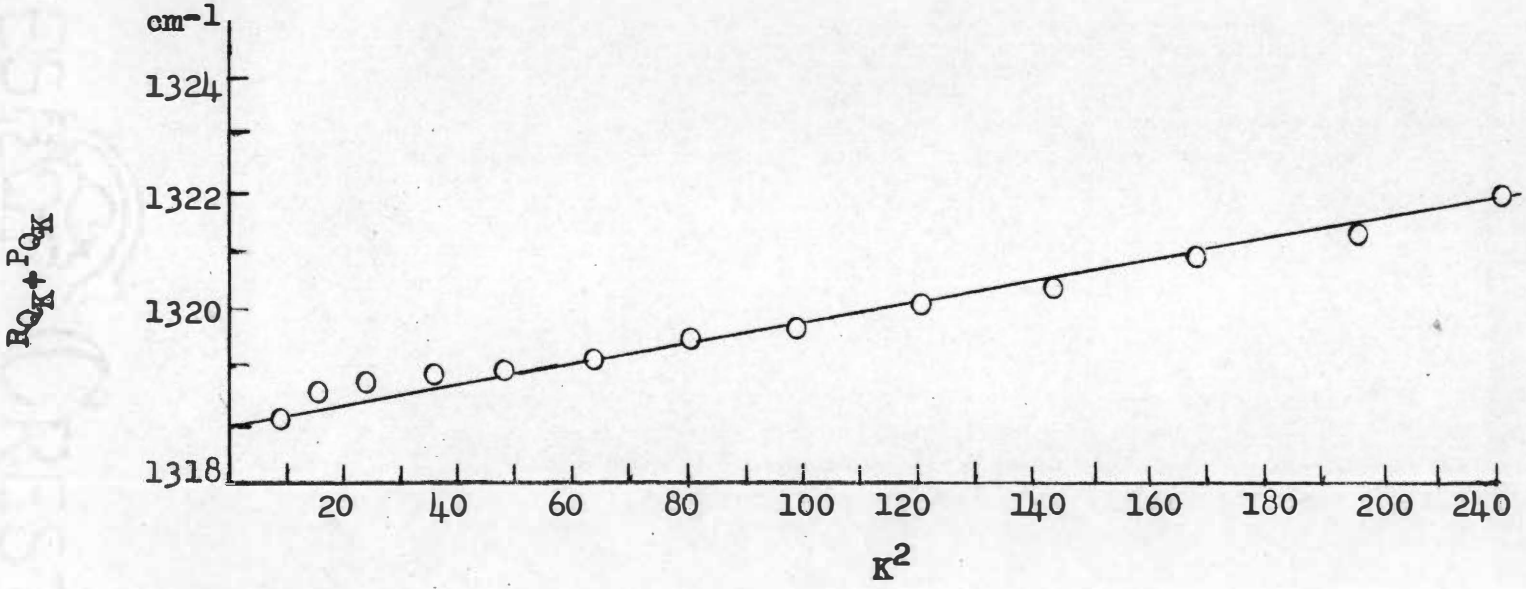

Figure 42. A plot of ($R_{Q_K} + P_{Q_K}$) versus K^2 for the Q lines of ν_5 of DCOF

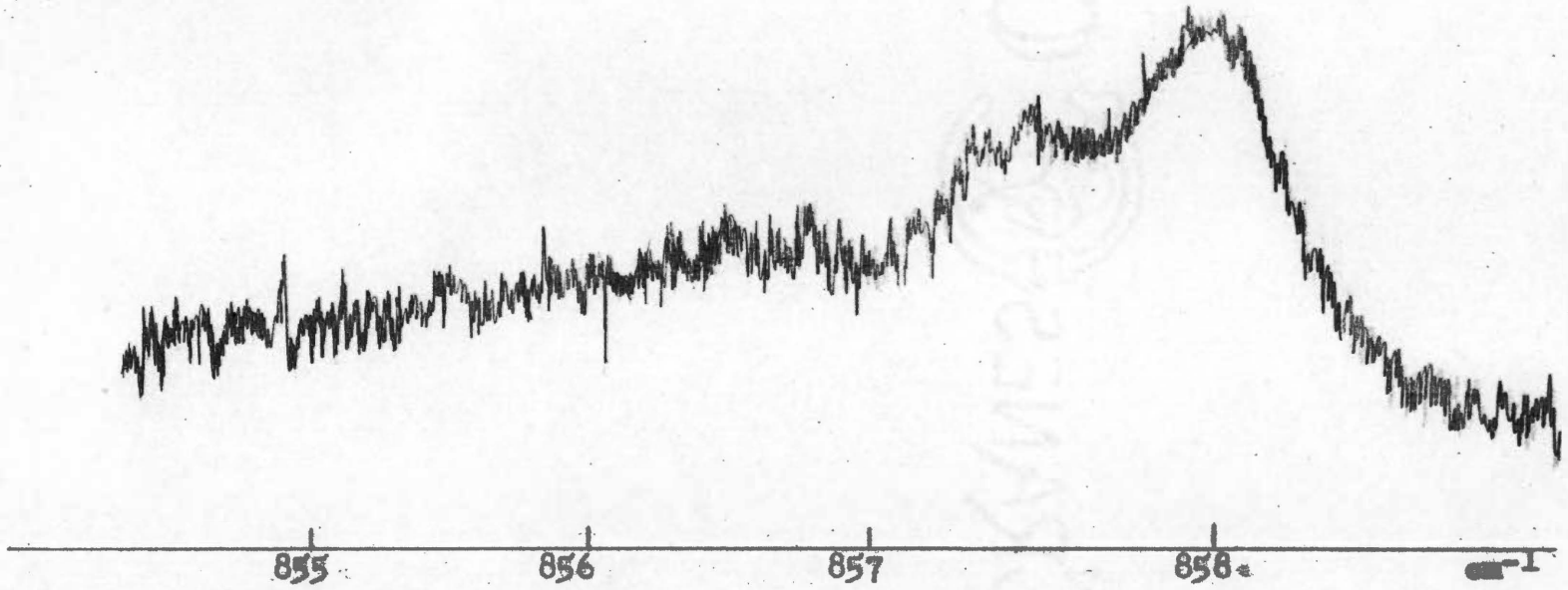

Figure 43. The ν_6 vibration-rotation band of DCOF

The Overtone and Combination Bands

$2\nu_2$

The overtone of the C=O stretching vibration in both molecules is observed as a relatively weak, fairly well resolved parallel band with the central Q branch not completely separated from the P branch. Figures 44 and 45 show the observed bands. Unfortunately, the only record of this band in HCOF which is suitable for reproduction as a figure was made with too high a pressure and a strong background. These bands were not assigned.

HCOF. All of the records of this band were made with a strong background. There are regions in both the P and R branches which are free from background interference. A number of lines were observed in each of these regions. The observed lines are listed in Table XXI. The exact location of the central Q branch is difficult to determine, because there is a water line in almost exactly the same location.

DCOF. As a result of the greater experience of the author when this band was observed, the background was almost completely removed. The observed lines of DCOF are listed in Table XXII.

$2\nu_3$ and $\nu_4+\nu_6$

A band is observed in DCOF at about 1930 cm^{-1} which Morgan, Staats, and Goldstein assigned as the overtone of the planar C-H bending vibration, $2\nu_3$. This band, shown in

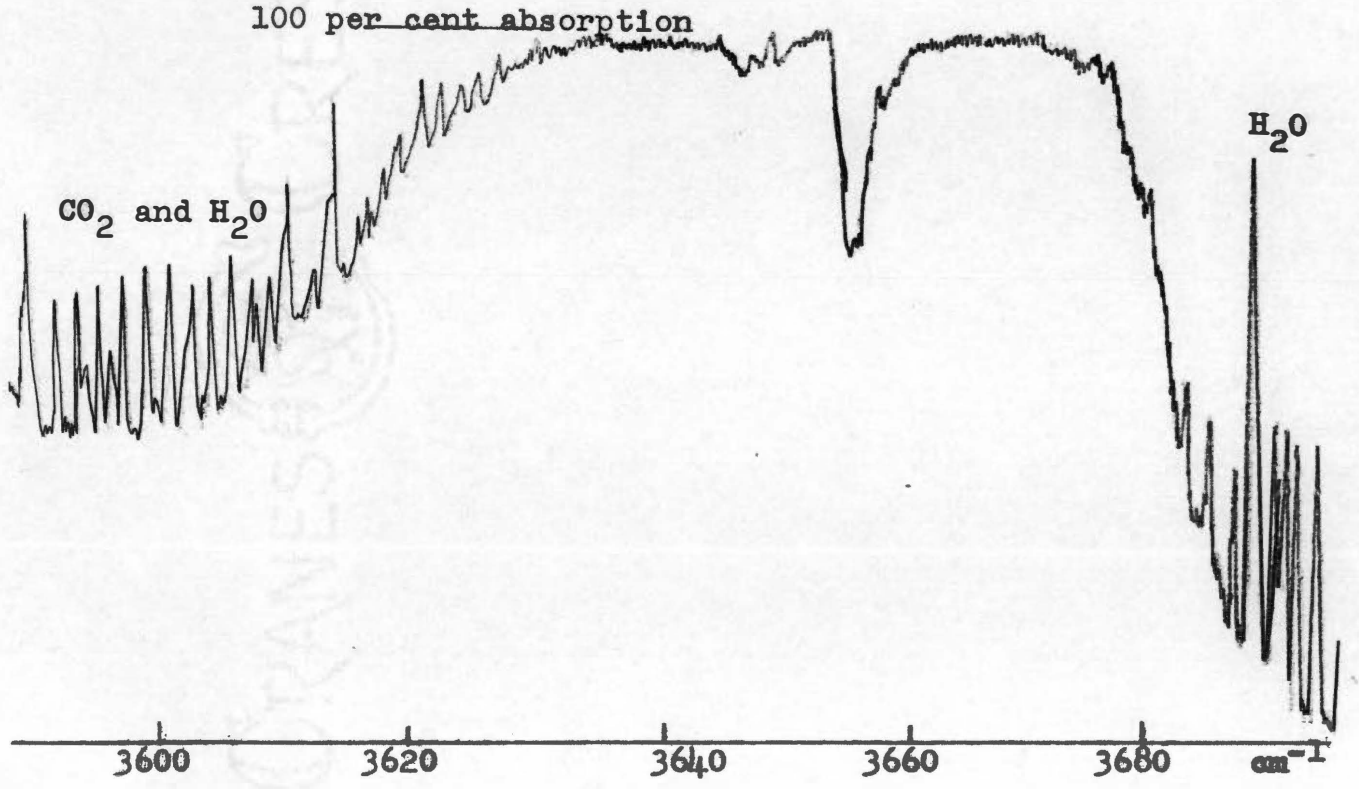

Figure 44. The $2\nu_2$ vibration-rotation band of HCOF

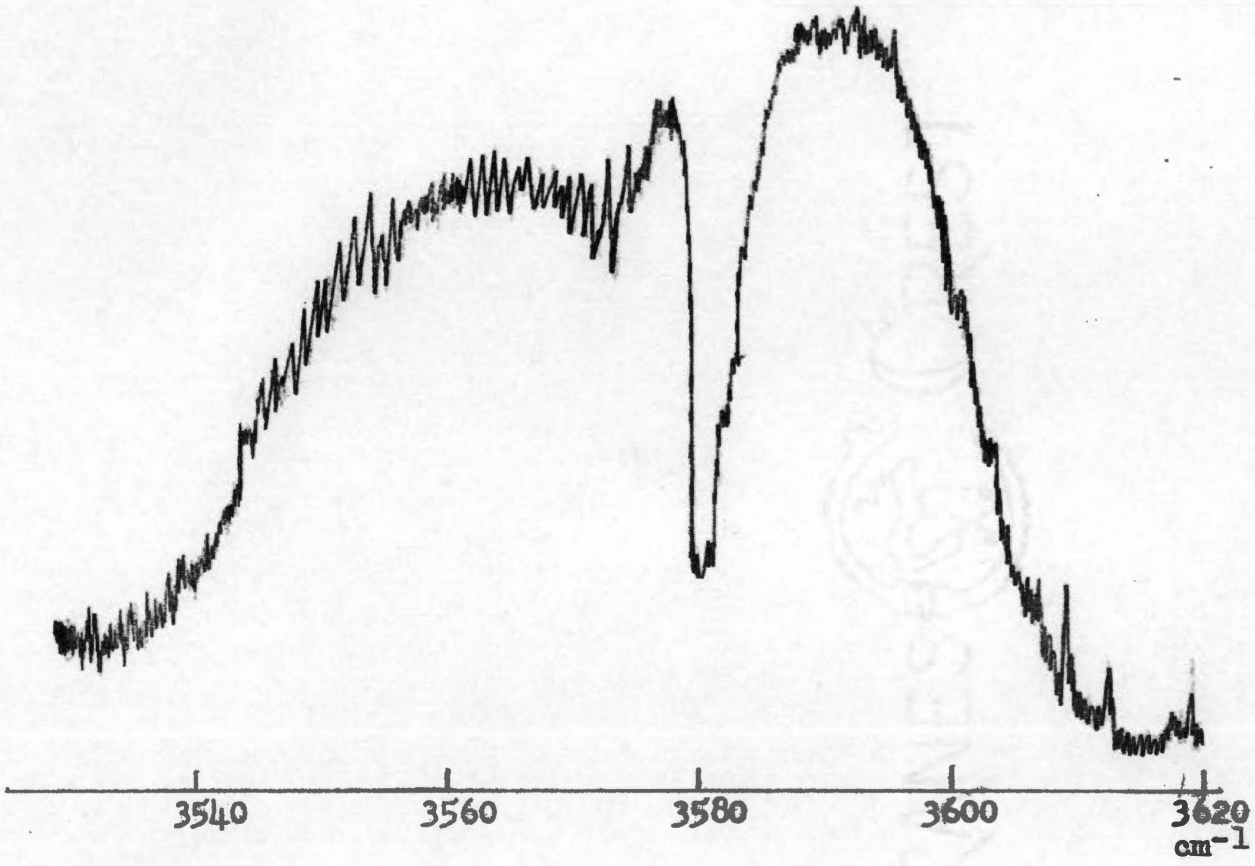

Figure 45. The $2\nu_2$ vibration-rotation band of DCOF

TABLE XXI

WAVE NUMBERS OF THE OBSERVED LINES IN $2\nu_2$ OF HCOF

Chart Number	$\tilde{\nu}$ (cm^{-1})	Chart Number	$\tilde{\nu}$ (cm^{-1})
-22	3630.09	0	3651.79
-20	3631.95	+2	3654.12
-19	3632.90	2?	3654.92
-17	3634.78	+3?	3656.76
-16	3635.69	+4	3657.67
-15	3636.57	+5	3658.34
-14	3637.41	6	3658.90
-12	3639.03	7	3659.72
-11	3639.88	8	3660.24
-10	3640.68	9	3660.91
-9	3641.56	10	3661.54
-8	3642.46	11	3662.16
-7	3643.17	12	3662.77
-6	3643.97	13	3663.44
-5	3644.72	14	3664.04
-4	3645.17	15	3664.56
-3	3645.66	16	3665.26
		17	3665.80
		23	3671.92
		24	3672.59
		25	3673.13

TABLE XXII

WAVE NUMBERS OF THE OBSERVED LINES IN $2\nu_2$ OF DCOF

Chart Number	$\tilde{\nu}$ (cm^{-1})	Chart Number	$\tilde{\nu}$ (cm^{-1})
-40	3542.21	-17	3564.39
-39	3542.75	-16	3565.34
-38	3543.89	-15	3566.11
-37	3544.79	-14	3567.00
-36	3545.99	-13	3567.76
-35	3546.89	-12	3568.74
-34	3547.88	-11	3569.56
-33	3548.97	-10	3570.55
-32	3549.75	-9	3571.30
-31	3550.99	-8	3573.12
-30	3552.02	-7	3572.57
-29	3553.20	-6	3573.80
-28	3553.88	-5	3574.15
-27	3554.91	-4	3574.88
-26	3555.58	-3	3575.52
-23	3558.66	-2	3576.20
-21	3560.86	-1	3576.82
-20	3561.74	0	3577.40
-19	3562.46	ν_o (est.)	3579.35
-18	3563.33		

TABLE XXII (continued)

WAVE NUMBERS OF THE OBSERVED LINES
IN $2\nu_2$ OF DCOF

Chart Number	$\tilde{\nu}$ (cm^{-1})	Chart Number	$\tilde{\nu}$ (cm^{-1})
1	3580.41	17	3591.31
2	3581.37	18	3591.86
3	3582.10	19	3592.49
4	3582.62	20	3593.05
5	3583.27	21	3593.62
6	3583.98	22	3594.15
7	3584.62	23	3594.68
9	3586.53	24	3595.30
10	3587.17	25	3595.65
11	3587.81		
12	3588.45		
13	3588.92		
14	3589.42		
15	3590.07		
16	3590.70		

Figure 46, exhibits two Q branches under higher resolution: one at 1928.4 cm^{-1} and the other at 1930.6 cm^{-1}. The Q branch at 1928.4 cm^{-1} is assigned to $\nu_4+\nu_6$, and the other Q branch, together with the P and R branches, is assigned to $2\nu_3$. The assignment of the bulk of the band to $2\nu_3$ seems to be entirely reasonable, since ν_3 is quite strong, and the assignment of the extra Q branch to $\nu_4+\nu_6$ seems to be unavoidable. There is no other assignment that would fit the observed band. The second overtone of the F-C=O bending vibration would be in approximately this region if it were observed, but since $2\nu_5$ is not observed, it is very improbable that $3\nu_5$ would be observed. The sample was originally quite pure, and none of the decomposition products absorb in this region, so it is unlikely that the absorption is due to an impurity. The observed lines of this band are listed in Table XXIII.

No corresponding bands are observed in HCOF.

$2\nu_4$

The overtone of the C-F stretching vibration, $2\nu_4$, appears to be a well resolved parallel band in both molecules, but a closer examination shows that many of the observed rotational lines are unresolved pairs of lines. It was at first planned to analyze these bands, but this was not done since it was felt that this would be a needless

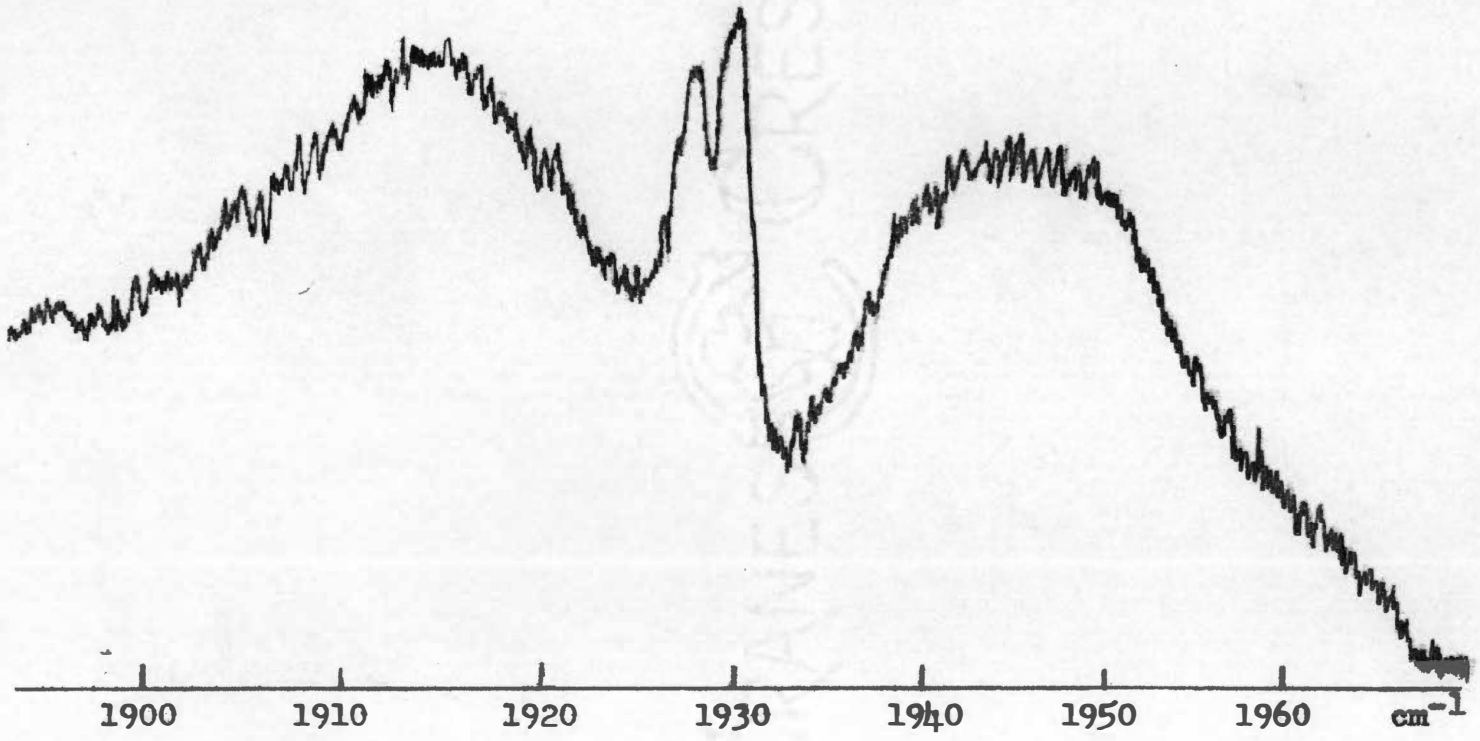

Figure 46. The $2\nu_3$ and $\nu_4+\nu_6$ vibration-rotation band of DCOF

TABLE XXIII

WAVE NUMBERS OF THE OBSERVED LINES IN $2\nu_3$ AND $\nu_4+\nu_6$ (TENTATIVE ASSIGNMENT) OF DCOF

J	R(J) (cm^{-1})	P(J) (cm^{-1})
0	1931.65	-
1	1932.14	-
2	1932.92	-
3	1933.71	-
4	1934.46	-
5	1935.56	-
6	1935.88	1927.29
7	1936.73	1926.52
8	1937.31	1925.74
9	1938.04	1924.89
10	-	1924.20
11	-	1923.53
12	-	1922.86
13	1940.48	1922.11
14	1941.16	1921.36
15	1941.81	1920.71
16	1942.37	1919.98
17	1942.98	1919.24
18	1943.61	1918.68
19	1944.37	1917.97
20	1945.09	1917.29
21	1945.83	1916.63
22	1946.54	1915.85
23	1947.45	1915.16
24	1948.22	1914.57
25	1948.91	1913.96
26	1949.59	1913.36
27	1950.25	1912.59
28	1950.84	1911.79
29	1951.43	-

duplication of the work of Wilson[3] and Wilkinson, who have examined the spectrum of HCOF and DCOF at wave numbers greater than about 1500 using a high resolution spectrometer. Figures 47 and 48 show these bands.

HCOF. Although this band appears to be parallel in type, there is no central Q branch, nor did one appear when the band was observed with an increased pressure. The observed lines are given in Table XXIV.

DCOF. There are no unusual features in this band, other than the unresolved rotational structure. The band appears to be well resolved, but a careful examination indicated that many of the lines are at least double. The observed lines are listed in Table XXV.

$\nu_3+\nu_4$

HCOF. When this band was recorded, the sample is known to have contained relatively large amounts of CO and CO_2, and probably some formic acid. The total amount of gas remaining was inadequate to give even moderately strong absorption. This band lies immediately on the high frequency side of a strong band due to CO_2 and might not have been noticed if it had not previously been reported by Morgan, Staats, and Goldstein. It is not shown in a figure.

---

[3] Wilson, private communication.

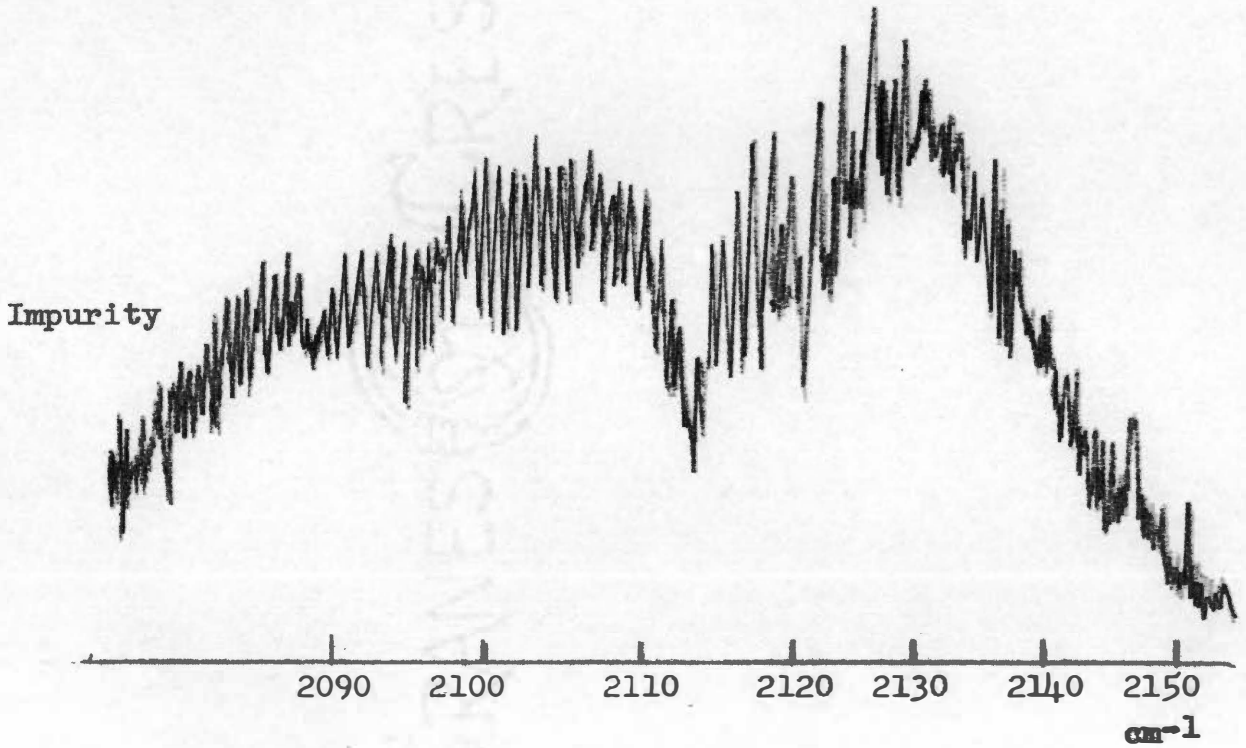

Figure 47. The $2\nu_4$ vibration-rotation band of HCOF

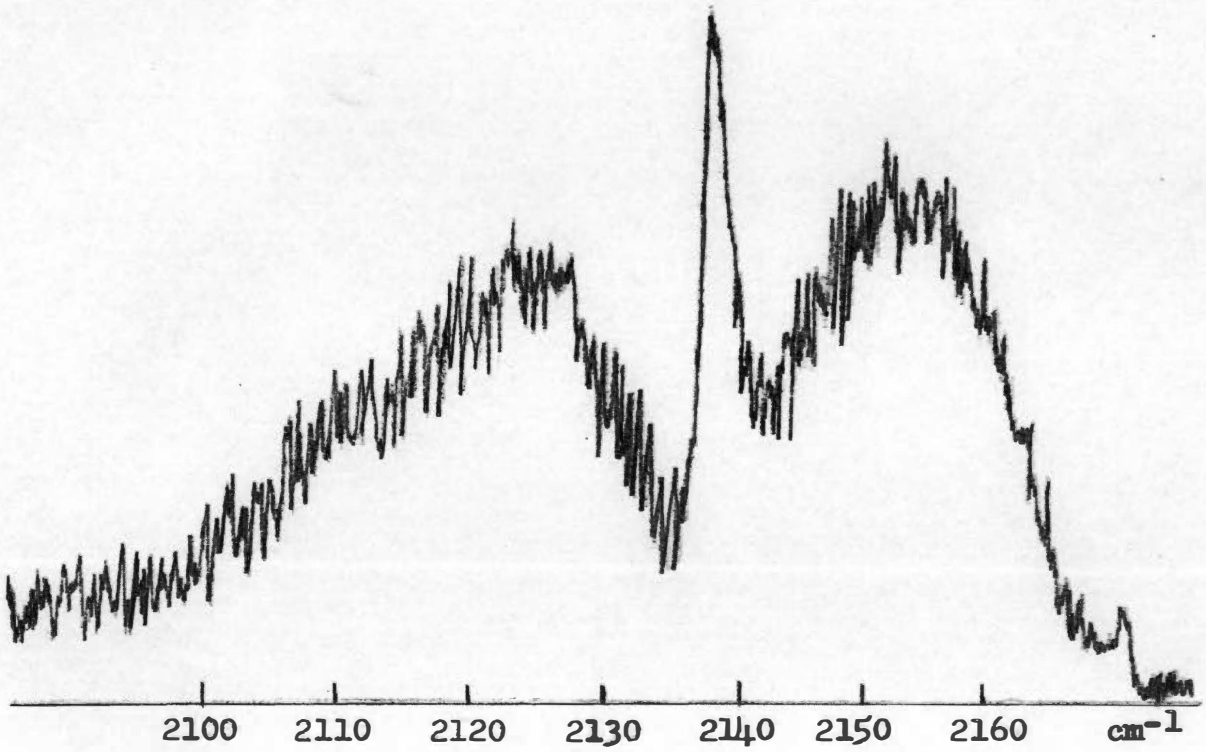

Figure. 48. The $2\nu_4$ vibration-rotation band of DCOF

TABLE XXIV

WAVE NUMBERS OF THE OBSERVED LINES
IN $2\nu_4$ OF HCOF

Chart Number	$\tilde{\nu}$ (cm^{-1})	Chart Number	$\tilde{\nu}$ (cm^{-1})
-52	2081.10	-18	2102.08
-50	2082.88	-17	2102.97
-49	2083.64	-16	2103.83
-48	2084.12	-15	2104.62
-47	2084.72	-14	2105.51
-46	2085.26	-13	2106.32
-45	2085.86	-12	2107.20
-43	2086.67	-10	2107.96
-42	2087.07	-9	2108.84
-41	2087.61	-8	2109.54
-40	2088.16	-7	2110.32
-39	2088.64	-6	2111.01
-38	2088.97	-5	2111.93
-37	2089.39	-4	2112.70
-36	2089.74	-3	2113.49
-34	2091.51	-2	2114.23
-33	2092.42	-1	2115.63
-32	2093.45		
-31	2094.32	+2	2116.39
-29	2095.33	+3	2117.15
-28	2095.94	4	2118.11
-27	2096.37	5	2118.89
-26	2096.92	6	2119.39
-25	2097.28	7	2120.21
-24	2097.75	8	2120.87
-23	2098.12	9	2121.62
-22	2098.60	10	2122.25
-21	2099.44	11	2122.87
-20	2100.29	12	2124.09
-19	2101.16	13	2124.62

TABLE XXIV (continued)

WAVE NUMBERS OF THE OBSERVED LINES IN $2\nu_4$ OF HCOF

Chart Number	$\tilde{\nu}$ (cm^{-1})	Chart Number	$\tilde{\nu}$ (cm^{-1})
14	2125.26	29	2132.58
15	2125.86	30	2133.16
16	2126.14	31	2133.79
17	2126.39	32	2134.37
18	2126.72	33	2134.90
18½	2127.04	35	2136.13
19	2127.31	36	2136.74
22	2128.49	37	2137.22
23	2129.05	38	2137.77
24	2129.50	39	2138.34
25	2130.23	40	2138.88
26	2130.67	44	2142.81
26½	2130.98	45	2143.27
27	2131.33	46	2143.77
28	2131.94	47	2144.40

TABLE XXV

WAVE NUMBERS OF THE OBSERVED LINES IN $2\nu_4$ OF DCOF

Chart Number	$\tilde{\nu}$ (cm^{-1})	Chart Number	$\tilde{\nu}$ (cm^{-1})
-79	2097.31	-46	2113.61
-78	2097.60	-44	2114.54
-76	2098.67	-43	2114.87
-75	2099.08	-42	2115.62
-74	2099.64	-41	2116.22
-73	2100.52	-40	2116.56
-72	2100.75	-39	2117.01
-71	2101.36	-38	2117.40
-70	2101.70	-37	2117.95
-69	2102.33	-36	2118.26
-68	2102.71	-35	2118.66
-67	2103.27	-34	2119.05
-66	2103.70	-33	2119.52
-65	2104.58	-32	2119.83
-64	2105.40	-31	2120.37
-63	2105.70	-30	2120.81
-62	2106.30	-29	2121.28
-61	2106.60	-28	2121.70
-60	2107.20	-27	2122.12
-59	2107.43	-26	2122.51
-58	2107.62	-25	2123.02
-57	2108.41	-24	2123.40
-56	2109.08	-23	2123.81
-55	2109.46	-22	2124.25
-54	2110.12	-21	2124.67
-52	2110.96	-20	2124.92
-51	2111.56	-19	2125.64
-50	2111.99	-17	2126.74
-48	2112.76	-15	2127.18
-47	2113.22	-14	2127.82

TABLE XXV (continued)

WAVE NUMBERS OF THE OBSERVED LINES IN $2\nu_4$ OF DCOF

Chart Number	$\tilde{\nu}$ (cm^{-1})	Chart Number	$\tilde{\nu}$ (cm^{-1})
-13	2128.01	16	2147.55
-12	2128.81	17	2148.17
-11	2128.94	18	2148.65
-10	2129.57	19	2148.95
-9	2130.30	20	2149.59
-8	2130.97	21	2150.08
-7	2131.57	22	2150.71
-6	2132.39	23	2151.39
-5	2133.17	24	2151.93
-4	2133.98	25	2152.54
-3	2134.72	26	2153.22
-2	2135.52	27	2153.79
-1	2136.18	28	2154.18
		29	2154.63
Q	2137.79	30	2155.32
+ ½	2138.70	31	2155.76
+1	2139.40	32	2156.52
2	2139.80	33	2156.96
3	2140.42	34	2157.74
4	2140.88	35	2158.32
5	2141.27	36	2158.95
6	2141.98	37	2159.38
7	2142.71	38	2159.95
8	2143.36	39	2160.49
9	2144.02	40	2161.14
10	2144.62	41	2161.67
11	2145.37	42	2162.06
12	2145.95	42½	2162.25
13	2146.35	43	2162.65
15	2146.93	44	2163.03

TABLE XXV (continued)

WAVE NUMBERS OF THE OBSERVED LINES IN $2\nu_4$ OF DCOF

Chart Number	$\tilde{\nu}$ (cm^{-1})
45	2163.54
46	2164.10
47	2164.56
48	2165.05
49	2165.60
50	2166.08
51	2166.48

DCOF. There are no remarkable features in this band. The parallel structure was not resolved, but the perpendicular component is well resolved. Carbon monoxide lines are observed as an internal background. Figure 49 shows this band, and the observed Q lines are listed in Table XXVI.

$\nu_3+\nu_5$

This band, observed only in DCOF, is seen as a relatively weak, unresolved, parallel-type band on the low frequency side of $\nu_4+\nu_5$. The background absorption caused by water vapor was only partly removed. Figure 50 shows this band.

$\nu_4+\nu_5$

HCOF. Figure 51 shows $\nu_4+\nu_5$ in HCOF, which, like $2\nu_4$, is generally parallel in appearance, but with no central Q branch. The band is relatively weak, and many of the observed lines are poorly defined. Table XXVII lists the observed lines.

DCOF. This band, of parallel type, is more intense than the corresponding band in HCOF, and more lines are observed, more clearly defined. The observed lines are listed in Table XXVIII, while Figure 52 shows this band.

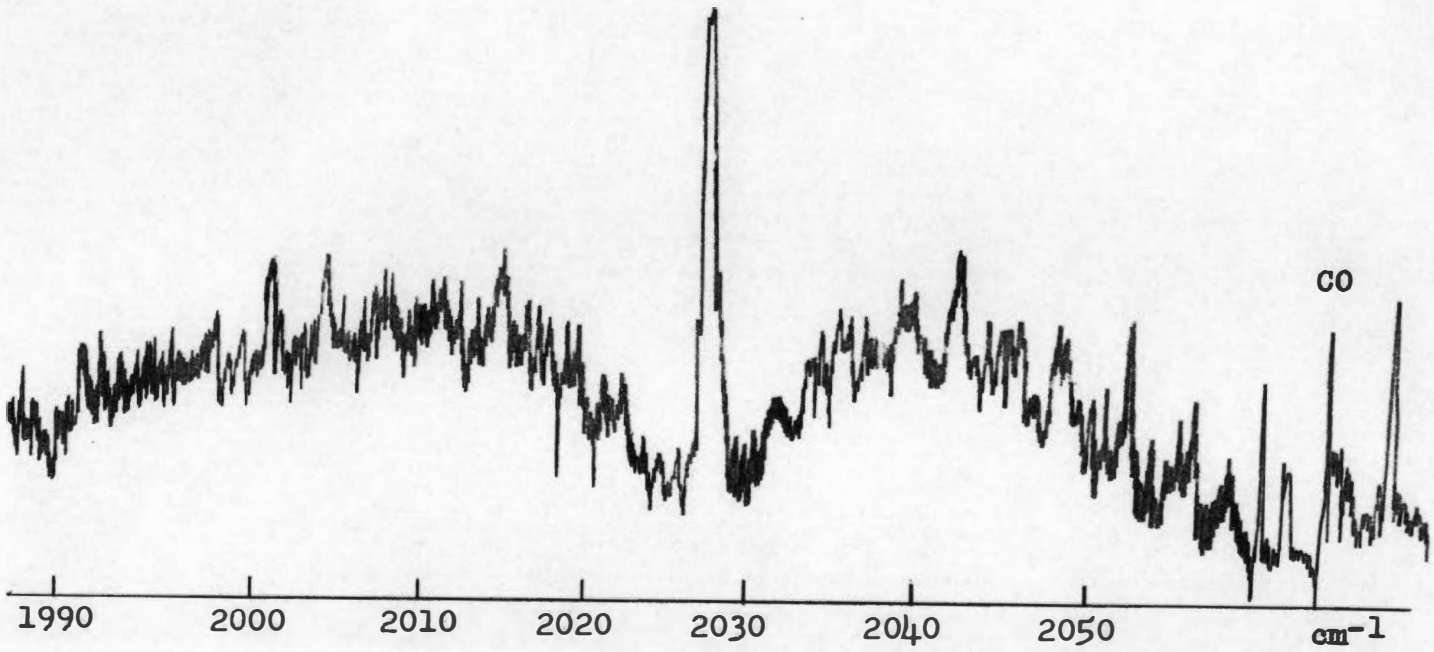

Figure 49. The $\nu_3+\nu_4$ vibration-rotation band of DCOF

TABLE XXVI

WAVE NUMBERS OF THE OBSERVED Q LINES IN $\nu_3+\nu_4$ (TENTATIVE ASSIGNMENT) OF DCOF

K	R_{Q_K} (cm^{-1})	P_{Q_K} (cm^{-1})
0	-	-
1	2033.29	-
2	2037.61	2023.20
3	2040.88	-
4	2044.21	2015.55
5	2048.31	2011.91
6	-	2008.38
7	-	2004.71
8	-	2001.14

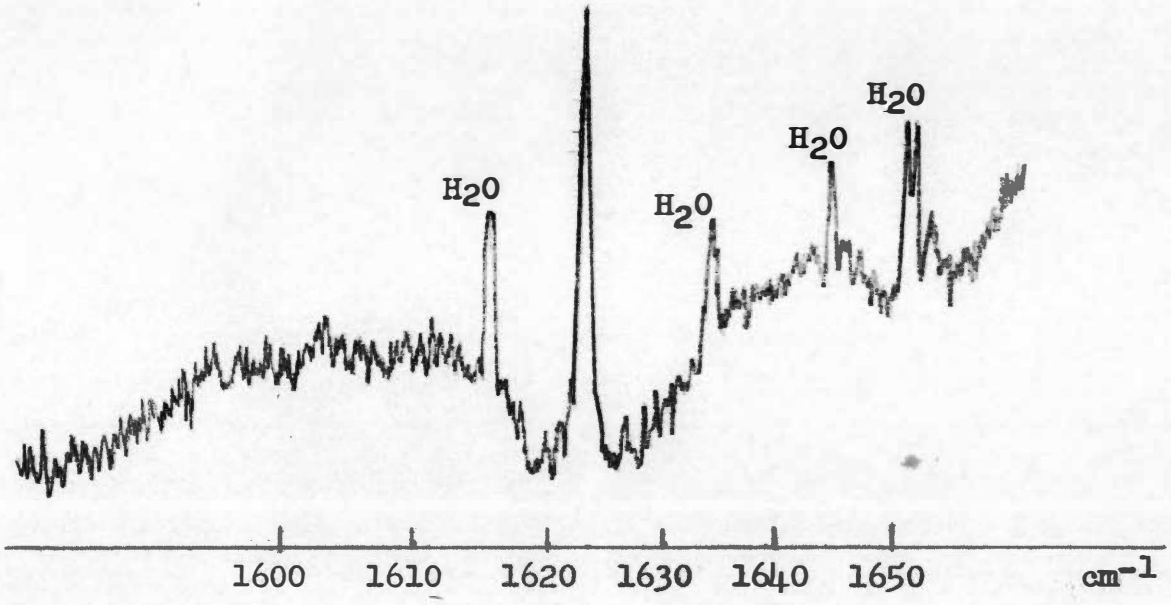

Figure 50. The $\nu_3+\nu_5$ vibration-rotation band of DCOF

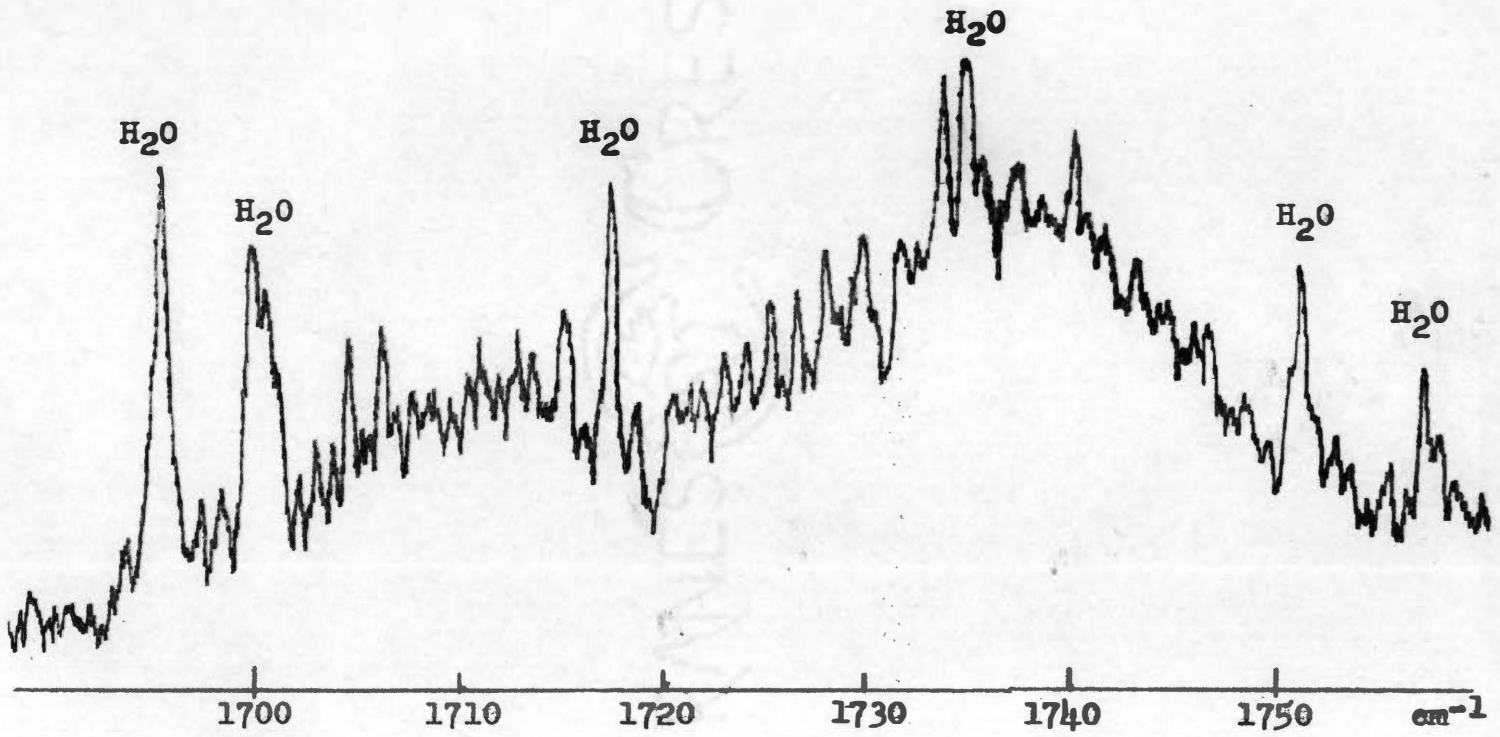

Figure 51. The $\nu_4+\nu_5$ vibration-rotation band of HCOF

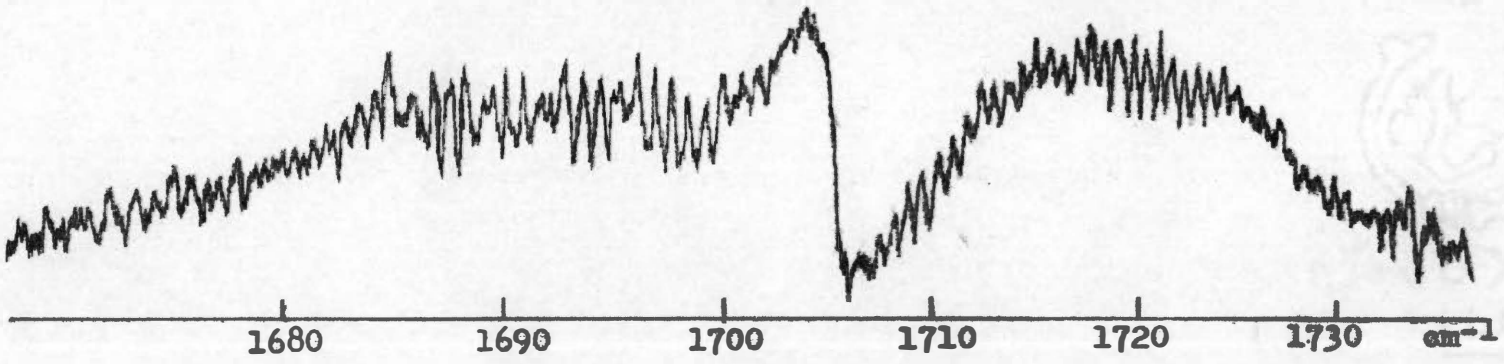

Figure 52. The $\nu_4+\nu_5$ vibration-rotation band of DCOF

TABLE XXVII

WAVE NUMBERS OF THE OBSERVED LINES IN $\nu_4 + \nu_5$ OF HCOF

Chart Number	$\tilde{\nu}$ (cm^{-1})	Chart Number	$\tilde{\nu}$ (cm^{-1})
-18	1702.16	+1	1720.50
-17	1702.83	2	1721.30
-16	1703.78	3	1722.02
-15	1704.72	4	1723.01
-14	1705.54	5	1724.09
-13	1706.44	6	1725.25
-12	1707.28	7	1726.59
-11	1708.11	8	1727.04
-10	1708.99	9	1727.90
-9	1709.83		
-8	1710.54		
-7	1711.33		
-6	1712.29		
-5	1712.04		
-4	1713.94		
-3	1714.49		
-2	1716.00		
-1	1716.99		

TABLE XXVIII

WAVE NUMBERS OF THE OBSERVED LINES IN $\nu_4+\nu_5$ (TENTATIVE ASSIGNMENT) OF DCOF

J	R(J) (cm^{-1})	P(J) (cm^{-1})
0	-	-
1	1707.50	-
2	1708.13	-
3	1708.87	1703.27
4	1709.58	1702.80
5	1710.27	1702.31
6	1710.87	1701.76
7	1711.50	1700.71
8	1712.21	1699.95
9	1712.92	1699.18
10	1713.46	1698.42
11	1714.17	1697.62
12	-	1696.94
13	1715.66	1696.11
14	1716.20	1695.14
15	1716.88	1694.37
16	1717.51	1693.63
17	1717.99	1692.89
18	1718.84	1691.96
19	1719.49	1691.04
20	1720.14	1690.27
21	1720.80	1689.21
22	1721.42	1688.40
23	1722.06	1687.73
24	1722.76	1686.93
25	1723.46	1686.16
26	1724.09	1685.73
27	-	1684.99
28	-	1684.31
29	-	1683.75

TABLE XXVIII (continued)

WAVE NUMBERS OF THE OBSERVED LINES IN $\nu_4+\nu_5$ (TENTATIVE ASSIGNMENT) OF DCOF

J	R(J) (cm^{-1})	P(J) (cm^{-1})
30	-	1683.01
31	-	1682.10
32	-	-
33	-	1680.73

CALCULATED RESULTS

Rotational Constants

The frequencies of the observed lines were calculated for every resolved band. A rotational analysis was completed for all of the observed fundamentals except ν_6 in DCOF. The reciprocal moments of inertia, the band centers, and the other constants listed in Tables XXIX (for HCOF) and XXX (for DCOF) were obtained from the graphs of the combination relations reproduced on the preceding pages. None of the overtone or combination bands were analyzed because of the work of Wilson and Wilkinson already mentioned.

The moment of inertia I_A can, of course, be calculated from the constants in the tables. It is not possible, however, to calculate the moments of inertia I_B and I_C from these data alone.

Position of the Hydrogen Atom

The relative positions of the carbon, fluorine, and oxygen atoms in formyl fluoride have been obtained from electron diffraction data[4]. It is desirable to know also the relative position of the hydrogen atom. If we assume that formyl fluoride is planar, only two coordinates are necessary to determine the position of the hydrogen atom.

---

[4] M. E. Jones, K. Hedberg, and V. Schomaker, J. Amer. Chem. Soc. 77, 5278 (1955).

TABLE XXIX

THE ROTATIONAL CONSTANTS OF HCOF (cm^{-1})

Band	(A''-B'')	(A'-B')	(A'-B')-(A''-B'')	B''	B'	(B'-B'')	ν_0(⊥)	ν_0(∥)	ν_0(av.)	$D_K^{''}$ X10^5	$D_K^{'}$ X10^5	D_J
ν_1	2.658	2.644	-0.017	0.3675	0.3670	-0.00007	2981.2	2980.9	2981.0	5	6	0
ν_2	-	-	-	0.3662	0.3642	-0.0023	-	1836.9	1836.9	-	-	0
ν_3	2.655	2.650	-0.009	-	-	-	1342.5	-	1342.5	-	-	-
ν_4	2.660	2.720	-	0.3683	0.3652	-0.0028	1064.8	1064.8	1064.8	8	2	0
ν_5	2.670	2.691	0.021	-	-	-	662.5	-	662.5	9	-	-

TABLE XXX

THE ROTATIONAL CONSTANTS OF DCOF (cm^{-1})

Band	$(A''-B'')$	$(A'-B')$	$(A'-B')-(A''-B'')$	B''	B'	$(B'-B'')$	ν_0(I)	ν_0(II)	ν_0(av.)	D''_K X10^5	D'_K X10^5	D_J
ν_1	1.807	1.790	-0.016	0.3646	0.3645	-0.0002	2261.7	2261.3	2261.7	3	.2	0
ν_2	-	-	-	0.3651	0.3631	-0.0015	-	1796.8	1796.8	-	-	0
ν_3	1.799	1.796	-0.004	0.3637	0.3638	0.0001	968.0	967.8	967.9	0	0	0
ν_4	1.808	1.824	0.011	0.3660	0.3649	-0.0012	1073.3	1073.0	1073.2	3	5	0
ν_5	1.809	1.813	0.009	-	-	-	657.5	-	657.5	3	-	-

Both B" and (A"-B") depend on the position of the hydrogen atom, and it is possible to set up equations relating these to the coordinates of the hydrogen atom. It is more practical, however, to calculate the moments of inertia for a series of positions, and to compare the results with the results obtained experimentally. The position of the hydrogen atom is thus obtained by the method of successive approximations. Unfortunately, the moments of inertia are relatively insensitive to the position of the hydrogen atom. Table XXXI gives a comparison of the experimental values of the reciprocal moments of inertia with those calculated for several different values of the coordinates of the hydrogen atom. It should be noted that the values which give reasonably good agreement with the experimental values correspond to a C-H bond length of 1.05 Å or less. A table of bond lengths given by Gordy, Smith, and Trambarulo[5] lists no C-H distance less than 1.056 Å, and then only in the configuration C≡C-H. Nevertheless, without considering the effect of the uncertainty in the other bond lengths, it does not seem possible to bring a value for the C-H distance greater than about 1.06 Å into accord with the experimental results.

---

[5]Walter Gordy, William V. Smith, and Ralph F. Trambarulo, Microwave Spectroscopy (John Wiley and Sons, Inc., New York, N.Y. 1953) p. 371f.

TABLE XXXI

A COMPARISON OF THE EXPERIMENTAL AND CALCULATED VALUES OF THE RECIPROCAL MOMENTS OF INERTIA

Position of the H Atom: C-H Distance Å and HCF Angle	B"(cm^{-1}) HCOF	(A"-B") (cm^{-1}) HCOF	B"(cm^{-1}) DCOF	(A"-B") (cm^{-1}) DCOF
1.08 119.0°	0.3663	2.610	0.3585	1.783
1.05 119.0°	0.3666	2.658	0.3591	1.831
1.046 110.8°	0.3670	2.666	0.3598	1.836
1.039 109.5°	0.3672	2.680	-	-
Experimental Values	0.3673	2.661	0.3648	1.806

Vibrational Constants

It is desirable to know the ω_i's and x_{ij}'s of equation (4) on page 9, or, at least, to know some of the ω_i^o's and x_{ij}^o's of equation (5) on page 9. The first step, of course, is to determine the vibrational band centers of the observed bands. These may be substituted into equations (4) and (5), which may then be solved for the unknowns.

The band centers of the fundamentals, other than ν_6, were determined by rotational analysis. The band centers of the other bands we observed were estimated by an examination of the bands. The band centers used in the vibrational analysis were values we obtained in this way for the bands that we observed, other than $\nu_3+\nu_4$. For those additional bands which Morgan, Staats, and Goldstein observed, and for $\nu_3+\nu_4$, we have used their values for the band centers.

It proved to be impossible to find any of the ω_i's, but several of the ω_i^o's were obtained. Those constants which could be obtained are listed in Table XXXII.

The values of the x_{ij}'s are uncertain. In particular the difference in sign of x_{34} for HCOF and DCOF should be noted. The results are quoted to one decimal place because the probable error is unknown.

TABLE XXXII

VIBRATIONAL CONSTANTS

Constant	HCOF (cm^{-1})	DCOF (cm^{-1})
ω_2^o	1847.9	1803.9
ω_3^o	-	970.5
ω_4^o	1070.3	1076.7
$x_{22} = x_{22}^o$	-11.0	- 7.1
$x_{33} = x_{33}^o$	-	- 2.6
$x_{44} = x_{44}^o$	- 5.5	- 3.5
$x_{14} = x_{14}^o$	-	-14.9
$x_{34} = x_{34}^o$	10.7	-12.5
$x_{35} = x_{35}^o$	-	- 0.9
$x_{45} = x_{45}^o$	- 8.0	-24.9
$x_{46} = x_{46}^o$	-	- 2.2

CHAPTER V

CONCLUSION

Nine bands were observed in HCOF and thirteen in DCOF. A rotational analysis was completed on five of the fundamental bands in each molecule. The ground state moments of inertia are internally consistent. The value of B which is quoted is actually $\overline{B} = \frac{1}{2}(B+C)$. As the symmetric top approximation is used throughout, no information was obtained about the actual values of B and C themselves. We know, however, that they cannot differ by very much because the symmetric top approximation gives consistent results.

The moments of inertia were used to determine the approximate position of the hydrogen atom. The moments of inertia, however, are relatively insensitive to the position of the hydrogen atom.

The band centers were used to determine some of the vibrational constants. Several ω_1^0's were calculated, but none of the ω_1's could be determined. If the combination band $\nu_2+\nu_4$ could be observed, it would then be possible to find ω_4.

A rotational analysis could probably be completed on several of the combination bands. It seems likely that some of these, notably $2\nu_4$, in both molecules, might require that

the symmetric top approximation be abandoned.

The results quoted here might be improved considerably if some of the bands could be examined under higher resolution. It seems that the parallel component of ν_5 (in both molecules) could be resolved with only a slight improvement in resolution. The unresolved regions in ν_2, apparently caused by interference between the lines, might also be cleared up.

It seems likely that higher resolution would force one to give up the symmetric top approximation entirely. In any case, in a complete analysis of these molecules, it would be desirable to consider their asymmetry. Tables[1,2] have been made by machine calculation which may be used to calculate the rotational energy levels of the asymmetric top for J up to 40. These tables would allow the asymmetry to be considered with a minimum of labor.

---

[1]Richard H. Schwendeman, A Table Of Coefficients For The Energy Levels Of A Near Symmetric Top. ONR contract N5ori 1866, Task Order XVI, Harvard University, 1957.

[2]G. W. King, R. M. Hainer, and P. C. Cross, J. Chem. Phys., 11, 27 (1943).

BIBLIOGRAPHY

BIBLIOGRAPHY

Dennison, David M. Rev. Mod. Phys. 3, 280 f (1931).

Edlen, B. J. Opt. Soc. Am. 43, 339 (1953).

Goldstein, Herbert. Classical Mechanics. Cambridge, Mass.: Addison-Wesley Press Inc., 1951.

Gordy, Walter, Smith, W. V., Trambarulo, R. F. Microwave Spectroscopy. New York: John Wiley and Sons, Inc., 1953.

Herzberg, G. Molecular Spectra and Molecular Structure II. Infrared and Raman Spectra of Polyatomic Molecules. New York: D. Van Nostrand, Inc., 1945.

Jones, M. E., Hedberg, K., and Schomaker, V. J. Amer. Chem. Soc. 77, 5278 (1955).

King, G. W., Hainer, R. M., and Cross, P. C. J. Chem. Phys. 11, 27 (1943).

Mashentsev, A. I. J. Gen. Chem. (U.S.S.R.) 16, 203 (1946).

Morgan, H. W., Staats, P. A., and Goldstein, J. H. J. Chem. Phys. 25, 337 (1956).

Nesmejanow, A. N., and Kahn, E. J. Ber. 67B, 370 (1934).

Nielsen, A. H. J. Tenn. Acad. Sci. 22, 241 (1947).

Plyler, E. K., Benedict, W. S., and Silverman, S. J. Chem. Phys. 20, 180 (1952).

_____, Blaine, L. R., and Conner, W. S. J. Opt. Soc. Am. 45, 104 (1955).

Rao, K. N. The Ohio State University, Columbus, Ohio. Private communication.

Schiff, L. I. Quantum Mechanics. New York: McGraw-Hill Book Co., Inc., 1949.

Schwendeman, Richard H. A Table Of Coefficients For The Energy Levels Of A Near Symmetric Top. Harvard Univ.: ONR contract N5ori 1866, Task Order XVI, 1957.

Slawsky, Z. I., and Dennison, D. M. J. Chem. Phys. 7, 509 (1939).

Wang, S. C. Phys. Rev. 34, 243 (1929).

Wilson, M. Kent. Tufts College, Medford, Mass. Private communication.